

Effect of Deicing Chemicals on the Strength and Deterioration of Concrete

by

Ccee Chan, EIT

A Thesis submitted to the Faculty of Graduate Studies of

The University of Manitoba

in partial fulfilment of the requirements of the degree of

MASTER OF SCIENCE

Structural Engineering Division
Department of Civil Engineering
University of Manitoba
Winnipeg, Manitoba
Canada

Copyright 2006 by Ccee Chan

THE UNIVERSITY OF MANITOBA
FACULTY OF GRADUATE STUDIES

COPYRIGHT PERMISSION

**Effect of Deicing Chemicals on the Strength
and Deterioration of Concrete**

BY

Ccee Chan

**A Thesis/Practicum submitted to the Faculty of Graduate Studies of The University of
Manitoba in partial fulfillment of the requirement of the degree
MASTER OF SCIENCE**

Ccee Chan © 2007

Permission has been granted to the Library of the University of Manitoba to lend or sell copies of this thesis/practicum, to the National Library of Canada to microfilm this thesis and to lend or sell copies of the film, and to University Microfilms Inc. to publish an abstract of this thesis/practicum.

This reproduction or copy of this thesis has been made available by authority of the copyright owner solely for the purpose of private study and research, and may only be reproduced and copied as permitted by copyright laws or with express written authorization from the copyright owner.

Abstract

Many studies have demonstrated that deicing chemicals often exacerbate concrete damage originating from freeze-thaw cycles. In North America, chloride-induced deterioration has been of major concern for many years. Furthermore, there has been an increasing demand for alternate deicers as traditional deicing chemicals have been associated with environmental and corrosion damage. The new deicers include calcium chloride, magnesium chloride, and potassium acetate. The deleterious effects caused by these deicing chemicals have not been fully documented. The purpose of this investigation is to examine the performance of current and potential deicing chemicals in the presence of freeze-thaw cycles. The performance of deicing chemicals is evaluated on the basis of changes in mechanical properties, and extent of concrete deterioration.

An experimental program was undertaken at the University of Manitoba to evaluate the effects of several deicing chemicals currently used or considered for use by the industry in the presence of freeze-thaw cycles. The deicing chemicals selected for this investigation were sodium chloride, corrosion-inhibited calcium chloride, corrosion-inhibited magnesium chloride (ICE-BAN 200M), and potassium acetate. In order to carry out the objectives of this investigation, 118 concrete cylinders, 10 concrete prisms, and 12 reinforced concrete beams were fabricated in order to determine the changes in scaling resistance, and physical and mechanical properties of the concrete elements. The samples were exposed to the deicing chemicals and placed in an environmental chamber where they were subjected to freeze-thaw cycles ranging from $-25^{\circ}\text{C} \pm 3^{\circ}\text{C}$ to $23^{\circ}\text{C} \pm 2^{\circ}\text{C}$ over a period of 6 months. Concrete deterioration during the freeze-thaw cycles was evaluated on the basis of mass loss or gain and degree of scaling. The changes in the mechanical properties of concrete were determined in terms of loss of tensile, compressive and flexural strength, and changes in the static modulus of elasticity. The results of the samples were compared to control samples that were not exposed to freeze-thaw cycles or deicing chemicals. The results of the compression test were also compared to samples stored in deicing solutions in the absence of freeze-thaw cycles.

Finally a Water Soluble Chlorides Test was carried out by the National Testing Laboratories to evaluate the penetration of corrosion-inducing chlorides with depth.

The results indicate that of the 4 deicing chemicals considered, the magnesium chloride solutions produced the greatest severity of strength deterioration. The potassium acetate samples exhibited an earlier strength reduction; however, the severity of degradation was approximately equivalent or surpassed by the calcium and magnesium chloride solutions with progressive cycles. The delayed deterioration may have been partly attributed to the presence of corrosion inhibitors in the $CaCl_2$ and $MgCl_2$ solutions, which may have acted to reduce the permeability of the concrete samples. The loss of compressive strength in the potassium acetate samples, however, demonstrates that there may be a deleterious reaction that occurs between the potassium acetate deicer and the cement paste. The NaCl samples experienced only a slight reduction in overall strength, but displayed significant surficial deterioration and chloride penetration. The decreased strength in the sodium chloride samples is attributed to the expansive internal pressures caused by the combination of the freeze-thaw cycles and the salt solution, as well as the reduction in surface area caused by scaling as a result of these damage mechanisms. The decreased strength in the calcium chloride, magnesium chloride and potassium acetate samples was believed to be caused by chemical reactions that occurred between the deicing chemical and the concrete paste. The resulting formation of new mineral phases in the cracks and voids may have caused expansive physical pressures leading to cracking, and loss of inter-particle bonds between the paste and the aggregate.

The results of this study have many important implications in the effort to obtain a greater understanding of the impact that alternative deicing chemicals may have on the long-term durability of concrete materials. The results of this investigation suggest that the proposed deicing chemicals react with concrete through various deterioration mechanisms to reduce the strength and durability of concrete structures. This research will assist transportation industries to better select effective yet benign deicing chemicals. As a result, the long-term durability and life of transportation infrastructure and assets will be maintained.

Acknowledgements

I would like to thank my advisor Dr Dagmar Svecova for her encouragement, support, and guidance during this project. I would also like to express sincere gratitude towards my fellow graduate student Sharyar Davoudi for all of his invaluable assistance during the experimental program, which would otherwise have not been possible. As well, I also would like to thank Hugues Vogel and Jeremy Walker for their assistance. Thank you all for your support and friendship during my time as a masters student.

The experimental program would also have not been carried out without the invaluable assistance provided by Moray McVey, Grant Whiteside, and Chad Klowak. A sincere thank you is also extended towards Liting Han and Evangeline Rivera for their assistance in using the DAQ and strain gages.

I would also like to acknowledge the support provided by the Department of Transportation and Government Services, especially Terry Zdan, Leonnie Kavanagh, Glen Fempel, and Tony Capizzi.

Assistance from Western Road Management, Winnipeg Airport Authority, and Fort Distributors for their contribution of the deicing chemicals is greatly appreciated.

Financial assistance received from Environment Canada, Western Economic Diversification Canada, Natural Resources Canada, and Portland Cement Association of Canada is highly appreciated.

Finally I am very thankful to my family and friends for their support and understanding while I was working on my thesis.

Contents

- 1 Introduction** **1**
 - 1.1 Problem Definition 1
 - 1.2 Climate Change 2
 - 1.2.1 Impact of Climate Change on Transportation Infrastructure 3
 - 1.2.2 Climate Modeling 5
 - 1.3 Current Winter Maintenance Practices 7
 - 1.4 Research Objectives and Scope 12
 - 1.5 Organization of Thesis 12

- 2 Literature Review** **14**
 - 2.1 Concrete 14
 - 2.2 Mechanisms of Frost Attack in Concrete 15

2.3	Influence of Deicing Chemicals on Concrete Freeze-Thaw Attack	18
2.4	Previous Research on Concrete Deterioration by Deicing Chemicals	22
2.4.1	Sodium Chloride	22
2.4.2	Calcium Chloride	24
2.4.3	Magnesium Chloride	26
2.4.4	Potassium Acetate	27
2.4.5	Corrosion Inhibitors	28
2.5	Considerations for the Experimental Program	29
2.5.1	Importance of Free Liquid on Surface	29
2.5.2	Minimum Temperature	30
2.6	Methods of Detecting Deterioration	30
3	Experimental Program	32
3.1	Overview	32
3.2	Test Samples	33
3.3	Testing Materials	38
3.3.1	Deicing Chemicals	38
3.3.2	Concrete	38

3.4	Freeze-Thaw Cycling	39
3.4.1	Temperature Regime	39
3.4.2	Concrete Cylinders	43
3.4.3	Concrete Prisms	44
3.4.4	Concrete Beams	45
3.5	Continuous Immersion	45
3.6	Compressive Strength Tests	47
3.7	Tension Tests	47
3.8	Modulus of Elasticity	50
3.9	Flexural Strength Tests	50
3.10	Water Soluble Chlorides Test	54
4	Analysis of Concrete Deterioration	55
4.1	Overview	55
4.2	Scaling Test	55
4.3	Mass Change	67
5	Analysis of Strength Deterioration	71

5.1	Overview	71
5.2	Compressive Strength Tests	72
5.3	Tensile Strength Tests	78
5.4	Statistical Analysis	81
5.4.1	Analysis of Variance	81
5.4.2	Compressive Strength Analysis Using ANOVA	84
5.4.3	Tukey's HSD Procedure for Compressive Strength	86
5.4.4	Tensile Strength Analysis Using ANOVA	90
5.4.5	Tukey's HSD Procedure for Tensile Strength	91
5.5	Flexural Strength Tests	94
5.5.1	Load Deflection Behavior	94
5.5.2	Cracking Load	100
5.5.3	Ultimate Load	102
5.6	Modulus of Elasticity	102
5.7	Water Soluble Chlorides Test	111
6	Summary, Conclusions, and Recommendations	115
6.1	Summary	115

6.2	Conclusions	118
6.2.1	Scaling	118
6.2.2	Mass Change	119
6.2.3	Compressive Strength	120
6.2.4	Tensile Strength	123
6.2.5	Flexural Strength	124
6.2.6	Static Modulus of Elasticity	126
6.2.7	Water Soluble Chlorides Test	127
6.3	Recommendations for Future Research	129

List of Figures

1.1	Aspects of Transportation Sensitive to Climate Change (Adopted from Mills & Andrey, [46])	4
1.2	Annual Freeze-Thaw Cycles over Time for Northern Manitoba	8
1.3	Annual Freeze-Thaw Cycles over Time for Central Manitoba	9
1.4	Annual Freeze-Thaw Cycles over Time for Southern Manitoba	10
2.1	Mechanisms of Osmotic Pressure Theory (Adopted from Pigeon and Pleau [52])	16
2.2	Concrete Scaling Caused by Freeze-Thaw Cycles in the Presence of Deicing Chemicals (Adopted from Portland Cement Association)	19
3.1	Casting of Concrete Cylinders and Prisms	33
3.2	Preparation of Concrete Prisms for Application of Deicing Chemicals	35
3.3	Beam Geometry (All Dimensions in mm)	36
3.4	Casting of Reinforced Concrete Beams	37

3.5	Arrangement of Specimens in Chamber	40
3.6	Temperature Readings -18°C to 23°C	41
3.7	Temperature Readings -25°C to 23°C	42
3.8	Concrete Cylinders in Submerged in Deicing Chemicals	43
3.9	Filtering Apparatus	46
3.10	Compression Testing Machine	48
3.11	Position of Aligning Jig Under Crosshead	49
3.12	Aligning Jig	49
3.13	Static Modulus Test	51
3.14	Beam Instrumentation	52
3.15	Beam Configuration	53
4.1	Average Scale Rating of Test Samples with Progressive Freeze-Thaw Cycles .	56
4.2	Progression of Deterioration for Severely Scaled Prism Ponded with Sodium Chloride	58
4.3	Progression of Deterioration for the Second Prism Ponded with Sodium Chloride	59
4.4	Progression of Deterioration for Specimen Ponded with Calcium Chloride . .	60
4.5	Progression of Deterioration for Specimen Ponded with Magnesium Chloride	62

4.6	Progression of Deterioration for Specimen Ponded with Potassium Acetate	63
4.7	Progression of Deterioration for Specimen ponded with Distilled Water	65
4.8	Cumulative Residual Mass of Scaled-off Particles	66
4.9	Mass-Change of Samples under Freeze-Thaw Cycles	67
4.10	Mass-Change of Samples vs Immersion Time	70
5.1	Mean Compressive Strength of Samples after Freeze-Thaw Cycling	72
5.2	Mean Compressive Strength after 6 Months of Continuous Immersion	76
5.3	Tensile Strength of Samples after Freeze-Thaw Cycling	79
5.4	Comparison of Means After 50 Cycles	88
5.5	Comparison of Means After 100 Cycles	88
5.6	Comparison of Means Between 50 and 100 Cycles	89
5.7	Comparison of Means After 100 Cycles	92
5.8	Comparison of Groups Between 50 and 100 Cycles	93
5.9	Condition of Sodium Chloride Specimen Prior to Flexure Test	95
5.10	Condition of Calcium Chloride Specimen Prior to Flexure Test	95
5.11	Condition of Magnesium Chloride Specimen Prior to Flexure Test	95
5.12	Condition of Potassium Acetate Specimen Prior to Flexure Test	95

5.13	Condition of Distilled Water Specimen Prior to Flexure Test	95
5.14	Condition of Control Specimen Prior to Flexure Test	95
5.15	Load Deflection Behavior of Control Specimen	96
5.16	Load Deflection Behavior of Sodium Chloride Specimens	97
5.17	Load Deflection Behavior of Calcium Chloride Specimens	97
5.18	Load Deflection Behavior of Magnesium Chloride Specimens	97
5.19	Load Deflection Behavior of Potassium Acetate Specimens	98
5.20	Load Deflection Behavior of Distilled Water Specimens	98
5.21	Crack Pattern of Control Specimen #1	103
5.22	Crack Pattern of Control Specimen #2	103
5.23	Crack Pattern of Sodium Chloride Specimen #1	103
5.24	Crack Pattern of Sodium Chloride Specimen #2	103
5.25	Crack Pattern of $MgCl_2$ Specimen #1	103
5.26	Crack Pattern of $MgCl_2$ Specimen #2	103
5.27	Crack Pattern of $CaCl_2$ Specimen #1	104
5.28	Crack Pattern of $CaCl_2$ Specimen #2	104
5.29	Crack Pattern of K-Acetate Specimen #1	104

5.30 Crack Pattern of K-Acetate Specimen #2	104
5.31 Crack Pattern of Distilled Water Specimen #1	104
5.32 Crack Pattern of Distilled Water Specimen #2	104
5.33 Stress-Strain Behavior of Test Samples at 50 Cycles	106
5.34 Stress-Strain Behavior of Test Samples at 100 Cycles	107
5.35 Moment-Curvature Relationship for Sodium Chloride Specimens	109
5.36 Moment-Curvature Relationship for Calcium Chloride Specimens	109
5.37 Moment-Curvature Relationship for Magnesium Chloride Specimens	110
5.38 Moment-Curvature Relationship for Control Specimens	110
5.39 % Concentration of Water Soluble Chlorides with Depth	112

List of Tables

1.1	Deicing Chemicals Used by Various Agencies	11
3.1	Experimental Program	34
3.2	Visual Rating Scheme for Scaling Resistance	45
5.1	Concrete Compressive Strength Loss with Respect to Control Samples	73
5.2	Change in Mean Concrete Compressive Strength	74
5.3	Continuously Immersed Samples Compared to Control Samples	75
5.4	Continuously Immersed Samples Compared to Freeze-Thaw Samples	77
5.5	Concrete Tensile Strength Loss With Respect to Control Samples	80
5.6	Change in Mean Concrete Tensile Strength	80
5.7	Analysis of Variance for Compressive Strength at 50 Cycles	85
5.8	Analysis of Variance for Compressive Strength at 100 Cycles	85

5.9	Analysis of Variance for Effect of Number of Freeze-Thaw Cycles	86
5.10	Analysis of Variance for Tensile Strength at 50 Cycles	90
5.11	Analysis of Variance for Tensile Strength at 100 Cycles	91
5.12	The Effect of Number of Freeze-Thaw Cycles on Tensile Strength	91
5.13	Cracking Load	101
5.14	The Effect of Deicing Chemical Exposure on Ultimate Load	102
5.15	The Effect of Deicing Chemicals on the Static Modulus of Elasticity	105
5.16	Change in Chord Modulus of Elasticity Values Compared to Control Samples	108
5.17	Apparent Modulus of Elasticity	110
6.1	Effect of Deicing Chemicals on the Strength and Deterioration of Concrete .	117

Chapter 1

Introduction

1.1 Problem Definition

There is a general consensus based on current climate models that the climate is changing today at a rate and magnitude that differs from previous climate changes. Since weather and climate affect the planning, design, construction, and maintenance of transportation infrastructure, changes in climate must be taken into account to prevent premature deterioration of infrastructure that can potentially lead to structural failure.

Current climate models suggest a trend towards increasing freeze-thaw cycles in central and southern Manitoba. This is discussed further in the next section. Many studies have shown that deicing chemicals often exacerbate concrete damage originating from freeze-thaw cycles. In North America and Europe, the chloride-induced deterioration of concrete structures has been a major concern for many years. In addition, it has also been recognized that the use of deicing salts in winter roadway maintenance operations is one of the major causes of the rapid degradation of concrete roads and bridges [42]. In order to implement cost-effective winter maintenance strategies for future snow and ice control, research on how different deicing

chemicals combined with the impact of cumulative freeze-thaw cycles must be carried out to gain a better understanding of how these factors affect the degradation of concrete surfaces. Despite the current awareness on the detrimental effects of deicing chemicals, the degree of damage caused by current and future deicing and anti-icing chemicals have not been fully examined and documented. While numerous studies have been carried out describing the destructive effects of freeze thaw cycles and deicing chemicals [12],[13],[15],[24],[39],[55],[67],[68], the effects of these combined conditions on concrete strength have not been fully investigated. In addition, the effects of potassium acetate and corrosion-inhibited deicers on the behavior of concrete are not well documented as these are relatively new deicing chemicals. If these chemicals are to be implemented in future winter maintenance strategies, a better understanding of the damaging effects of these chemicals under different exposure conditions must be obtained.

1.2 Climate Change

The Intergovernmental Panel on Climate Change (IPCC) defines weather as the fluctuating state of the atmosphere characterized by the temperature, wind, precipitation, clouds, and other weather elements. IPCC [33] defines climate as the average weather in terms of the mean and its variability over a certain time-span and a certain area. Climate can be defined quantitatively using the expected values of the meteorological elements such as the average temperature, precipitation, wind, pressure, cloudiness, and humidity [25].

Climate varies with location, depending on latitude, distance to the sea, vegetation, and presence or absence of mountains or other geographical factors. Climate varies also in time; from season to season, year-to-year, decade to decade or on much longer time-scales, such as the ice ages. Statistically significant variations in either the mean state of the climate, or its variability, typically persisting for decades or longer, are referred to as climate change [33].

Climate change may occur as a result of natural internal processes, external forcings, which are processes that disturb the energy balance between incoming radiation from the sun, and outgoing terrestrial radiation from the earth or persistent anthropogenic changes in the composition of the atmosphere or in land use [33].

1.2.1 Impact of Climate Change on Transportation Infrastructure

Despite significant amounts of research carried out in the area of climate change, its impact on transportation infrastructure is a new topic that has only been addressed in recent years. For example, the most recent IPCC report on impacts, adaptation and vulnerability of climate change devotes less than 1 of over 1000 pages to transportation-related impacts and sensitivities [46]. A study conducted by Mills and Andrey [46] identifies the potential transportation sensitivities caused by anthropogenic climate change and how they may potentially affect transportation infrastructure. Figure 1.1 summarizes the areas in transportation that may be impacted by changes in climate.

Mills and Andrey [46] categorizes the weather elements affecting transportation sensitivities into temperature-related sensitivities and precipitation-related sensitivities. Temperature sensitivities include extreme heat and cold, freeze-thaw cycles, permafrost degradation, and reduced ice cover. Precipitation-related sensitivities include sea-level rises and storm surges. The impacts of climate change on future precipitation patterns currently, however, are much less certain than those for temperature, due in part to the highly variable nature of precipitation, and the inability of current global climate models to resolve certain precipitation processes. The changes in temperature, however, can be predicted with moderate confidence [33]. Mills and Andrey [46] conclude that there are many gaps which exist in the understanding of climate change impacts, and available adaptation strategies and costs. The study notes the need for more research on the vulnerability of Canadian roads to changes in thermal conditions including freeze-thaw cycles. A preliminary attempt to quantify the

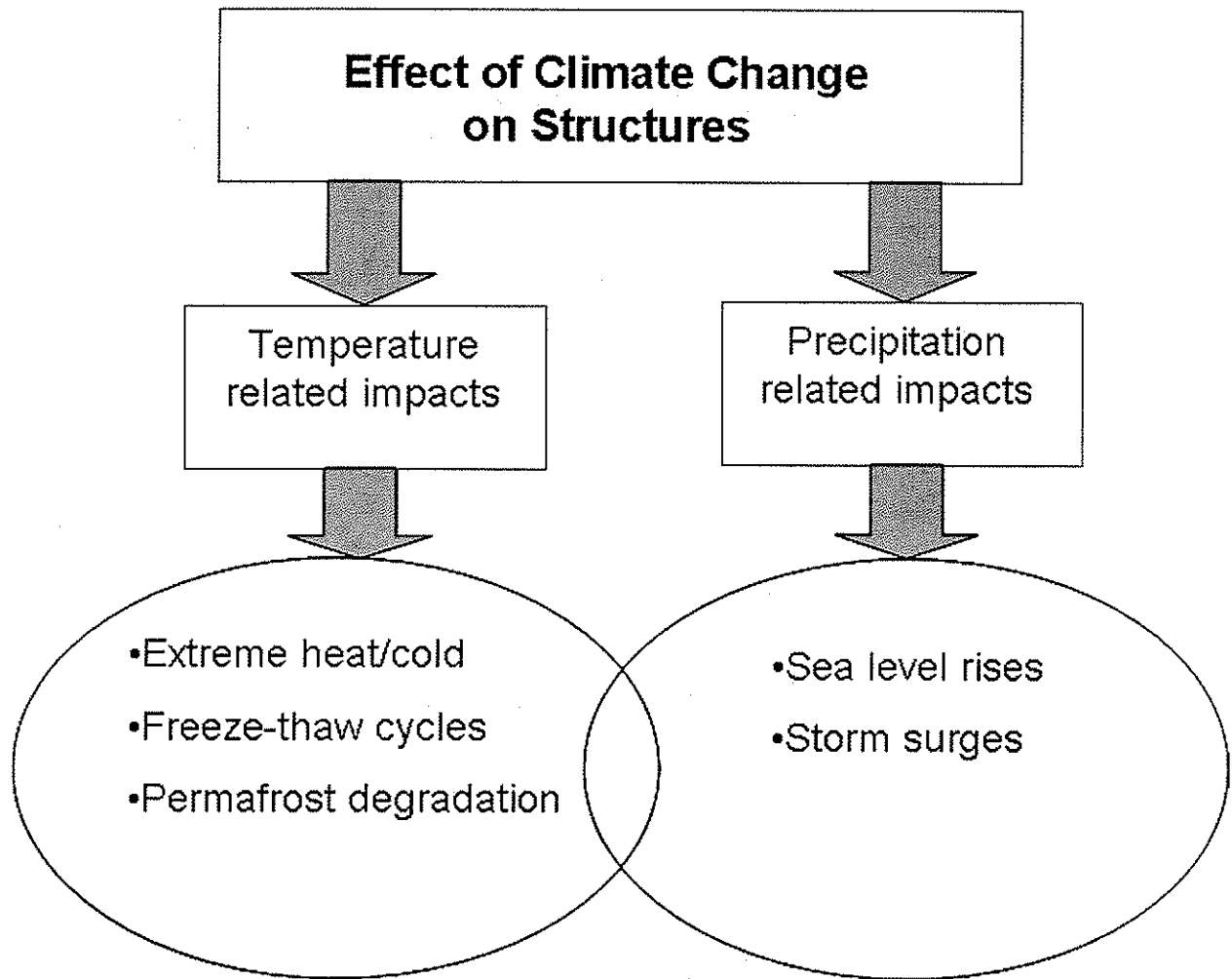


Figure 1.1: Aspects of Transportation Sensitive to Climate Change (Adopted from Mills & Andrey, [46])

changes in the freeze-thaw cycles over time was made in this investigation and is described in the following sections.

1.2.2 Climate Modeling

General Circulation Models

The behavior of the climate system, the components and their interactions, can be studied and simulated using climate models. A climate model can range from a relatively simple bulk model to a comprehensive model of the earth-atmosphere-ocean system. Depending on the detail of quantitative description of the physical characteristics and processes one wishes to obtain, an appropriate model can be selected [9].

The primary objective of climate modeling in this research is to develop a climate change scenario over Manitoba in order to assess the possible impacts on transportation infrastructure due to climate induced loads. General Circulation models (GCM) are complex computer models of the climate system that can be used to simulate human-induced climate change. GCMs are based on fundamental conservation laws of mass, momentum and energy, which are used to describe the dynamics of the atmosphere and oceans [33]. These physical laws are expressed as non-linear mathematical equations, and must be solved numerically using well-established mathematical techniques. GCMs often run to simulate current climates and those under double CO_2 conditions and other transitory scenarios. Recent GCMs attempt to represent the atmosphere, oceans, and land surfaces, as well as describe the apportioning and transport of heat, moisture and more recently CO_2 by the earth system [9],[18].

AGCM2

The climate data used in this project is obtained from the Second Generation Atmospheric General Circulation Model (AGCM2). The AGCM2 is the second coupled atmospheric-ocean model developed by the Canadian Center for Climate Modeling and Analysis [11]. A fully coupled climate model simulates the atmosphere and ocean jointly, including exchanges of momentum, heat, and water between them [33]. Hartmann [25] describes the atmospheric component as being a model created for the purpose of weather forecasting, and the basic framework of the numerical model of the atmosphere as a spatial grid-work that represents the mathematical equations described in the above section. A grid system with sides corresponding to the latitude and longitude of the globe is used because fields representing such processes as convection and radiative heating require interpolation of grid points [25]. The size and number of grid boxes are limited by the amount of computer power available, and the time period over which the model must be integrated. The atmospheric model in AGCM2 has 10 vertical levels and a horizontal resolution of about 300 km. The atmospheric model is coupled with a highly simplified oceanic model, and also takes into account land surface, and sea ice [11].

The quality of the simulations is assessed by comparing the climate scenario obtained from the model to actual observations made in the present climate. This allows for more confidence in the quality of the model, and provides a baseline for future projections of human-induced climate change [11]. Once the quality of the model is established, AGCM2 uses the transient method to make projections of future climate. This involves coupling a 3-D ocean model to the atmospheric model. To operate the model, the ocean and atmospheric models are “spun up” individually, (this refers to the computing time required for computer model to balance the internal equations of physics), and then coupled together so that the atmosphere and ocean interact on a daily basis [28]. The transient method requires a time-dependent profile of greenhouse gas and aerosol concentrations. These are derived from emission scenarios [33]. The climate data obtained from AGCM2 for this research uses a double CO_2 scenario.

Climate Projections using AGCM2

Future climate change projections were carried out for northern, central and southern Manitoba. From AGCM2, the daily temperature data was obtained for Manitoba for the years 1965-2100. The center of the grid of the data obtained for southern Manitoba was 97° Longitude, and 50° Latitude. As mentioned in the previous section, this data applies to a 300 km x 300 km square radius. Similarly, the center of the grid for central Manitoba was 97° Longitude and 53° Latitude, and 97° Longitude and 57° Latitude for northern Manitoba. From the temperature data, changes in diurnal freeze-thaw cycles over time were determined. Hershfield's [29] definition of a freeze-thaw cycle as occurring if the temperature fluctuates across the freezing point on the same calendar day was used to determine the total number of freeze-thaw cycles. The total number of freeze-thaw cycles per year was determined and plotted. Figures 1.2, 1.3, 1.4 illustrate the trends for freeze-thaw cycles for northern, central and southern Manitoba. An inspection of the plot for northern Manitoba does not reveal a trend towards increased diurnal freeze-thaw cycles due to changes in climate. Plots for freeze-thaw cycles over time for central and southern Manitoba, however, show that based on the temperature data given by the climate model, the number of freeze-thaw cycles will increase over time. This will lead to an increased use of deicing chemicals on roads and bridges across Manitoba.

1.3 Current Winter Maintenance Practices

A survey of winter maintenance strategies used by several Provincial Highway agencies reveals that many of the departments use deicing chemicals as the main method of snow and ice removal. Hassan et al. [26] defines deicing as a reactionary operation to break the bond between already-bonded snow or ice and the pavement. The chemicals melt the ice by depressing the freezing point. Depending on the type of chemical, this is achieved by either

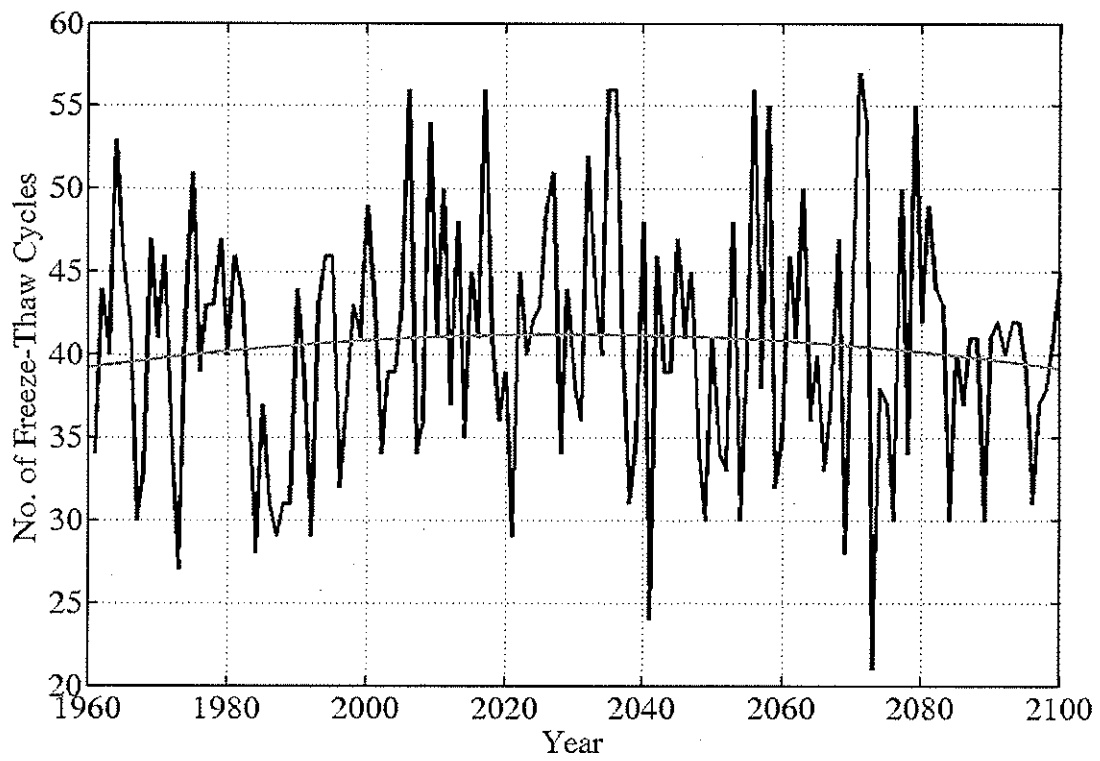


Figure 1.2: Annual Freeze-Thaw Cycles over Time for Northern Manitoba

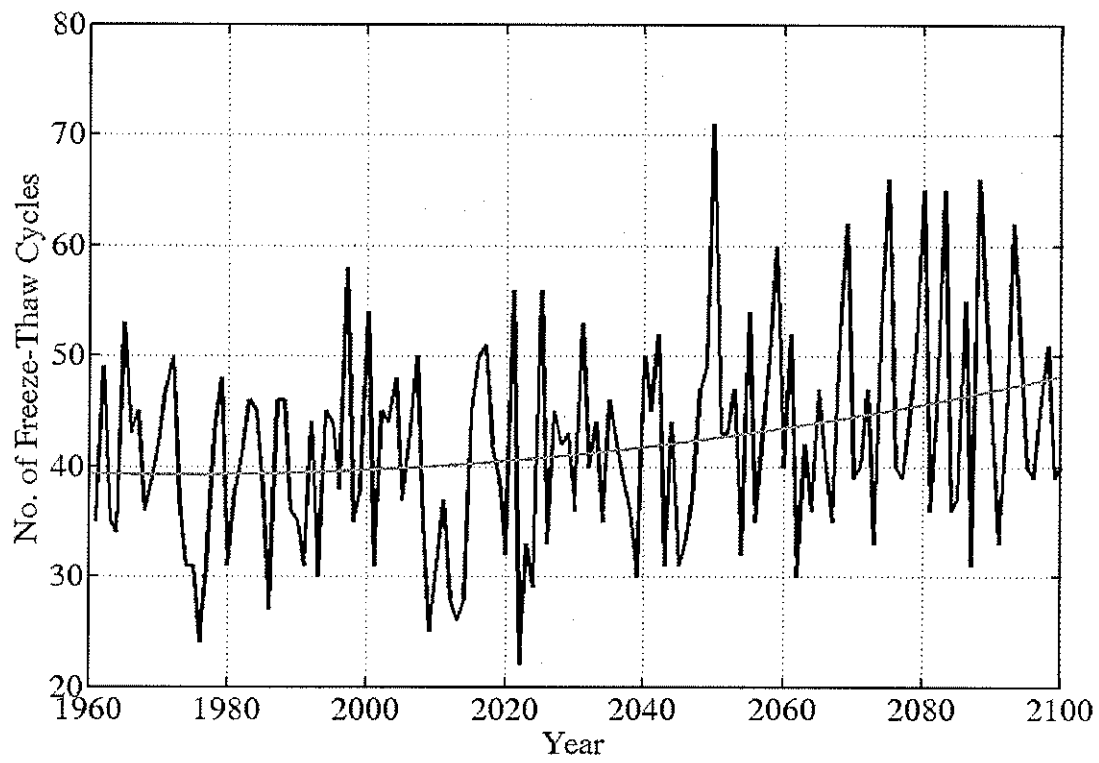


Figure 1.3: Annual Freeze-Thaw Cycles over Time for Central Manitoba

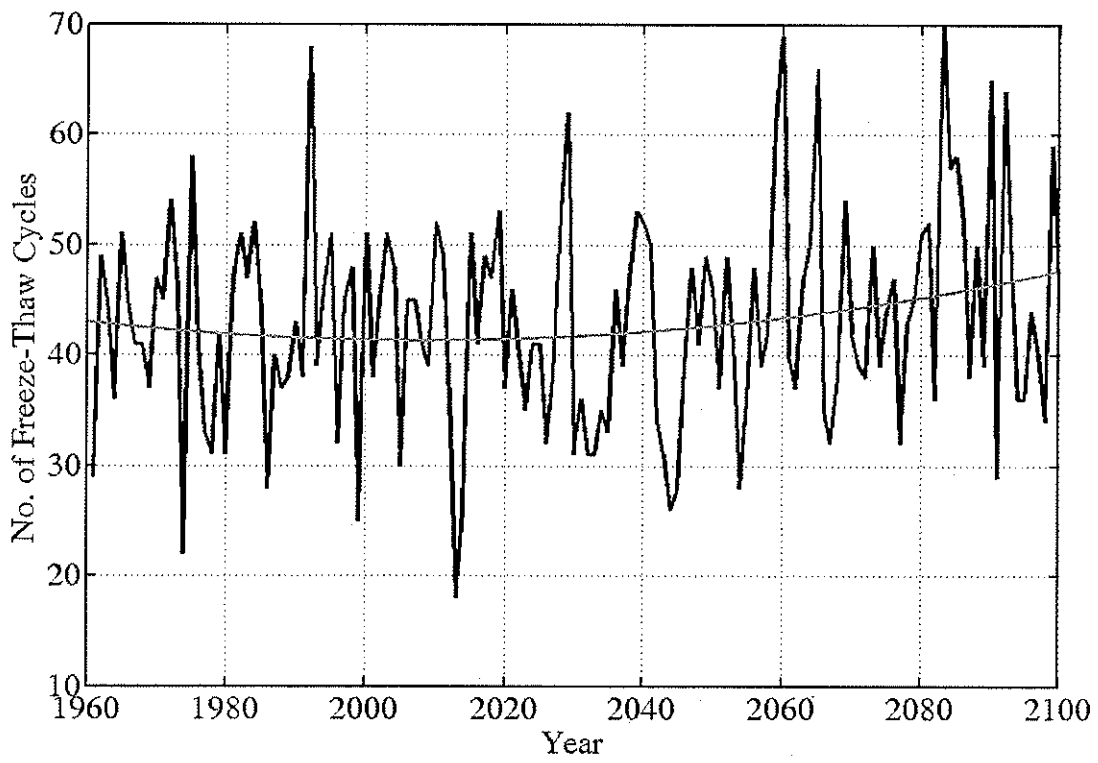


Figure 1.4: Annual Freeze-Thaw Cycles over Time for Southern Manitoba

Table 1.1: Deicing Chemicals Used by Various Agencies

Highway Agencies	De-icing Chemical	Pre-wetting Chemical
Manitoba Highways	Sodium Chloride (NaCl)	
Saskatchewan Highways	Sodium Chloride (NaCl)	Magnesium Chloride ($MgCl_2$)
Alberta Highways	Sodium Chloride (NaCl)	Magnesium Chloride ($MgCl_2$) Calcium Chloride ($CaCl_2$)
Quebec Highways	Sodium Chloride (NaCl)	Calcium Chloride ($CaCl_2$)

releasing heat to system during dissolving of the chemical or absorbing heat from an outside source such as the pavement or outside air during dissolving [48]. A survey of types of deicing chemicals used by Provincial Highways Departments in Canada indicates that Sodium Chloride, Calcium Chloride and Magnesium Chloride are the primary deicers used. Table 1.1 summarizes the deicing chemicals used by various deicing agencies.

The deicing chemicals chosen for this investigation were based on a review of the current deicers used by various Canadian transportation agencies, and conversations with the Manitoba Department of Transportation and Government Services regarding deicing chemicals considered for future use. The Department is currently considering the use of two new deicing chemicals: a corrosion-inhibited calcium chloride and corrosion-inhibited magnesium chloride (ICE-BAN 200M). These have been provided for the investigation by the company, Western Road Management which is based in Winnipeg, Manitoba and supplies the Department of Transportation and Government Services with deicing chemicals during their winter maintenance program. The investigation program will compare the effects of these deicers with sodium chloride, which is the primary deicer currently used by the department, and with potassium acetate, provided by the Winnipeg Airport Authority. Though potassium acetate is not generally used on bridge surfaces, it is the primary deicing chemical used on corrosion-sensitive operations such as the deicing of runways and taxiway pavements. As a result, it was also included in the current comparative investigation.

1.4 Research Objectives and Scope

Based on the problem definition described in the above section, the purpose of this investigation is to examine the performance of current and potential deicing chemicals in the presence of freeze-thaw cycles. The performance of deicing chemicals is evaluated on the basis of changes in mechanical properties, and extent of concrete deterioration.

The scope of the study is limited to the performance of sodium chloride, corrosion-inhibited calcium chloride, corrosion-inhibited magnesium chloride, and potassium acetate deicing chemicals. This investigation focuses primarily on the changes in mechanical properties of concrete as a result of freeze-thaw cycles. Although chemical interactions and changes in the concrete pore structure are acknowledged to occur throughout the experimental program, the chemical reactions are not measured in this study, and a microscopic analysis was outside the scope of this thesis.

1.5 Organization of Thesis

The thesis is organized into six chapters. Chapter 1 describes the problem, objectives, and scope of the study, as well as the climate modeling scenario used in determining the impact of climate change on freeze-thaw cycles in Manitoba. A review of literature is carried out in Chapter 2. Chapter 3 describes the experimental program undertaken to determine the damaging effects of the selected deicing chemicals on concrete. The fabrication of the test specimens and environmental conditions are described in this section. The mechanical apparatus and experimental procedures are also discussed. The experimental data and results are presented in Chapter 4 and 5 for the concrete and strength deterioration respectively. The extent of concrete deterioration is evaluated on the basis of mass loss/gain, and scaling. The changes in mechanical properties as a result of freeze-thaw cycles and chemical deterioro-

ration, are measured in terms of changes in tensile, compressive, and flexural strength, and static modulus of elasticity. A monotonic load is applied in all strength tests. Chapter 6 summarizes the conclusions drawn regarding the performance of the deicing chemicals and recommendations for future research.

Chapter 2

Literature Review

2.1 Concrete

Concrete is a composite material composed primarily of aggregate, cement, and water [47]. The type of cement used in general is Portland cement and all references to concrete in this thesis refer to Portland Cement Concrete. When the cement is mixed with water, the components undergo a series of chemical reactions referred to as hydration, and the major hydration products are finely structured porous solids known as cement gel. This gel consists primarily of calcium silicate hydrate (CSH) and calcium hydroxide (CH). Popovics [53] suggests that the gel particles bond to each other, to the aggregate particles, and to the other bodies in the concrete, and that this bond action is primarily responsible for the strength of concrete. In addition to the inter-particle bonds, other factors that influence concrete strength include the paste strength, aggregate strength, and porosity. As described in the following sections, the action of freeze-thaw cycles and deicing chemicals result in various mechanisms of deterioration that may act to compromise both the inter-particle bonds and concrete micro-structure.

2.2 Mechanisms of Frost Attack in Concrete

The deterioration of concrete as a result of frost attack has been studied for over five decades. Early attempts to explain this damage were based on the fact that water expands by 9% when it freezes. It was assumed that when concrete had reached a critical saturation of 91.7%, it would not be able to accommodate the increased volume, and damage would result. However, Powers [54] reasoned that concrete always contains enough air-filled space to accommodate the ice formed inside fully saturated concrete. He instead proposed that the 9% expansion of water during freezing in saturated concrete caused the water to migrate to a less saturated region. The viscous resistance to this flow as a result of the low porosity of concrete produced hydraulic pressures. The magnitude of this pressure depended on the rate of freezing, degree of saturation, the coefficient of permeability of the paste, and the length of the flow path from the saturated region to an unsaturated region. If this pressure exceeded the strength of concrete at a point, the freezing action caused fractures to occur. However, if water was able to migrate to an air void, ice would form in that void, and the hydraulic pressure would disappear.

Through extensive studies, Powers and Helmuth [55] observed that hydraulic pressure was not the only mechanism of frost damage. Powers [56] forwarded the osmosis pressure theory to address some of the limitations in the hydraulic pressure hypothesis. When freezing occurs, there exists a period of super cooling where ice forms only in the pore cavities that would support ice at that freezing temperature. The smaller the cavity size, the lower the melting point of the crystal and the less likely ice would be created in that cavity. Thus, what would develop in a given pore supporting ice during freezing is ice formed from pure water surrounded by a somewhat concentrated solution of water that has not been completely frozen. The solutes originally in the frozen water would now move to the surrounding water in the pore, thus increasing the solute concentration of the surrounding water, and lowering the overall melting point of the solution. At this point, the equilibrium is broken

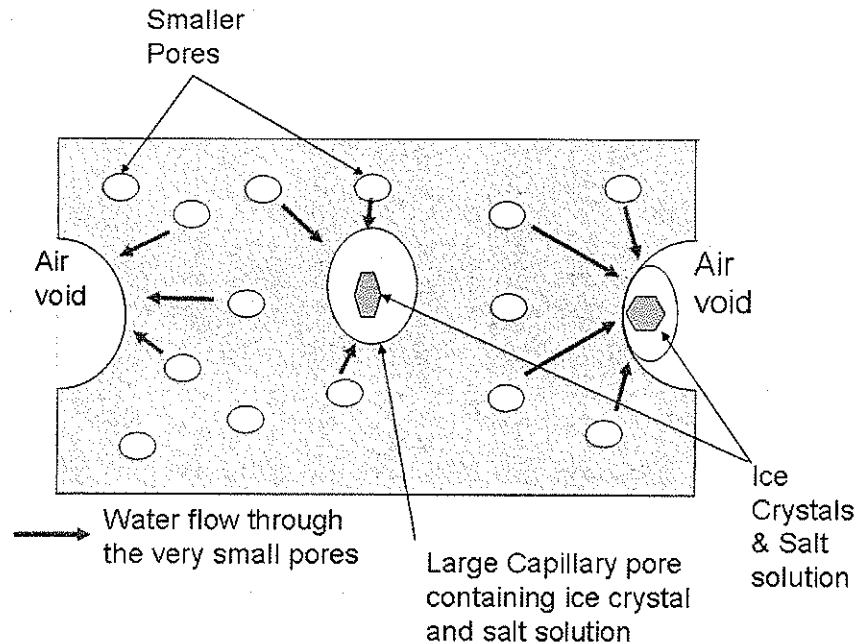


Figure 2.1: Mechanisms of Osmotic Pressure Theory (Adopted from Pigeon and Pleau [52])

between the pore water solution with the increased solute concentration and the water in the smaller surrounding pores where ice has not formed and the solute concentration has not increased. Due to the principle of osmosis, the pure water in the surrounding pores will migrate towards the larger pores where ice has formed, in order to reestablish equilibrium between the concentrations. This results in further growth of the body of ice in the pore cavity. When the cavity becomes full of ice and solution, any further growth of the ice crystal causes dilative pressures to develop, and the paste to eventually fail. Figure 2.1 is an illustration of the osmotic pressure theory.

Litvan [37],[38] proposed a mechanism of frost deterioration based on previous experimental data which suggests that water accumulated in a porous solid is prevented by surface forces from freezing when the temperature reaches below 0°C . Because the unfrozen water in the pores has a higher vapor pressure than ice, there will be a non-equilibrium situation that exists between the unfrozen pore water and the ice that forms on the outer surface of a

specimen. Equilibrium in the cement paste is achieved by the migration of the pore water to either the surface, or a larger capillary pore where formation of ice is possible. The vapor pressure in the smaller pores decreases as a result of the net loss of water in the pores, thereby achieving equilibrium. Any further cooling at temperatures below zero causes more ice to form, and the requirement of more water to be expelled from the pores in order to reduce its vapor pressure to that of the bulk ice. Continuing reductions in temperature results in more water expulsion and an accumulation of ice in the larger pores. According to Litvan [38], damage of the cement or concrete occurs when the distance for the water to migrate to the surface or cavity is too large and/or when the rate of water expulsion necessitated by rapid cooling is so high, it cannot be realized by the paste. In both of these cases, the passageways may become blocked with ice, generating high stresses and subsequent cracking. Furthermore, if there is a flaw in the concrete such as cracking, damage may also be caused by the expulsion of pore water into the cracked section. Solidification of this water causes the fissure to propagate, and further cooling results in accumulation of more water. Since this water is not necessarily reabsorbed back into the pore during the thawing cycle, this also explains the cumulative destructive effect of freeze-thaw cycles [52].

From the previous paragraphs, it is evident that much work has been carried out in an attempt to explain the frost damage on concrete. However, there is no single proposed model that can satisfactorily explain all the experimental results reported in literature. Pigeon and Pleau [52] concluded after a review of frost damage literature that despite initial appearances of contradictions in the models, the three theories compliment each other in many respects, and serve to explain certain portions of the overall phenomenon. Pigeon and Pleau [52] point out that the hydraulic pressure theory clearly explains the relationship between frost damage, and the maximum distance water can migrate before reaching an air void. The generation of internal stresses is also clearly explained. Litvan's theory in part contradicts the hydraulic pressure theory, because the movement of water in order to reestablish equilibrium is toward the freezing site, rather than away. The internal stresses, however, from both theories are caused by the forced movement of water between voids. With regards to the

osmotic pressure theory and Litvan's theory, Pigeon and Pleau [52] explains that both models do not necessarily contradict one another, but rather analyzes two different phenomena. The osmosis pressure theory clearly defines the destructive effects of a longer freezing period, because long freezing periods promote ice-crystal growth in the pores and thus a greater difference in chemical potential between water in the large and small pores. It does not, however, explain the influence of freezing rate. Litvan's theory, clearly explains the influence of freezing rate, and the possible destructive effects that can occur if the freezing rate is too high.

Regardless of the mechanism of deterioration, however, all three theories recognize the beneficial effects of air entrainment. In the osmosis pressure theory, the role of the air voids is to compete with the capillary pores during ice formation. When the less concentrated unfrozen water migrates towards the ice, it will reach an air bubble that has ice and water, but is far from being full. Thus, once the unfrozen water reaches the ice in the air bubble it will stop its migration. If the air voids are sufficiently closely spaced, the paste is protected from frost damage. Litvan's explanation of the beneficial effects of air entrainment is that the air voids act as a reservoirs where expelled water can migrate during freezing. The closeness of the air bubbles decreases the distance water must travel, and thus protects the cement paste.

2.3 Influence of Deicing Chemicals on Concrete Freeze-Thaw Attack

"Deicing chemicals often exacerbate the concrete damage caused by freeze-thaw cycles. Besides creating pressures through osmosis and crystallization, deicing chemicals often keep concrete pores at or near maximum fluid concentration, thus increasing the risk of frost damage" [68]. These mechanisms are explained in further detail in this section. Physical deterioration by deicing chemicals is generally found to be in the form of scaling. This type



Figure 2.2: Concrete Scaling Caused by Freeze-Thaw Cycles in the Presence of Deicing Chemicals (Adopted from Portland Cement Association)

of deterioration is exclusively a surface phenomenon, in which structures may show a progressive loss of small cement or mortar particles by crumbling and spalling, but relatively little loss in strength and resilience of the material [54]. In addition to reducing the serviceability of a structure, surface scaling is known to favor the ingress of deicing chemicals into the interior of the concrete which consequently increases the risk of deterioration by other phenomena such as alkali-aggregate reactions and corrosion of reinforcing steel [42]. Figure 2.2 illustrates the cumulative effect of successive freeze-thaw cycles and disruption on a concrete surface. The theories proposed in the previous section are believed to be at least partly responsible for surface scaling, since it has been demonstrated in many studies that air entrainment works to protect concrete from scaling [52].

Powers [56] demonstrated that when concrete pavement is made without entrained air, the repeated freezing and thawing of water on the concrete surface leads to a localized failure described as scaling. This damage is greatly increased when sodium or calcium chloride is used to melt the ice formed on the surface. Using the hydraulic and osmosis pressure

theories, Powers explained that the scaling was primarily due to the destructive stress caused by hydraulic and osmotic pressures in the paste. As explained in the previous section, when freezing occurs in cement pastes, ice is formed within the capillary cavities. The cavities contain a dilute solution of water and dissolved materials, which at a sufficiently low temperature, will become partially frozen. Thermodynamic equilibrium is achieved by the migration of the solute ions, and the pure water to the frozen water, causing osmotic pressures to develop. When deicing salt is added to the pavement surface, some of the salt diffuses slowly into the concrete. Due to the low permeability of the cement-gel, the salt will build up in the capillary spaces rather than in the dense cement-gel resulting in an increased saturation of the concrete [22]. The high salt concentration in the cavity will increase the osmotic potential of water to flow towards the cavity to the salt solution, but at a given minimum temperature will produce less ice than before. The result is two contradictory effects. On the one hand, the reduction in ice causes a reduction in the pressure produced—either osmotic or hydraulic, as the capillary will not be taken up by the space of the ice; and on the other hand, it increases the maximum pressure that can develop, whether osmotic or hydraulic as there is more water flowing into the capillary. Powers also observed that chemically dissimilar materials such as alcohol, ethylene glycol, and urea have the same destructive effects, and that the maximum destructiveness was observed at deicing chemical concentrations of 4%. Based on this information, and supporting results by Verbeck and Klieger [67], Powers also concluded that the destructive effects of deicers were due primarily to physical rather than chemical actions.

Litvan [39] also expanded his previous frost damage theory to include the deleterious influence of deicing chemicals. By measuring the expansion of small rectangular specimens immersed in NaCl solutions of known concentration, the research demonstrated that specimens immersed in a 5% NaCl solution expanded more than those stored in stronger and weaker solutions. Litvan [39] hypothesized that this was due to the migration of pore water to the surface of the specimen during the cooling process. As the liquid approached the surface, the solution would crystallize, causing blockage at the end of the capillary channels leading to the external

surface. Subsequent flow from the interior would therefore be impeded resulting in the creation of a highly non-equilibrium situation and extremely large expansions. Litvan further concluded that the deicing agents cause a higher degree of saturation in concrete due to the decreased vapor pressure of the solution caused by the dissolved salts. Thus, the ambient water vapor will have a greater tendency to condense into a salt solution rather than water. In addition, the lower freezing point caused by the increased solute content would cause the water to migrate to the surface at lower temperatures, at which the viscosity of the solution may be quite high, and at which salt crystals may have already formed on the external surface. This would further impede the flow and diminish the frost resistance.

While the above theories account for many of the mechanisms of deicer scaling attack, several macroscopic models based on experimental results have been developed by investigators in order to explain specific scaling mechanisms observed in laboratory data [52]. Brown and Cady [10] proposed that two principle mechanisms of deterioration existed- one physical in nature, and the other chemical that accounted for the diverse observations of previous investigators. The physical mechanism was related to the deicer concentration gradient and hydraulic pressures. Because scaling is often in the form of small, flat flakes breaking away from the concrete surface, Brown and Cady hypothesized that the concentration of deicing solution in the concrete pores above the fracture plane was too high to produce sufficient freezing required for failure. However, below the surface, the degree of deicer concentration decreased, and the the formation of ice generated hydraulic pressures large to produce scaling in the form of flakes [10][52]. Brown and Cady determined that a chemical mechanism must exist because degradation occurred in concrete subjected to strong chloride solutions in their own experimental work as well as in previous research conducted by Neville [50].

Hansen [23] suggested that the growth of crystals in a concrete pore cavity could exert disruptive pressures causing scaling on the surface of the structure. It was hypothesized that repeated freeze-thaw cycles caused concrete to become supersaturated with a salt solution. Crystallization of the salts would initially take place in the the pores large enough to support

nucleation of the crystal. The growth of the crystals in the larger pores occurred when the solute ions in a surrounding solution migrated to the salt crystal, causing further growth. This enabled salt crystals to exert increasing pressure on the cement gel.

Though deicer salt scaling is now recognized as the most important frost problem in many countries, and there is extensive research and testing that has been initiated, much still remains to be learned concerning the fundamental mechanisms causing deicer salt scaling. The technical literature is still full of contradictions that cannot be readily explained [52]. It is likely that the increases in osmotic pressure, thermal stress, level of saturation, deicer concentration, and the other theories mentioned above, all play a role in deicer salt scaling. In combination, these mechanisms are far more damaging for concrete exposed to deicers when subjected to freeze-thaw cycles than without deicers [64].

2.4 Previous Research on Concrete Deterioration by Deicing Chemicals

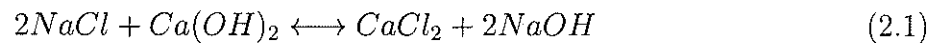
This section describes the previous research related to concrete deterioration caused by deicing chemicals used in the present investigation. Previous experimental work on the effects of sodium chloride, calcium chloride, magnesium chloride, and potassium acetate will be reviewed. The effect of corrosion inhibitors on concrete will also be discussed.

2.4.1 Sodium Chloride

The deterioration of concrete as a result of the application of sodium chloride is believed by many researchers to be primarily a physical rather than a chemical mechanism [1]. Early studies by Verbeck and Kleiger [67] showed that the maximum deterioration occurred when

an intermediate concentration of deicer salt was used. Verbeck and Kleiger [67] used chemically dissimilar materials which included sodium chloride, calcium chloride, ethyl alcohol and urea. Regardless of the deicing chemical, the relatively weak concentration caused greater deterioration than stronger solutions. Later studies by Powers [56], Litvan [39], and Brown and Cady [10] revealed similar results.

Recent investigations have indicated that while salt scaling is primarily a physical mechanism, there is evidence that chemical interactions may be occurring [64]. Suryavanshi [63] indicated that chloride intrusion reduces the total accessible pore volume and porosity, though the degree of reduction decreases with increasing w/c ratio. The reduction in pore volume is attributed to the formation of chemical products which partially block the coarser pores and converts them into finer pores. This is because the coarser pores have a larger internal pore wall surface area for nucleation compared to finer pores. As a result, the precipitates forming from the interaction between sodium chloride and cement will preferentially precipitate in the coarser pores. Heller et al. [27] observed that sodium chloride penetrating into the concrete transforms to calcium chloride by an ion exchange reaction with portlandite. The reaction is given as follows:



The reaction forms the compounds Friedel's salt, and calcium chloride, which are more voluminous compared to sodium chloride. Because the volume per mol of Friedel's salt and calcium chloride is 10 times and 2 times greater than sodium chloride respectively, the decrease in coarser pores may be due to the precipitation of Friedel's salt and calcium chloride rather than sodium chloride [63]. Suryavanshi [63], however, cautions that while the number of pores may be reduced in the outer layers, this does not likely enhance the overall durability of the concrete materials, and that resistance of concrete to chloride penetration is not solely related to pore structure alone.

2.4.2 Calcium Chloride

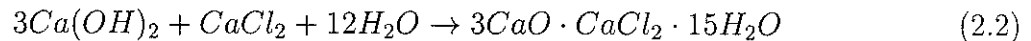
Many studies have indicated that attack by calcium chloride is not as chemically benign as believed by early investigators [10],[12],[13],[15],[50]. Colleparidi [15] explained that the chemical damage is often masked by the freeze-thaw deterioration that often occurs simultaneously in field concrete structures.

Neville [50] compared the behavior of concrete under the influence of strong and weak solutions using changes in frequency and weight as a measure of deterioration for several types of concrete mixes. Specimens immersed in a weak solution (5% $CaCl_2$ by weight) all showed an increase in weight throughout the testing period. Specimens immersed in a saturated solution, however, experienced a decrease in weight with the exception of specimens having a high water-cementitious materials ratio. In these specimens, there was a steady increase in weight despite observations of deep cracks and warping after exposure. Neville [50] concluded that the degradation of concretes with high water-cement ratios was the result of the deposition of crystals in voids previously occupied by water. The weight gain was due to the absorption of the ambient solution, which led to the formation of crystals. Because the specimens with low w/c ratios experienced exfoliation and eventual disintegration, Neville [50] hypothesized that the deterioration of specimens with low water-cement ratios was due to the compounds leaching out of the cement paste.

Progressive investigations have shown that when the chloride ions in an aqueous calcium chloride solution diffuses into cement paste, hydroxyl ions from the bulk cement paste diffuse towards the surface and combine with the Ca^{2+} ions in order to counter-balance the charge [63]. The reaction precipitates as portlandite ($Ca(OH)_2$). Chatterji [12] explains that continued diffusion of calcium chloride into the cement paste leaches the $Ca(OH)_2$ from the paste thereby leaving a coarser pore structure. The pores may be filled with new materials produced by the reaction between calcium chloride, calcium hydroxide, and carbonation. Cody et al. [13] observed that the growth of the newly precipitated salts produced expan-

sive pressures inducing fractures at the interface between the coarse aggregate and cement paste [13].

Collpardi et al. [15] further investigated the damaging mechanisms caused by exposure to $CaCl_2$ and observed that the damage mechanism described by Chatterji [12] is accompanied by the formation of hydrated calcium oxychloride. The reaction is given as follows:



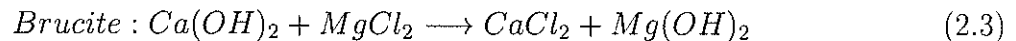
The formation of calcium oxychloride is an expansive physical action which causes a disruptive hydraulic pressure analogous to the pressures formed during ice formation [15].

More recently, Wang et al. [68] carried out a comparative study on evaluating the effects of sodium chloride, calcium chloride, corrosion inhibited calcium chloride, potassium acetate and an agri-deicing chemical on cement paste and concrete specimens. The damaging effects of deicing chemicals were evaluated on the basis of mass loss, scaling, compressive strength, and chemical penetration. Mass change measurements of concrete samples immersed in calcium chloride revealed that samples experienced a gain in mass until 30 freeze-thaw cycles (up to 60 cycles), and then began to lose mass with further cycles. Because this trend was similar in the paste samples, the authors hypothesized that the deterioration of the sample was related to the disintegration of the paste. Paste samples immersed in corrosion-inhibited calcium chloride solution experienced alternate mass loss and gain until 55 cycles whereby continuous mass loss occurred. The authors believed this inferred that the corrosion inhibitor postponed deterioration, but could not delay scaling once it occurred. The results also indicated that the rate of scaling of samples in the corrosion-inhibited solution was greater than for the solution without. Compressive strength tests for the calcium chloride samples showed that both concrete and paste specimens experienced dramatic losses in strength when compared to samples immersed in distilled water. The results showed that while the samples in the calcium chloride solution lost strength much earlier than the specimens in

the corrosion-inhibited solution, the overall strength was approximately the same at the end of the freeze-thaw cycles. This reinforced the idea that the corrosion inhibitor delayed the onset of deterioration, but did not diminish damage once it began [68]. Scaling of samples in both solutions was also very severe at the end of the cycling period. Ion penetration tests showed that for a given depth, both the pure calcium chloride and corrosion-inhibited calcium chloride solutions had over two times the chloride content than sodium chloride. Both deicers had a much higher chloride concentration for a given depth than the other deicing chemicals. This agrees with the results of the compressive strength and scaling tests which demonstrated that deterioration by calcium chloride was most severe.

2.4.3 Magnesium Chloride

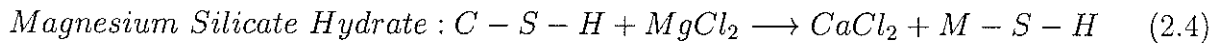
During recent years, there has been an increased interest in deicing chemicals other than sodium chloride as a result of environmental and corrosion concerns [44]. Consequently, the use of magnesium chloride has increased. Research on magnesium chloride has shown that its effect on concrete is not as benign as once was believed. When magnesium chloride is applied onto concrete it is not chemically innocuous. Ftikos and Parissakis [21] demonstrated using high resolution scanning electron microscopy (SEM) that the presence of Mg^{2+} and Cl^{-} ions in cement reacted with the major hydration products in the cement paste. The magnesium (Mg^{2+}) ions reacted with portlandite ($Ca(OH)_2$) to produce the non-cementitious material magnesium hydroxide (brucite). The reaction is given as follows:



According to Kleinlogl [31], the formation of magnesium hydroxide provided a protective film which could temporarily delay the onset of deterioration. However, as the protective film of magnesium hydroxide was washed away, new concrete surfaces were exposed to attack, and the cumulative effect acted to destroy the concrete. Furthermore, precipitation of brucite

minerals within concrete is potentially an expansive reaction, which may lead to de-bonding of the aggregate between the paste-aggregate interface [13], [14], [35], [64].

The accumulation of the chloride (Cl^-) ions in the cement paste reacted with calcium silicate hydrate (C-S-H) to form extremely porous calcium silicate hydrate and magnesium silicate hydrate (M-S-H). The equation is given as follows:



Lee et al. [34], observed that the formation of magnesium silicate hydrate in cement pastes caused severe crumbling of the paste and debonding of the aggregate particle. A comparative study by Cody and Spry [13] also demonstrated that concrete deterioration was most severe when magnesium chloride solutions were used. In their case, deterioration was observed in the form of brownish discoloration and severe crumbling. The authors believed that the chemical reactions between magnesium chloride and the concrete-aggregate paste involved both replacement and dissolution reactions with different concrete phases, and precipitation of new mineral phases in cracks and voids. Furthermore, the precipitation of the minerals likely produced crystal growth pressures which result in concrete expansion and destruction.

2.4.4 Potassium Acetate

A review of literature revealed very little research carried out on the effects of potassium acetate on concrete. A recent comparative study was carried out by Wang et al. [68] evaluating the performance of potassium acetate with respect to sodium chloride, calcium chloride, corrosion-inhibited calcium chloride, agri-deicing chemical, and distilled water. The damaging effects of deicing chemicals were evaluated on the basis of mass loss, scaling, compressive strength, and chemical penetration. Mass change measurements of concrete samples immersed in potassium acetate showed that the samples gained, rather than lost mass while

undergoing freeze-thaw cycles. Because it was observed that the samples experienced a slight degree of scaling, the authors hypothesized that the expected loss in mass from scaling was off-set by absorbed water and possible salt crystallization [68]. Compression tests carried out at every 20 cycles (up to 60 cycles) revealed very little strength loss throughout the cycling period. The chemical penetration of the deicers were evaluated on the basis of ion penetration tests. The authors presumed that the rate and depth of the chemical ion penetration was related to the degree of damage resulting from the reaction between concrete and deicing chemicals. Potassium profiles in the samples exposed to potassium acetate revealed that potassium levels were high in the surface layer, but decreased rapidly with depth from the concrete surface. Wang et al. [68] hypothesized that the reaction between the potassium acetate and the paste may only occur on the surface, resulting in only minor scaling damage.

2.4.5 Corrosion Inhibitors

In recent years, the use of corrosion inhibitors within deicing chemicals has become more frequent. The corrosion-inhibited deicing chemicals considered in this investigation are considered to be organic inhibitors. Vaysburd et al. [66] describes the primary function of a corrosion inhibitor as a chemical compound that checks, decreases, or prevents the reaction of steel with the surrounding environment. Corrosion inhibitors can be mixed directly within fresh concrete, or applied on the surface of existing concrete structures. Recent deicing chemicals such as those considered in this investigation have incorporated the action of an organic inhibitor directly within the deicer. Materials such as triethanolamine (TEA), corn products, or agricultural by-products have all been known to be used in commercial deicing chemicals as organic corrosion inhibitors [19]. Mindess [47] states that organic corrosion inhibitors reduce the permeability of concrete, thus limiting the access of oxygen and moisture to the reinforcement. Consequently, the ingress of chloride ions is also reduced. Very little research has been carried out on the effects of corrosion-inhibitors present in deicing chemicals on hardened concrete. As mentioned in the previous section, the study by

Wang et al. [68] indicates that the corrosion inhibitors may delay the onset of deterioration, but cannot reduce the severity of damage once it began.

2.5 Considerations for the Experimental Program

Verbeck and Kleiger [67] demonstrated that the laboratory procedure used to evaluate salt scaling significantly impacts the results obtained. In this section, the considerations related to experimental procedure are reviewed based on observations of past researchers. These factors include the requirement of free liquid on the surface of the sample in order for scaling to occur, and the increased damage caused by freeze-thaw cycles with a lower minimum temperatures [65],[36].

2.5.1 Importance of Free Liquid on Surface

Verbeck and Kleiger's study [67] showed that when samples did not have liquid present on the surface, scaling did not occur. In their study, three different procedures were tested. In the first procedure, specimens were frozen with pure water on the surface with a solution applied immediately onto the ice before thawing. In the second procedure, specimens were frozen and thawed with a salt solution applied onto the surface. In the third procedure, the specimens were frozen in a damp condition with deicing solution applied during the thawing cycle. Results of the experiment revealed that almost no scaling occurred when the third procedure was used. Sellevold [60] and Studer [62] have also observed that when the salt solution is missing due to leakage at the edges of the specimen, scaling of the specimen ceases to occur. Lindmark [36] believes that this indicates that outer moisture must be present in order for scaling to occur. Because these "saturation" conditions are largely unknown during natural frost cycles, Studer [62] presumes that the tests conducted in the laboratory represent

the most severe condition in that respect. However, in natural conditions, structural concrete is subjected to 50-100 times more freeze-thaw cycles than in the tests [62].

2.5.2 Minimum Temperature

Several investigations have demonstrated the increased damage caused by freeze-thaw cycles with lower minimum temperatures. Sellevold [60] demonstrated that less deterioration occurred at a minimum freezing temperature of -10°C than at -20°C . He pointed out that this is because the minimum temperature determines the amount of ice formed in a specimen regardless of the damage mechanism. Studer [62], however demonstrated that the effect of minimum temperature was not linear, with the effect being more severe at temperatures close to -18°C than at -13°C . Thus, according to Studer [62], the choice of a moderate minimum temperature in laboratory tests is supported then, by the fact that down to this value, the assumption of the linear effect of temperature on the amount of scaled-off material is more reasonable, and hence the extrapolation of the test results to the behavior of structural concrete under natural frost cycling appears more reasonable. Petersson [51] further investigated the effect of minimum temperatures, and conducted tests at temperatures as low as -24°C . Petersson's results showed that the lower the minimum temperature, the higher the scaling. However, the influence was much smaller and almost negligible after scaling exceeds $100\text{-}500\text{ g/m}^2$ and the temperature is below -18°C .

2.6 Methods of Detecting Deterioration

“Diagnosis of deterioration depends on the inferences which may be drawn from the measurements. The evidence provided from several measurements may provide a set of inferences which together are of considerable help in picturing the nature of the attack” [32]. A common

measurement of deterioration used in many studies is a measure of weight [32],[50],[58],[68]. Changes in weight of a specimen indicate several things. An increase in weight in an unsaturated specimen may be caused by the absorption of water or of ambient solution. A larger increase in weight may indicate that the absorbed liquid has a greater density than water. It may also indicate that crystals which are generally more dense than liquid are forming in the specimen and adding to the total specimen weight [32],[50]. If crystals cause expansion and open cracks, the ingress of liquid into the new space may cause more crystal deposition and further weight gain. A decrease in weight generally indicates hydrated cement compounds are being leached from the mortar and the binder material is dissolving [32]. As this progresses, sand grains, insoluble reaction products, and debris may deposit in the bottom of the container.

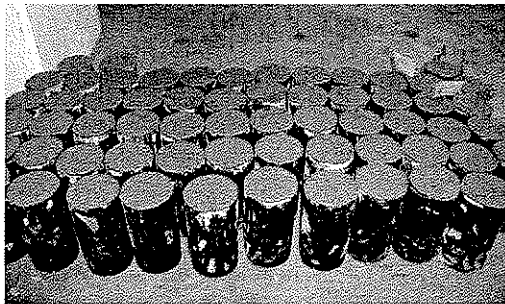
A common test method of assessing deicer salt scaling resistance is ASTM 672C Standard Test Method for Scaling Resistance of Concrete Surfaces Exposed to Deicing Chemicals [41]. This procedure qualitatively evaluates the salt scaling resistance of concrete using a visual examination to assess the degree of deterioration of the tested specimens. Despite the detailed guidelines given in the standard, the visual rating is often considered to be subjective and closely dependent on the type of surface tested [41]. To compensate for this, many laboratories also collect and weigh the scaled off particles at regular intervals in order to improve the reliability of the test. For this investigation, the mass of scaled-off particles is also collected and weighed to be used in conjunction with the visual inspection as a measure of deterioration.

Chapter 3

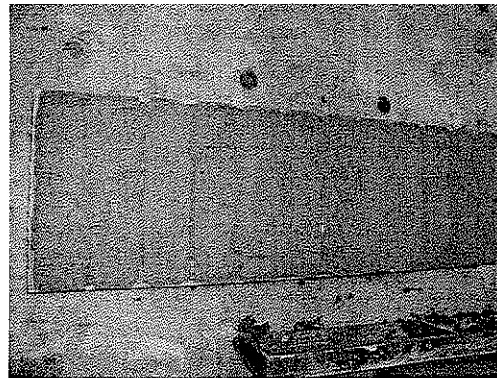
Experimental Program

3.1 Overview

To determine the destructive effects of various deicing chemicals used or considered for use by the industry on concrete surfaces, an experimental program was undertaken at the University of Manitoba. A total of 110 concrete cylinders, 10 prisms, and 12 reinforced concrete beams were exposed to four deicing chemicals including sodium chloride, corrosion-inhibited calcium chloride, corrosion inhibited magnesium chloride, and potassium acetate. The specimens were also subjected to freeze-thaw cycles ranging from $-25^{\circ}\text{C} \pm 3^{\circ}\text{C}$ to $23^{\circ}\text{C} \pm 2^{\circ}\text{C}$. In addition, 8 concrete cylinders were submerged in deicing chemicals and exposed only to laboratory air. Concrete deterioration was evaluated on the basis of mass loss or gain. The performance of the deicing chemicals with respect to scaling resistance was evaluated on the basis of ASTM 672C and mass of scaled-off particles. The changes in the mechanical properties of concrete were evaluated in terms of loss of tensile, compressive and flexural strength, and changes in the static modulus of elasticity. A test to determine the quantity of free chlorides in hardened concrete was also carried out by National Testing Laboratories



(a) Concrete Cylinders



(b) Concrete Prisms

Figure 3.1: Casting of Concrete Cylinders and Prisms

to evaluate the chemical penetration of corrosion-inducing chlorides present in the concrete.

3.2 Test Samples

The samples used in the experimental program are summarized in Table 3.1.

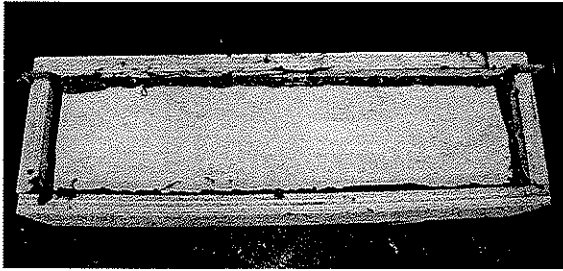
A total of 110- 102mm x 203mm (4" x 8") cylinders were fabricated for the experimental program. Figure 3.1(a) illustrates the concrete cylinders at the time of casting. The cylinders were removed from their molds after 48 hours and moist cured for 14 days in a curing room which met the requirements of ASTM C511 [3]. After 14 days, the cylinders were removed from the moist storage and stored in air for 14 days at room temperature. A thermocouple was inserted into the center of five cylinders so that the core temperature of the cylinders could be measured during the testing procedure.

Ten prisms were fabricated to carry out the scaling resistance tests described in the next section. The prisms were 110mm wide x 100mm deep x 440mm long. The dimensions were chosen to ensure that the surface area was at least 0.045 m^2 (75 in^2) and the depth was a

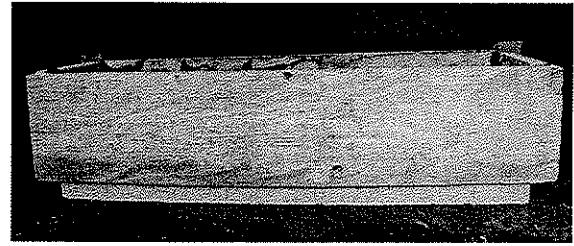
Table 3.1: Experimental Program

Sample	Deicer	No. of Samples	No. of Cycles	
Cylinders	Sodium Chloride	10	50	
		10	100	
	Calcium Chloride	2	None	
		10	50	
	Magnesium Chloride	10	100	
		2	None	
	Potassium Acetate	10	50	
		10	100	
	Distilled Water	2	None	
		10	50	
	Control	10	100	
		6	N/A	
	Total		118	
	Prisms	Sodium Chloride	2	100
Calcium Chloride		2	100	
Magnesium Chloride		2	100	
Potassium Acetate		2	100	
Distilled Water		2	100	
Total		10		
Beams	Sodium Chloride	2	100	
	Calcium Chloride	2	100	
	Magnesium Chloride	2	100	
	Potassium Acetate	2	100	
	Distilled Water	2	100	
	Control	2	N/A	
Total		12		

minimum of 75mm (3 in) as specified in ASTM 672C-98 [2]. Figure 3.1(b) illustrates the casting of the prisms in their formwork. The prisms were removed from their formwork after 4 days. They were then placed in the curing room with the cylinders and moist cured for 14 days. Afterwards, they were stored in air for 14 days at room temperature. Once the prisms were cured for 28 days, a plywood dam was built around the perimeter of the prism in order



(a) Application of Sealant



(b) Plywood Dam

Figure 3.2: Preparation of Concrete Prisms for Application of Deicing Chemicals

to contain deicing solution on the top surface of the block. The dam was glued onto the sides of the concrete prism using Devcon 2 Ton epoxy®, which was chosen for its flexibility at low temperatures. Crafcro Roadsaver 522™ was applied to the concrete-plywood perimeter along the top surface to seal the crack along this barrier. The application of deicing chemicals is described in further detail in the next section. The prisms and the dam were built in accordance to ASTM 672C-98 [2]. Figure 3.2 illustrates the prism with the plywood dam built along its perimeter.

Twelve rectangular reinforced concrete beams were cast to carry out the flexural strength portion of the experimental program. The beam cross-section was 100mm wide, 200mm deep and the beam was 1200mm in length. A cover of only 20mm was provided to accelerate the chloride penetration to steel and facilitate the on-set of corrosion. Two 10M steel reinforcing bars were used as tensile reinforcement with an effective depth of 169mm. Figure 3.3 illustrates the cross-section and reinforcement details.

The beam was designed for both flexure and shear in accordance to CSA A23.3-04. Twelve 6M steel stirrups spaced at 100mm were provided to ensure that the beam failed in flexure not in shear during the three-point bending test. Details of this test are described in later sections. Figure 3.4 illustrates the casting of the beam.

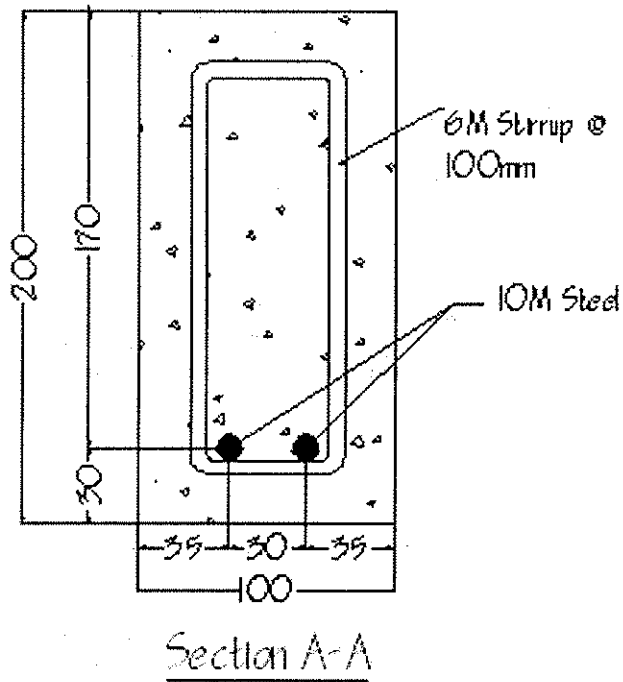
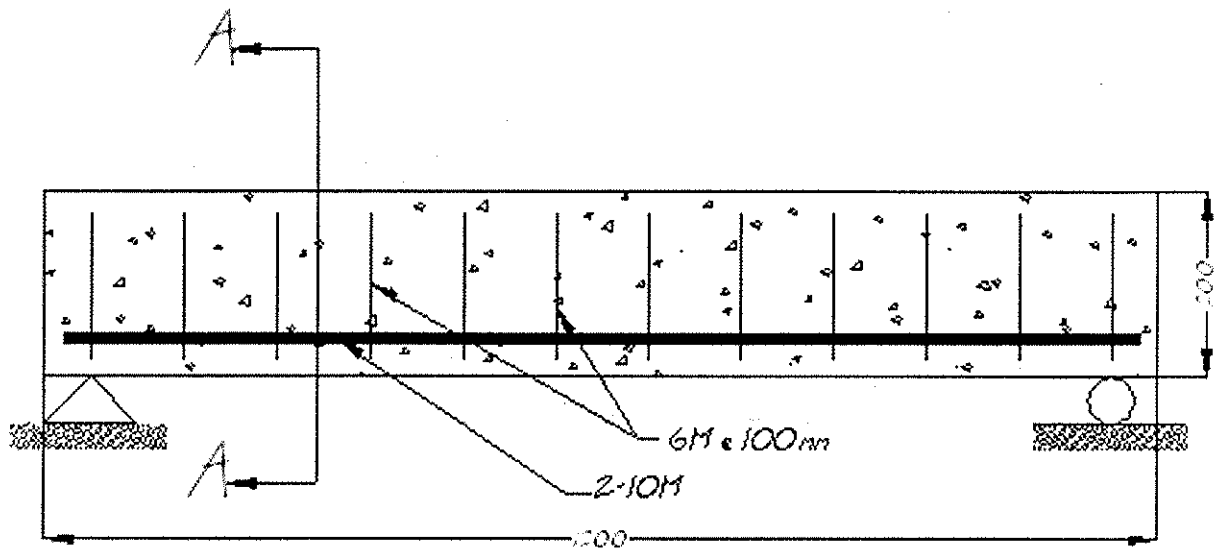


Figure 3.3: Beam Geometry (All Dimensions in mm)

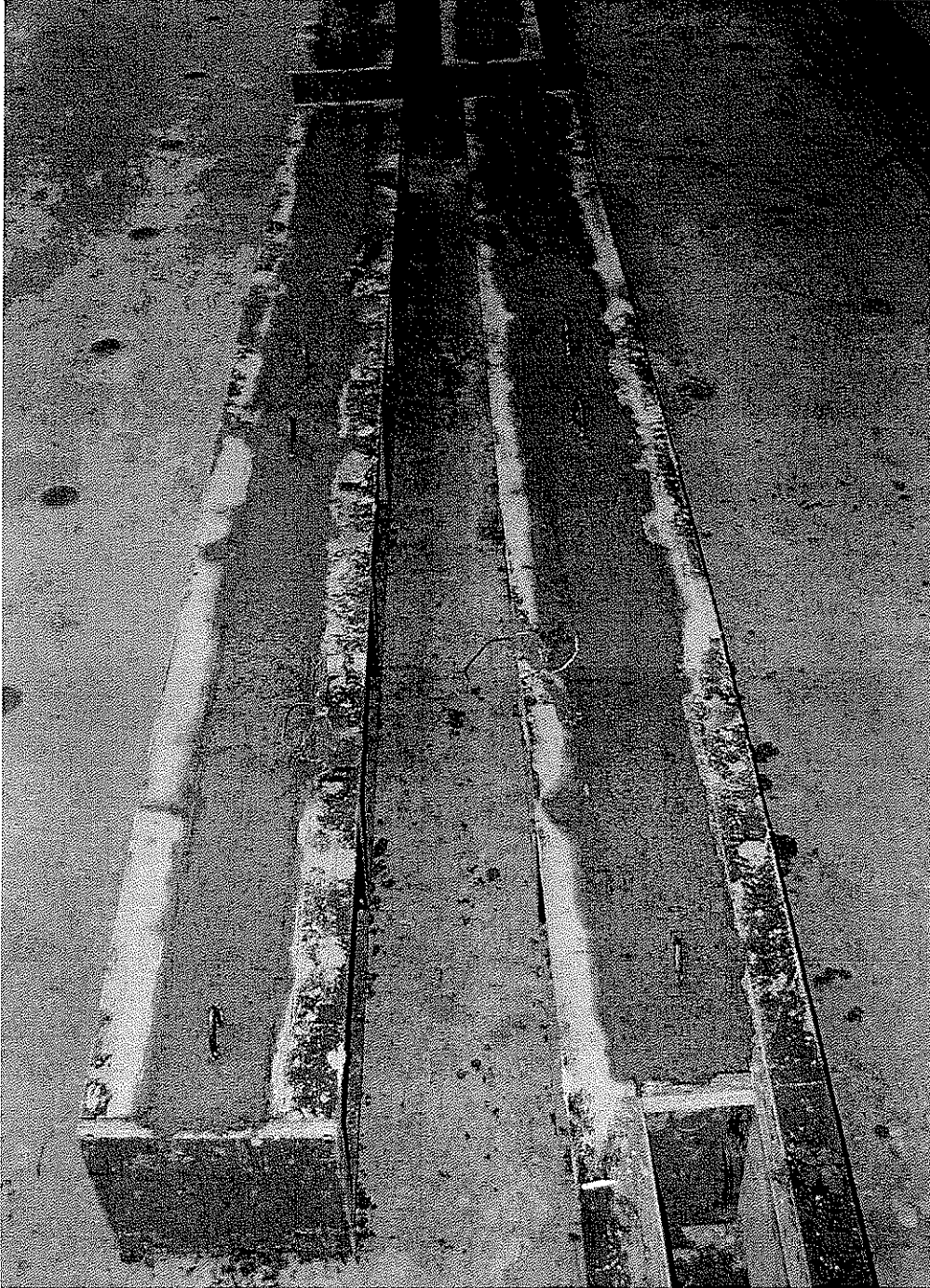


Figure 3.4: Casting of Reinforced Concrete Beams

3.3 Testing Materials

3.3.1 Deicing Chemicals

The deicing chemicals selected for this investigation were sodium chloride, corrosion-inhibited calcium chloride, corrosion-inhibited magnesium chloride (ICE-BAN 200M), and potassium acetate and were received directly from the suppliers. As mentioned previously, the deicers were chosen for their wide applications and potential industry considerations. The sodium chloride was obtained in liquid form as a 23% brine solution. The magnesium chloride deicer consisted of 29-31% magnesium chloride in water, and a corrosion inhibitor to reduce the damaging effects of corrosion. The corrosion-inhibitor was derived from corn by-products containing residue of fermented and distilled agricultural by-products including cane, beet sugar syrup, corn, barley, and other carbohydrates [19]. The calcium chloride solution was a 32% aqueous solution with an organic corrosion inhibitor. A 50% (by weight) aqueous potassium acetate solution was used in the investigation.

3.3.2 Concrete

Non-air entrained, Portland Cement Concrete was cast at Lafarge Canada on August 20, 2005 and transported to the University of Manitoba for fabrication of specimens. The use of a non-air entrained mix facilitated the achievement of scaling damage in a relatively short time period. This corresponds with specimen preparations carried out by other investigators [10], [61]. The order specified 25 MPa concrete with 80 mm slump. The same batch of concrete was used to cast all cylinders, prisms, and reinforced concrete beams. Detailed mix design was not provided to us by Lafarge Canada.

3.4 Freeze-Thaw Cycling

In this phase of the testing program, the concrete specimens were exposed to a combination of freeze-thaw cycles and deicing chemicals. The deterioration of prism and cylinder specimens were evaluated based on the degree of scaling and mass loss respectively. The changes in the tensile, compressive, and flexural strength as a result of this exposure condition were determined in the next phase of the experimental program.

3.4.1 Temperature Regime

After the concrete had reached an age of 28 days, all of the specimens were placed in a walk-in environmental chamber in order to undergo freeze-thaw cycling. The beams were positioned on top of large plywood planks with sheets of plastic placed underneath the wood members to capture the excess deicing chemicals sprayed on the beams and protect the chamber floor. The containers holding the concrete cylinders were placed along the side of the chamber to allow the thermocouple wires connected to selected cylinders to reach the Data Acquisition System (DAQ) located behind the chamber. The concrete prisms were placed near the front of the chamber. Figure 3.5 illustrates the layout of the specimens inside the chamber. The arrangement allowed for a walkway between the specimens so that the prisms could be moved in and out of the chamber, and that the beams and cylinders could be accessed during the cycling time.

The temperature during the first 50 cycles ranged from $-18^{\circ}\text{C} \pm 3^{\circ}\text{C}$ to $23^{\circ}\text{C} \pm 2^{\circ}\text{C}$. After 65 cycles, the minimum temperature was decreased to -25°C in order to accommodate other users of the chamber. Based on previous results by Peterson [51], the dependence of scaling on minimum temperature is more or less negligible when the minimum temperature is below -18°C to -20°C and the scaling exceeds $100 - 500\text{g}/\text{m}^2$. Since mass of scaled materials exceeded $100\text{g}/\text{m}^2$ for all deicing chemicals, the decrease in the minimum temperature was



Figure 3.5: Arrangement of Specimens in Chamber

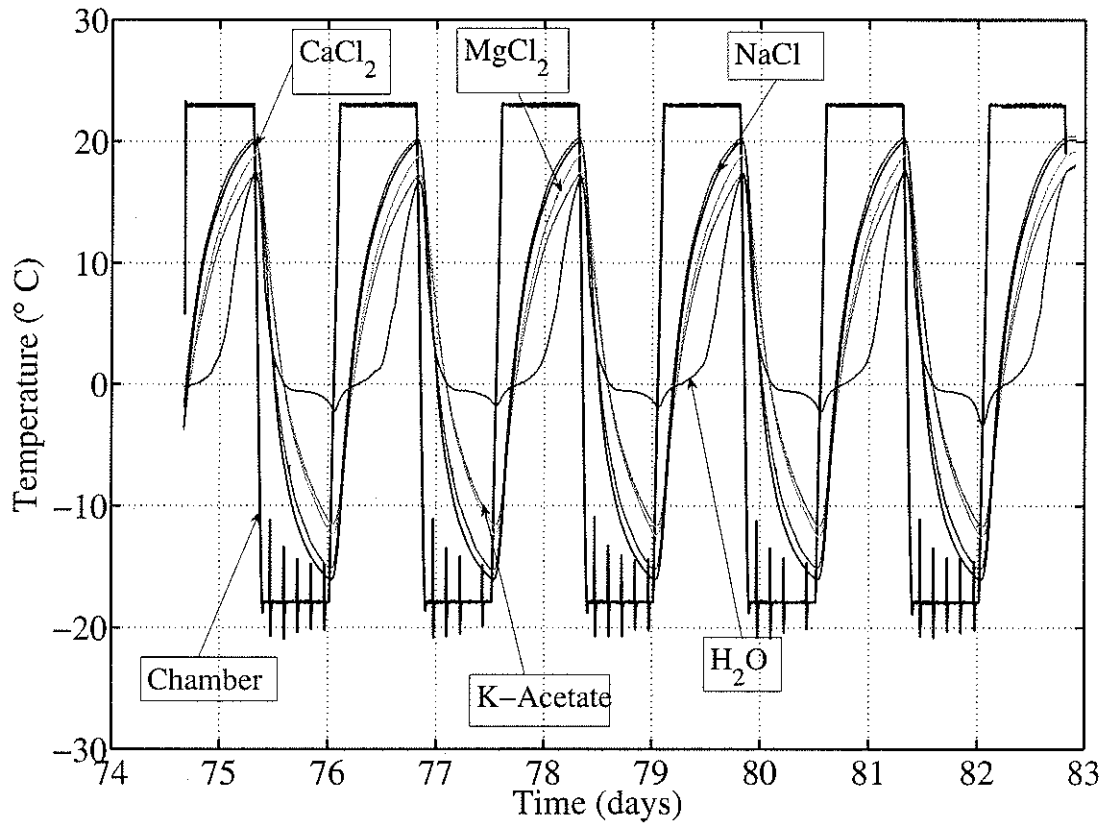


Figure 3.6: Temperature Readings -18°C to 23°C

believed not to affect the experimental results. Each cycle was approximately 36 hours long. The freezing portion of the cycle was 17 hours and the thawing portion of the cycle was 19 hours. The length of each freeze-thaw cycle was longer than the time recommended by the standard so that the temperature measured by the thermocouple inside of the sample was close to the temperatures measured by the chamber sensors and the recommended temperature range in the ASTM standard [2]. Typical chamber temperature readings are illustrated in Figure 3.6 and Figure 3.7.

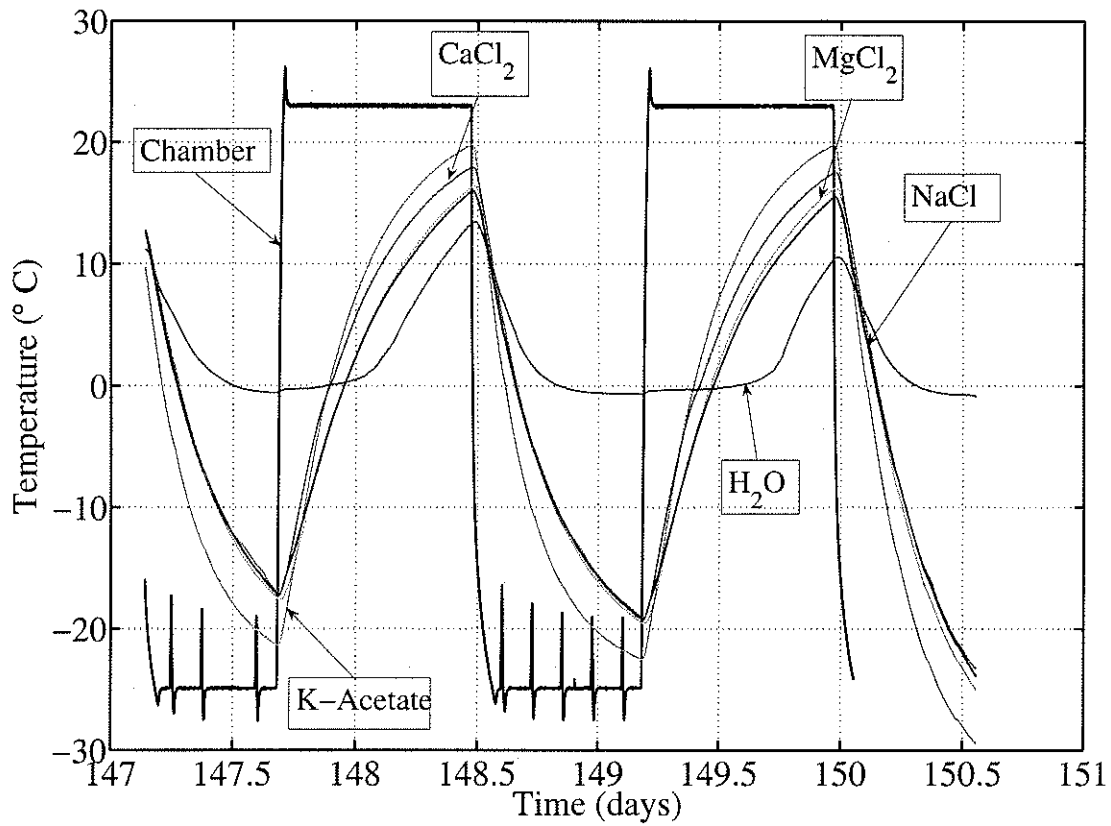


Figure 3.7: Temperature Readings -25 °C to 23 °C

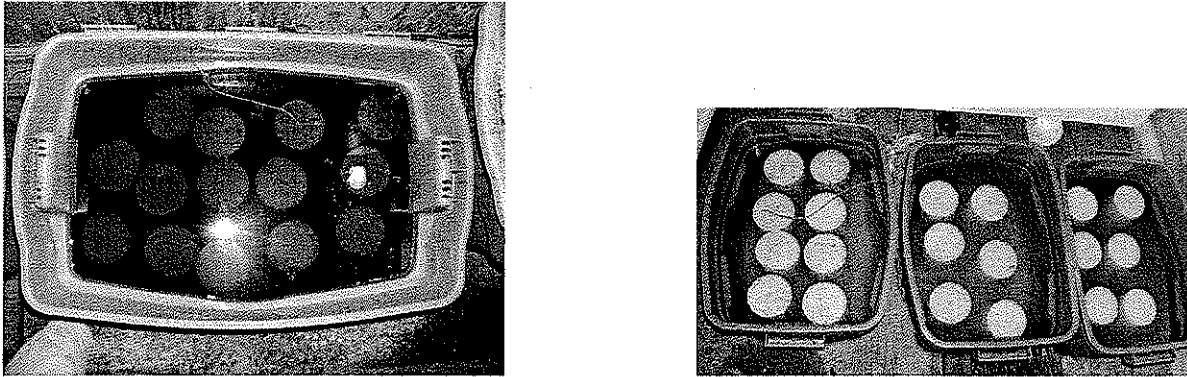


Figure 3.8: Concrete Cylinders in Submerged in Deicing Chemicals

3.4.2 Concrete Cylinders

The cylinders were submerged in a deicing solution and subjected to the alternating freeze-thaw cycles described in the above section. A distilled water solution was also used to evaluate the effect of freeze-thaw cycles without deicing chemicals and to be used as a comparison to the deicing chemical solutions. Figure 3.8 illustrates the method of submersion. To monitor the deterioration experienced by the cylinders during the freeze-thaw cycling, the weight of the saturated-surface dry samples was determined. The saturated weight of the cylinders was measured every 10 cycles beginning at the 10th cycle. In order to determine the weight, the specimens were taken out of the deicing solution and weighed after drying the surface with a clean piece of cloth.

Each deicing and distilled water solution had a cylinder with a thermocouple inserted in the center to ensure that the temperature of the cylinders matched the air temperature in the chamber. The temperatures of the cylinders were monitored using a Data Acquisition System (DAQ) which recorded all of the temperature data. Figure 3.6 shows the temperature readings for both the thermocouples and the chamber from 44 cycles to 50 cycles. The fluctuations in the freezing portion of the the chamber temperature plot are the result of the coils defrosting during the freezing process. These readings are representative of the

typical temperature readings obtained for the initial 50 cycles. As illustrated in the figure, the temperature in the cylinders submerged in deicing solution were sufficiently close to air temperature measured by the chamber sensors. The freezing temperature in the distilled water specimens however, did not reach the minimum air temperature in the chamber. During the freezing portion of the cycle, the plot reveals that the temperature in the water remained constant just below 0°C for approximately 4 hours, and then decreased to a minimum temperature of approximately -4°C . This is because during freezing, the energy in the system is spent on changing the state of matter and not on the temperature. Only when all of the water has been converted to ice will the temperature begin to drop. A longer freezing period would have allowed the minimum water temperature to reach that of the chamber. The temperature readings from 78 to 80 cycles are illustrated in Figure 3.7. As with the previous plot, these readings represent the typical temperature data for the final 50 cycles. The readings are similar to those in the initial 50 cycles, with sufficiently close comparisons between the air temperature and relatively constant water temperature readings during the freezing portion of the cycle.

3.4.3 Concrete Prisms

The top surfaces of the prisms were covered in approximately 6mm of deicing solution. Two prisms were used for each deicing chemical. Two specimens covered with distilled water only were also prepared for comparison purposes. All of the specimens were then placed in the environmental chamber to undergo freeze-thaw cycling. The levels of the solution were checked everyday to ensure the surfaces had approximately a 6mm layer of solution. Deicing solution was added as necessary to maintain the solution level at this depth. At the end of every five cycles, the deicing solution was flushed off the concrete surface and poured through a filter. The materials collected in the filter as a result of freeze-thaw damage were rinsed with distilled water and allowed to air-dry. The mass of the material was recorded to be used as a measure of damage. Figure 3.9 illustrates the filter apparatus. The specimens

Table 3.2: Visual Rating Scheme for Scaling Resistance

Rating	Surface Condition
0	No Scaling
1	Very slight scaling (1/8-in maximum depth, no coarse aggregate visible)
2	Slight to moderate scaling
3	Moderate scaling
4	Moderate to severe scaling
5	Severe scaling (coarse aggregates visible over entire surface)

were also visually graded at this point on a scale of 0-5 using a visual rating scheme adopted from ASTM 672C-98 [2]. Table 3.2 summarizes the grading scheme.

3.4.4 Concrete Beams

The surface of the beams was sprayed with deicing chemicals every 2.5 cycles using a polyethylene sprayer until the entire surface was saturated with the deicing solution. Two beams were used for each type of deicing chemical. A distilled water solution was also used as comparison. The flexural strength of the beams was determined after 100 cycles.

3.5 Continuous Immersion

In order to determine the effect of deicing chemicals in the absence of freeze-thaw cycles, 8 concrete cylinders were stored in containers containing deicing solution and exposed only to laboratory air. The test samples were submerged in deicing solution for 6 months, which was the same duration of time as the specimens in the environmental chamber. The change in mass was recorded throughout the test period, and the samples were placed on a palette and allowed to dry for 26 days before the compressive strength was determined.

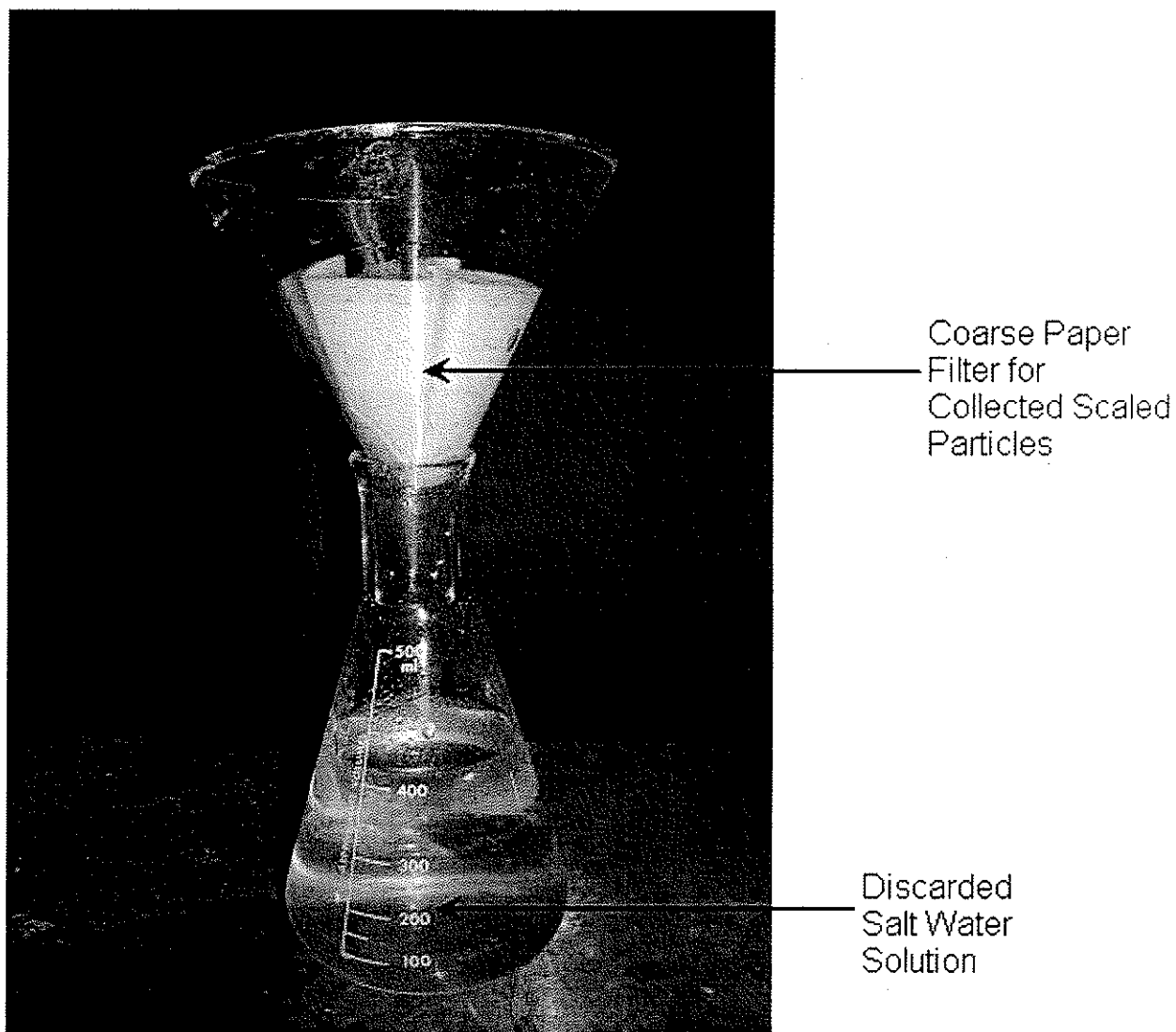


Figure 3.9: Filtering Apparatus

3.6 Compressive Strength Tests

After 50 and 100 freeze-thaw cycles were completed, 25 concrete cylinders (5 cylinders per deicing solution) were removed from the environmental chamber in order to be tested for compressive strength. The specimens were placed on a palette in the laboratory until testing. The specimens were weighed after 12 days and 26 days after removal from the chamber in order to determine the net mass loss or gain in the specimens. The test was carried out after 26 days. Three control cylinders not exposed to either freeze-thaw cycles or deicing solution were also tested in order to compare the strength of the cylinders.

Before testing began, the cylinders were capped with a sulphur mortar cap using the procedure described in ASTM C 617 [4]. The cap ensured that an even surface was obtained between the cylinder and the upper and lower bearing blocks on the compression testing machine. The test was carried out using a compression testing machine that met the requirements specified in ASTM C39-M [5]. A load rate of 1216 N/s to 2837 N/s was specified in the standard and used for the test. Figure 3.10 illustrates the compression testing machine.

3.7 Tension Tests

After 50 and 100 cycles, 15 cylinders were removed from the chamber and a splitting tension test was carried out. The splitting test specimens were placed with the compression test specimens on a laboratory palette and allowed to air dry until testing occurred. The cylinders were weighed after 12 and 26 days after removal from the chamber in order to determine the net loss or gain in mass in the specimen. The test was carried out after 26 days using the compression testing machine. A load rate of 689 to 1380 kPa/minute was specified in ASTM C 496-96 [6] and was used for the test. In order to carry out the splitting test, the cylinder



Figure 3.10: Compression Testing Machine

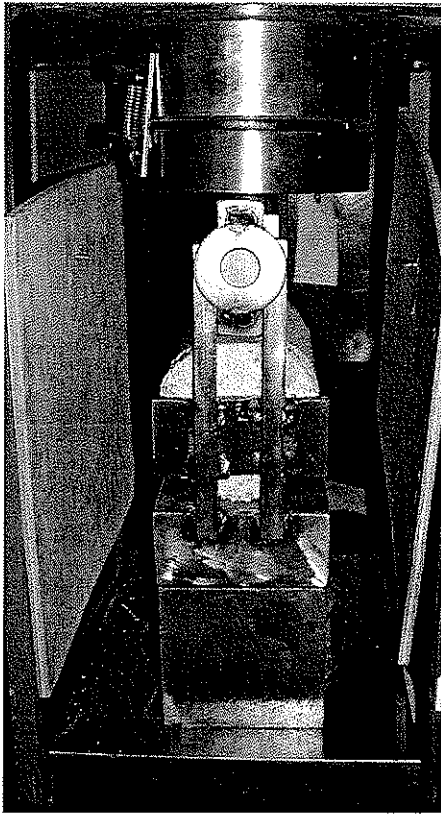


Figure 3.11: Position of Aligning Jig Under Crosshead

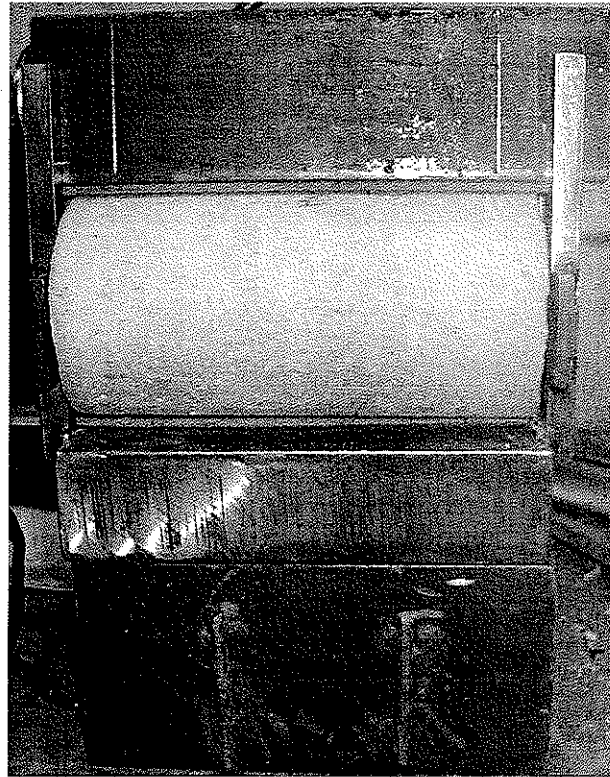


Figure 3.12: Aligning Jig

was placed on its side and positioned under the crosshead of the testing machine using an aligning jig centered under the cross head. A compressive force was applied along its length which induced high transverse compressive stresses at the top and bottom of the cylinder, and uniform tensile stresses across the rest of the diameter [40]. Figures 3.11 and 3.12 illustrate the tension test set-up and the aligning jig.

3.8 Modulus of Elasticity

After 50 and 100 cycles, a test to determine the static modulus of elasticity was carried out. 5 cylinders were removed from the chamber (one for each deicing chemical and distilled water) and placed with the tension and compression test specimens on a laboratory palette to air dry until the test was carried out. As with the previous specimens, the cylinders were weighed after 12 and 26 days after removal from the chamber in order to determine the net loss or gain in mass in the specimen. One cylinder not exposed to any environmental conditions was used as a control sample.

Before testing began, a 50mm strain gauge was attached length-wise to the side of the cylinder at the center using an adhesive. A wire was soldered onto the leads of the strain gauge in order to connect the strain gage to the Data Acquisition (DAQ) system and monitor the strain in the concrete during the test. A sulphur mortar cap was placed on the top and bottom surfaces of all test specimens to ensure an even loading surface was obtained between the concrete and the top and bottom bearing blocks. The test was carried out using a 1000kN capacity servo-hydraulic testing machine. A compressive load was applied to the cylinder until failure occurred. A 0.5 mm/minute load rate was used because it corresponded approximately to a load rate of 1000-2000 N/s which was used in the compression test. The load was applied continuously until failure occurred. Figure 3.13 illustrates the testing layout.

3.9 Flexural Strength Tests

After 100 cycles, the flexural strength tests on the beam specimens were carried out at W.R. MacQuade Structural Laboratory, at the University of Manitoba. The beams were simply supported at each end with the roller supports positioned so that the test span was 1m.

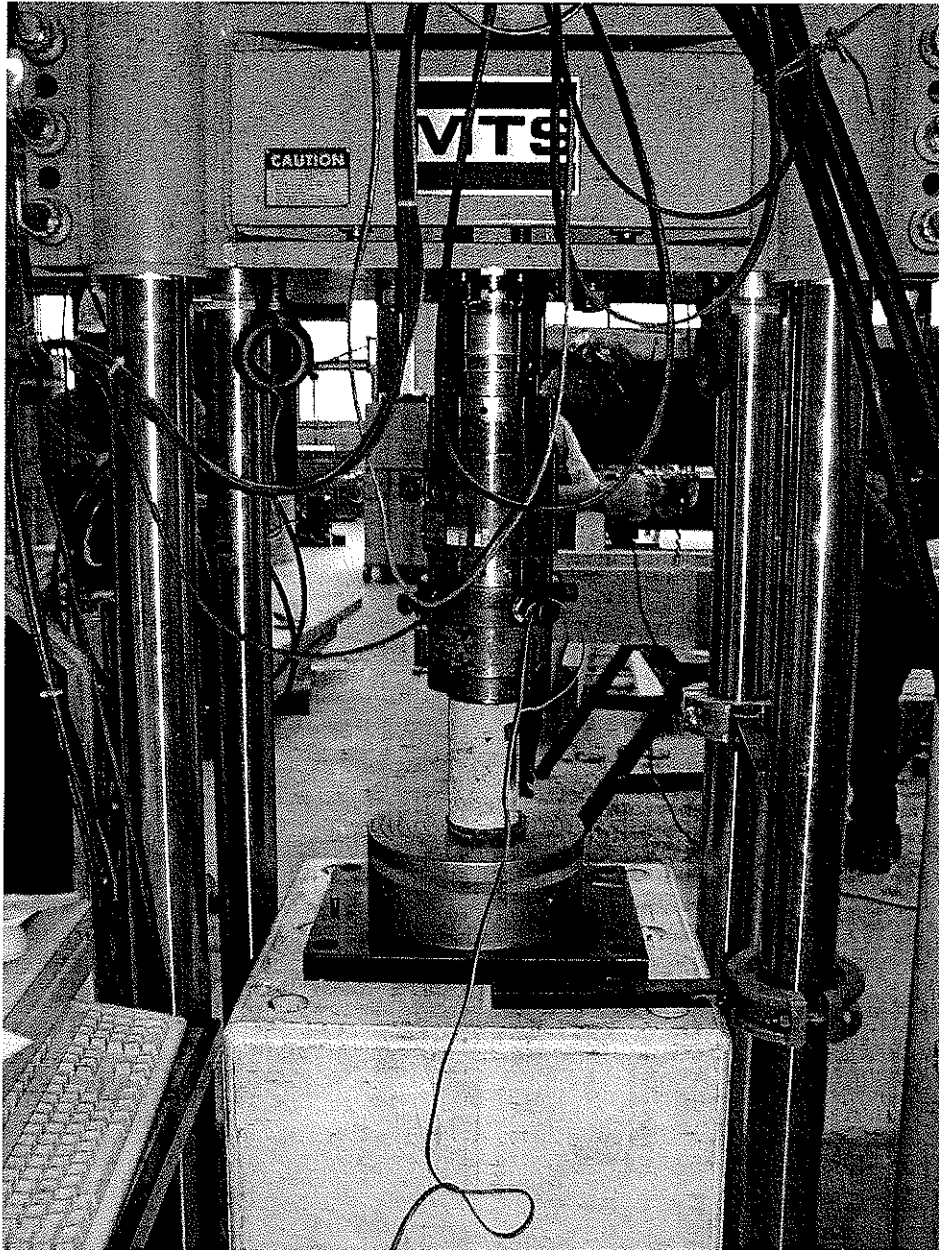


Figure 3.13: Static Modulus Test

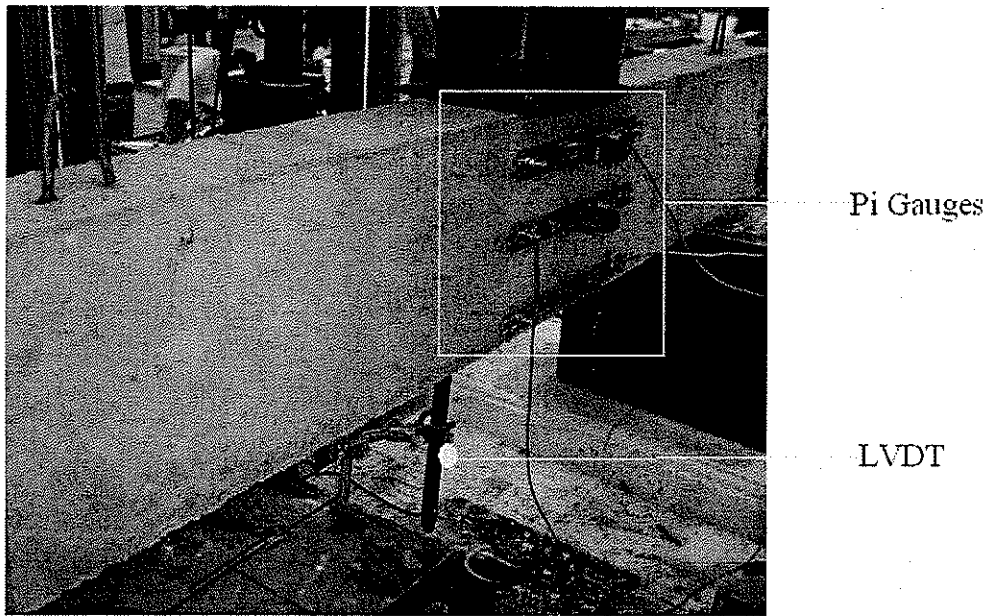


Figure 3.14: Beam Instrumentation

Before each test, the beams were instrumented so that the deflection and strain could be monitored during the test. Deflections were monitored using a Linear Variable Displacement Transducer (LVDT) that was placed at the point of maximum deflection at the mid-span of the beam. Three 200mm pi gauge transducers were placed under the load point at 175mm, 100mm, and 35mm from the bottom of the beam. This allowed the concrete strain at these levels to be monitored during the test. A strain gage was also attached onto the reinforcing bar during casting to monitor the strains in the steel. Figure 3.14 illustrates the beam instrumentation. The locations of the pi gages and LVDT on the beam are represented schematically in Figure 3.15.

Both the LVDT and the pi gage transducers were calibrated before the start of the test using a micrometer and the DAQ system. The LVDT or pi gage was attached length-wise to a micrometer that displaced the shaft of the transducer in small increments. The transducer was connected to the DAQ and the voltage change required to calibrate the gauges was recorded. The DAQ was also used during the test to record all of the readings from the

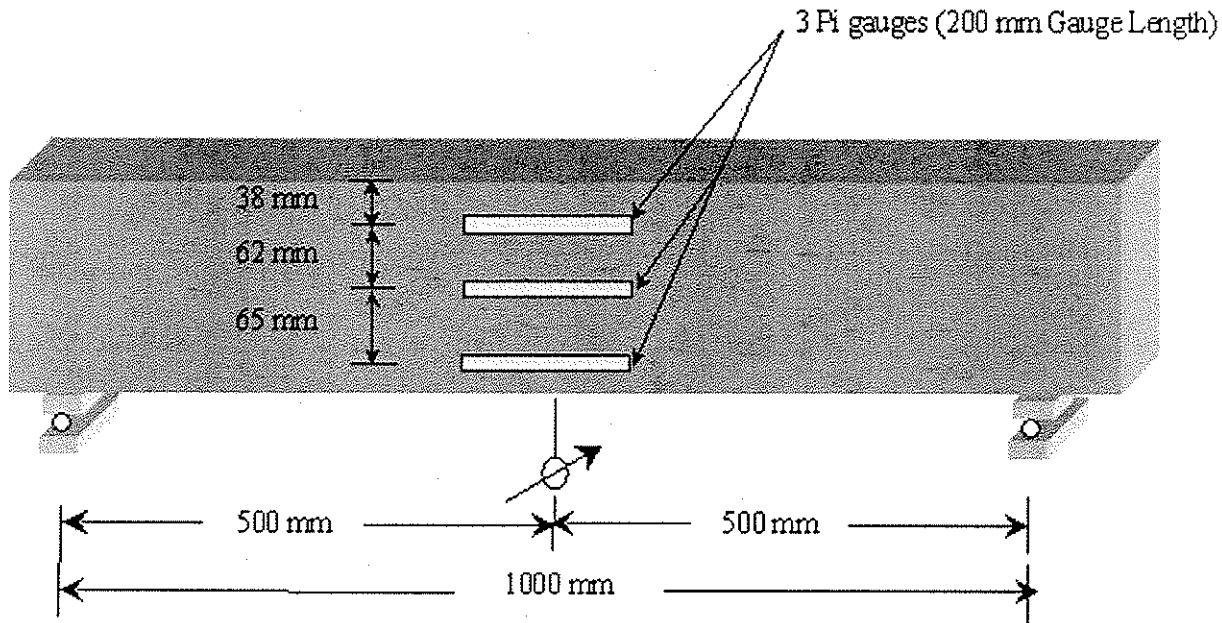


Figure 3.15: Beam Configuration

LVDT, pi gauges and the machine load and stroke. All of the beams were tested under a 1000kN capacity servo-hydraulic testing machine. A concentrated load was applied at mid-span at a load rate of 0.5 mm/minute. The load rating allowed the maximum load to be reached in approximately 35 minutes. All of the beams were tested under the same load rate so that any comparisons made between the test specimens would not be affected by the load rate. A mid-span load was chosen in order to obtain the maximum flexural moment in the beams. At the load point, a rubber bearing pad was used to distribute the load with the exception of the calcium chloride specimens. Because the exterior surface on these beams was severely scaled, plaster was used instead.

3.10 Water Soluble Chlorides Test

A test to determine the quantity of water soluble chlorides in hardened concrete samples was carried out by The National Testing Laboratories Limited. It is generally believed that the corrosion of the reinforcing steel occurs when mobile chlorides are present at the interface between the reinforcing steel and the concrete [30]. In order to carry out the test, slices approximately 10mm thick and 100mm x 100mm wide were cut using a diamond saw with water as a lubricant from the prism specimens after the scaling tests were completed. The slices were taken at regular intervals beginning at the specimen surface and ending at a distance of approximately 1/2 of the specimen depth. The samples were taken to The National Testing Laboratories Limited where they were ground to obtain a powdered sample. A boiling water leach was then carried out on the sample and the leachate was analyzed for water soluble chlorides using the AquaKem 200 Discrete Analyzer. The detection limit for chlorides on the AquaKem was 100 $\mu\text{g/g}$ with a ratio of 1 gram of a sample to 100mL of water.

Chapter 4

Analysis of Concrete Deterioration

4.1 Overview

This chapter describes the results of the scaling test and the systematic monitoring of the deterioration of the test samples during the progression of the freeze-thaw cycles. The saturated-surface dry weight of each cylinder was measured at the beginning of every 10th cycle, and used to determine the overall % change in mass through the freeze-thaw cycles.

4.2 Scaling Test

All of specimens used in the scaling experiment were inspected prior to the start of the test and were considered to be in good condition. It was observed that the prisms possessed several faint discolorations perpendicular to the length of the specimen. This was likely caused by the plastic cover that was placed over the prisms during the curing process. The results of the visual rating procedure carried out in accordance to ASTM 672C are presented

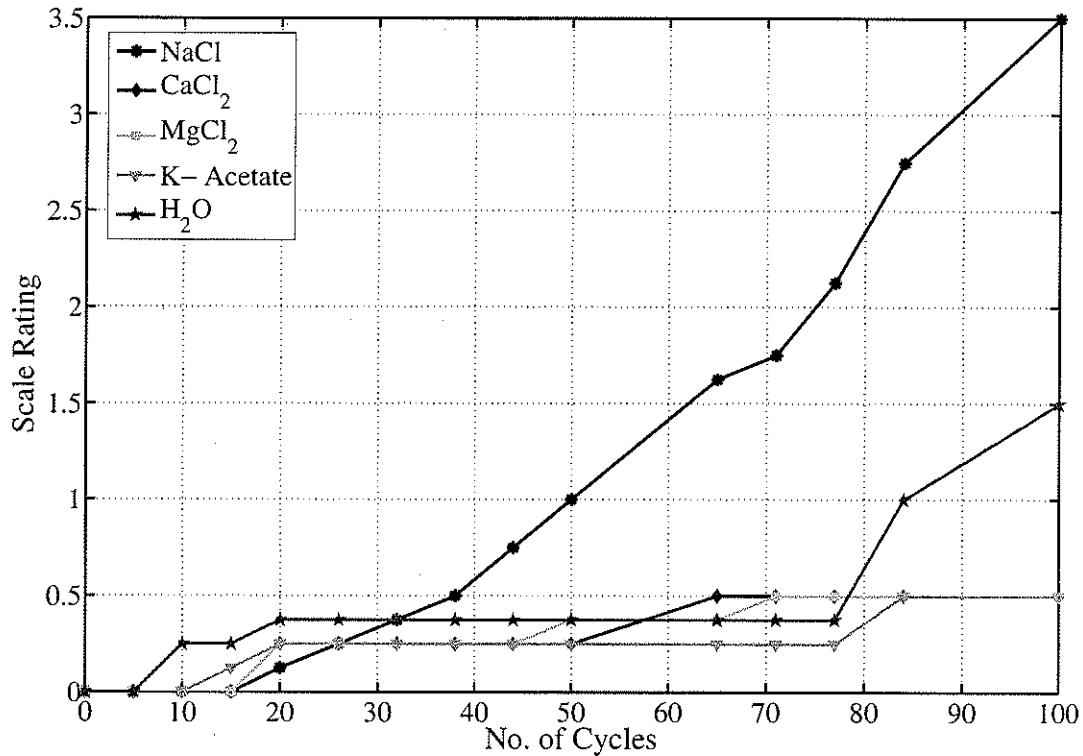


Figure 4.1: Average Scale Rating of Test Samples with Progressive Freeze-Thaw Cycles

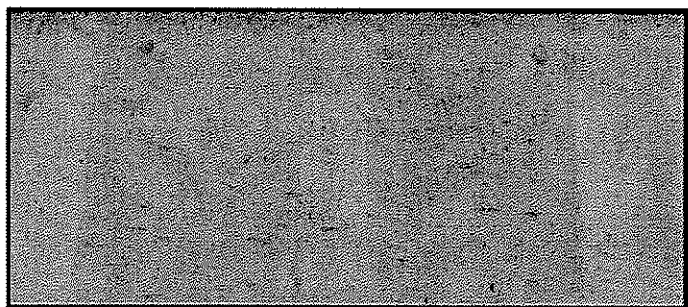
in Figure 4.1. The scale rating shown in the plot corresponds to the average rating given to the two specimens used for each deicing chemical.

A scale rating of 0 indicating no scaling at all was given to the sodium chloride specimens until 20 cycles where extremely light scaling on the surface was visible and the scale rating was increased to 0.125. At 50 cycles, slight scaling was observed in one of the two prisms ponded with sodium chloride. Scaling progressed in this prism with further cycles. By 77 cycles, coarse aggregate was visible on several portions of the surface due to the top concrete layer being scaled off in these sections. At 100 cycles, the entire surface layer had scaled off, exposing coarse aggregate over virtually the entire surface. Figure 4.2 illustrates the

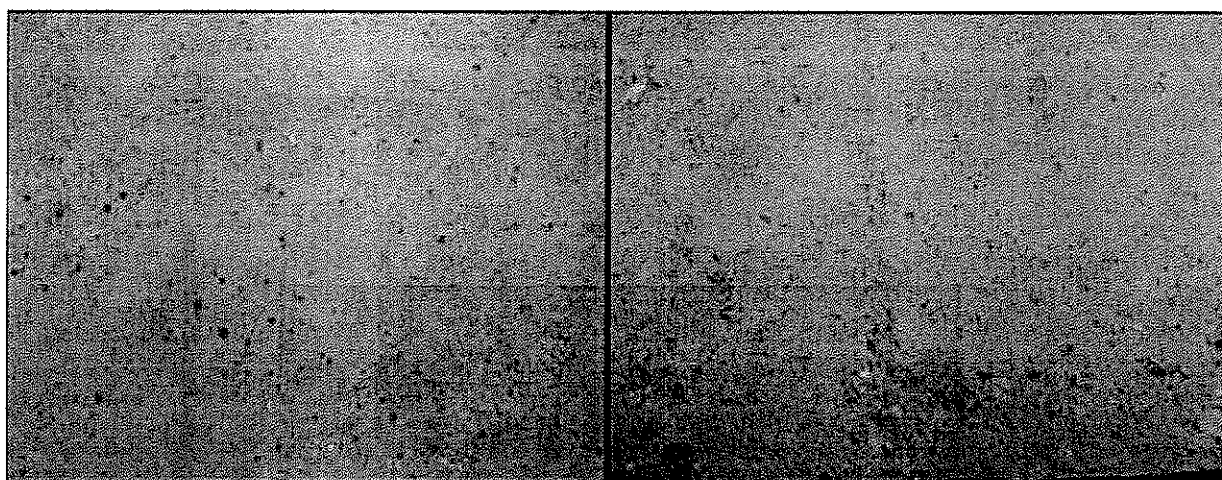
progressive deterioration of the severely scaled prism. In contrast, the second prism ponded with sodium chloride, placed in the same location, and exposed to the same freeze-thaw conditions in the environmental chamber did not experience the same degree of severity in the scaling process. At 50 cycles, both prisms exhibited the same level of scaling and had a scale rating of 1.00. However, where the scaling resistance of the first prism deteriorated extremely rapidly with further cycles, only small amounts of scaled material broke away from the surface in the second specimen each time the visual rating was carried out. At 100 cycles, only slight to moderate scaling was observed over the entire surface, with coarse aggregate visible in scattered areas. It is hypothesized that a similar degree of scaling to the other specimen would have occurred with continued cycles as the scaling progressed in a similar manner to the first prism but at a slower rate. Figure 4.3 illustrates the deterioration of the second prism. The potential reason for this discrepancy may be related to the finishing of the concrete surface. One prism may have been better finished than the other.

Both specimens ponded with calcium chloride exhibited the same magnitude of scaling relative to each other throughout the cycling process. As with the sodium chloride specimens, extremely light scaling began at 20 cycles warranting an increase in the scale rating of the specimens from "0" to "0.25". At 65 cycles, the depth of the voids appeared larger, and the scale rating was increased to 0.5 as small aggregates could now be observed in the voids. In addition, deposits of small white crystals were discovered in the many of the voids throughout the surface. Further freeze-thaw cycles did not warrant an increase in the scale rating, and at 100 cycles the scale rating was still constant at 0.5, though the accumulation of crystals in the voids did appear to increase. Figure 4.4 illustrates the progression of deterioration for the calcium chloride specimens.

Specimens ponded with magnesium chloride exhibited similar behaviors to those ponded with calcium chloride. At 20 cycles, small aggregate particles were visible in some of the larger voids, increasing the scale rating to 0.25. After 50 cycles, small aggregate particles were visible in all larger voids and some smaller voids increasing the scale rating to 0.5.

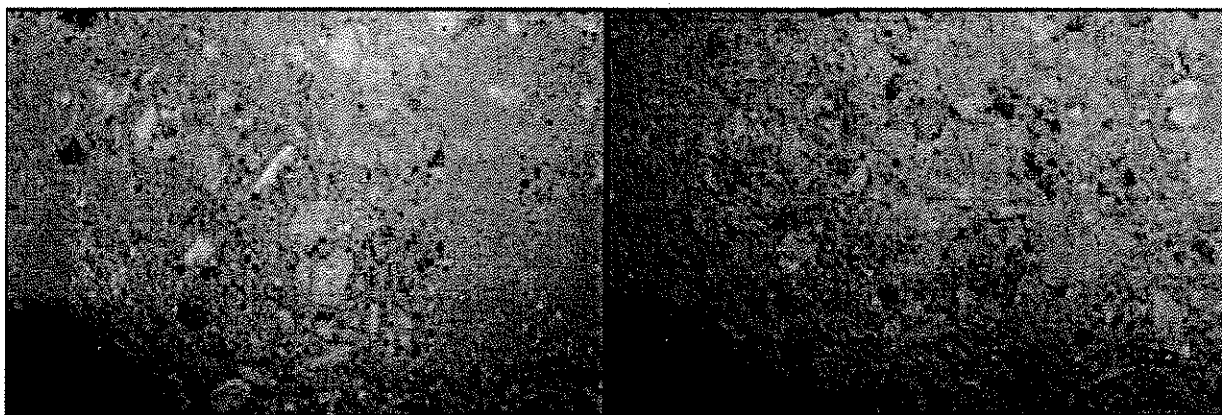


Initial Condition



20 Cycles

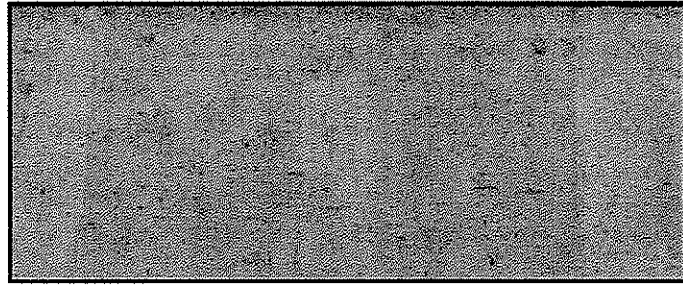
50 Cycles



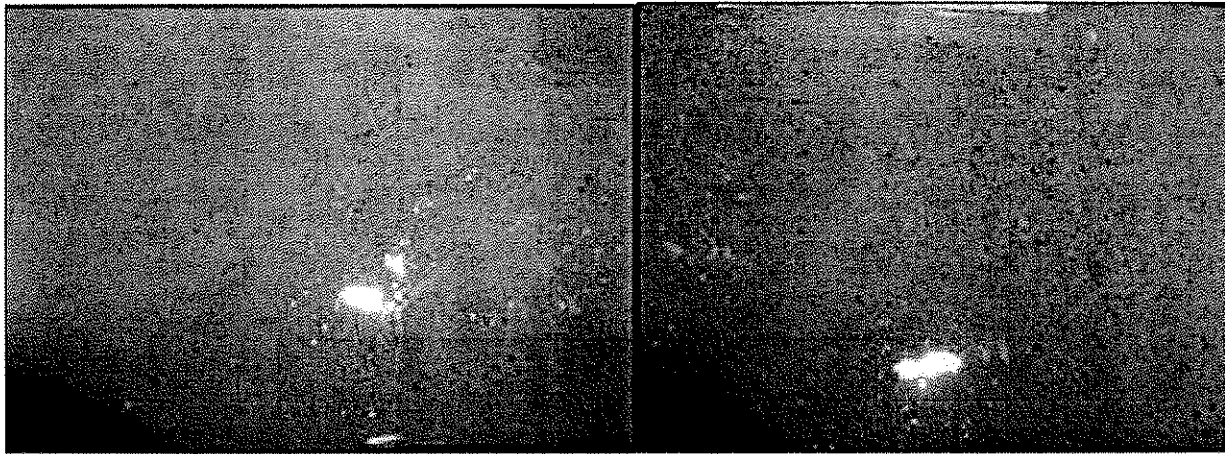
77 Cycles

100 Cycles

Figure 4.2: Progression of Deterioration for Severely Scaled Prism Ponded with Sodium Chloride

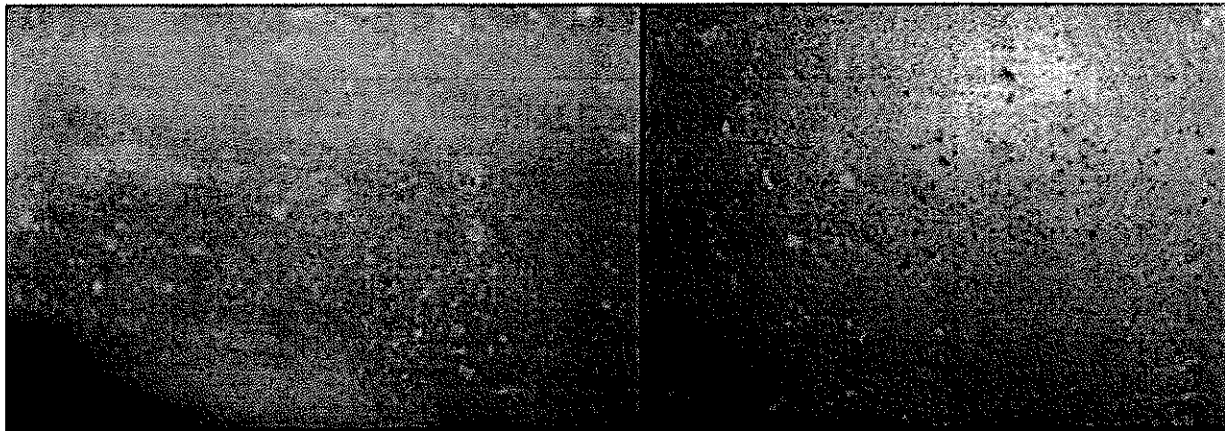


Initial Condition



20 Cycles

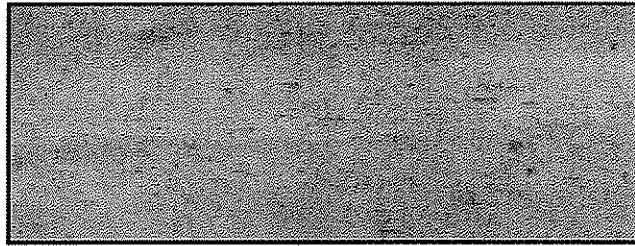
40 Cycles



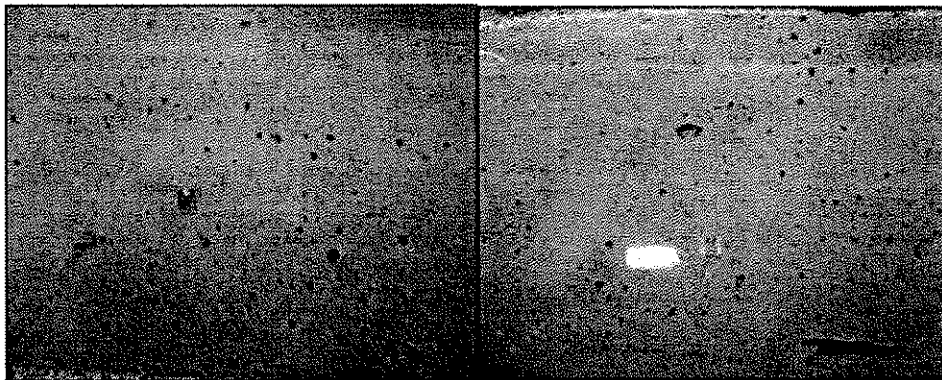
77 Cycles

100 Cycles

Figure 4.3: Progression of Deterioration for the Second Prism Ponded with Sodium Chloride

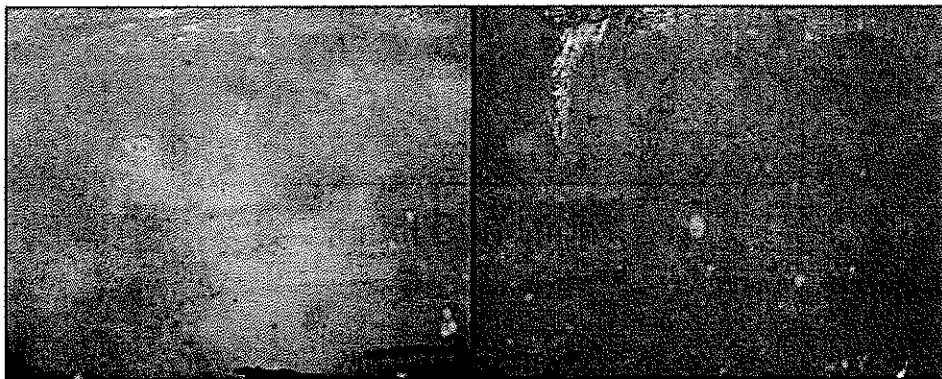


Initial Condition



20 Cycles

50 Cycles



84 Cycles

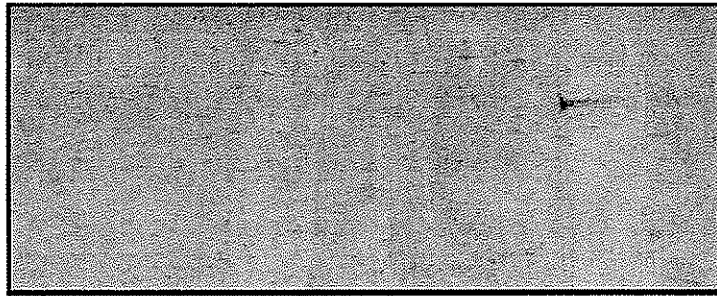
100 Cycles

Figure 4.4: Progression of Deterioration for Specimen Ponded with Calcium Chloride

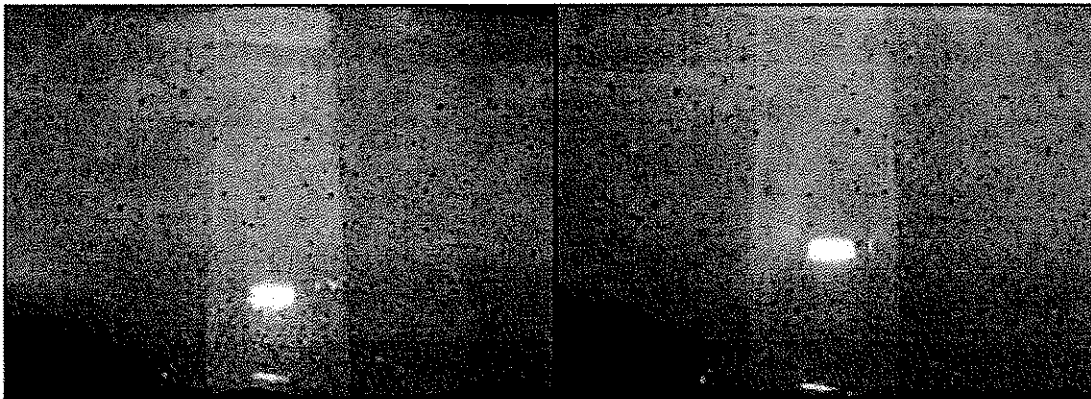
A dark brown discoloration was present in several areas throughout the surface, which was believed to have been caused by the collection of deicing chemical in the surface indentations. Completion of further cycles indicated that extremely light scaling occurred on the surface, but the quantity of scaling was so minimal that the scale rating was maintained constant at 0.5. At 84 cycles, deposits of small white crystals were also visible in many of the voids throughout the surface. At 100 cycles, the scale rating was still 0.5, however, there was an extremely minimal amount of scaled-off particles that were observed. Figure 4.5 illustrates the progression of deterioration of the magnesium chloride specimens.

Specimens ponded with potassium acetate also exhibited virtually no scaling throughout the entire scaling test. As with the other specimens, minimal scaling was observed starting at 20 cycles, increasing the scale rating from 0 to 0.25. No further deterioration could be seen that warranted an increase in the scale rating until 84 cycles, where the scale rating increased to 0.5 as a result of small scaled off particles observed on the surface. The final scale rating at 100 cycles was 0.5. At 50 cycles, an extremely light bluish discoloration was observed after the surface was dried as a result of the blue dye in the deicing chemical. After 100 cycles, the bluish surface coating was much darker. Figure 4.6 illustrates the progression of deterioration for the potassium acetate specimens.

Specimens ponded with distilled water experienced extremely light scaling after 10 cycles in which thin flakes of concrete were observed to be removed from the surface and was assigned a scale rating of 0.25. The average rating at 20 cycles was increased to 0.375 to account for the progression of scaling in a few areas of the prism surface. From 20-84 cycles, smaller particles were observed to break away from the surface, however the degree of scaling did not warrant an increase in the scale rating. An increase in the scale rating occurred at 84 cycles, whereby an increased volume of small cement flakes in the area where scaling initially occurred was observed to break away from the surface. The progression of damage was slight because the water ponded on the surface tended to evaporate in-between cycles, so that there were periods when the surface was dry until more water was re-applied. It is hypothesized

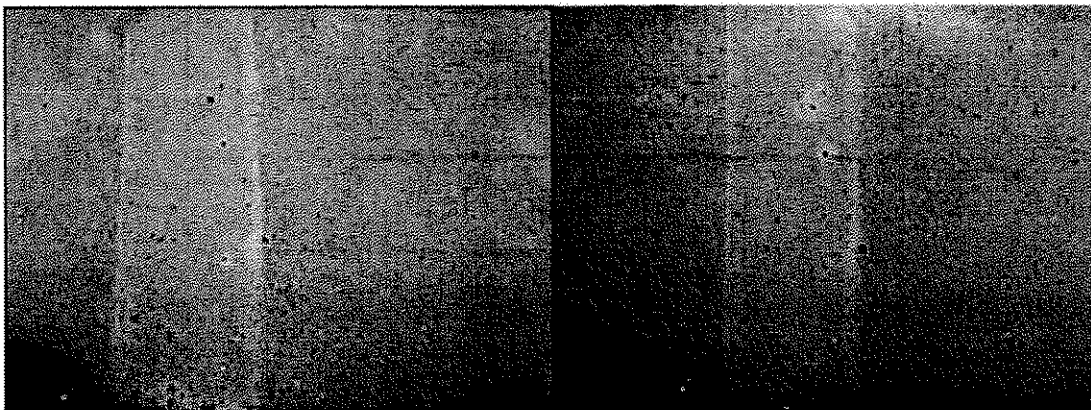


Initial Condition



20 Cycles

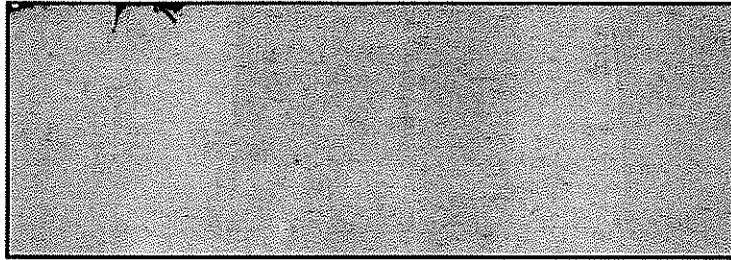
50 Cycles



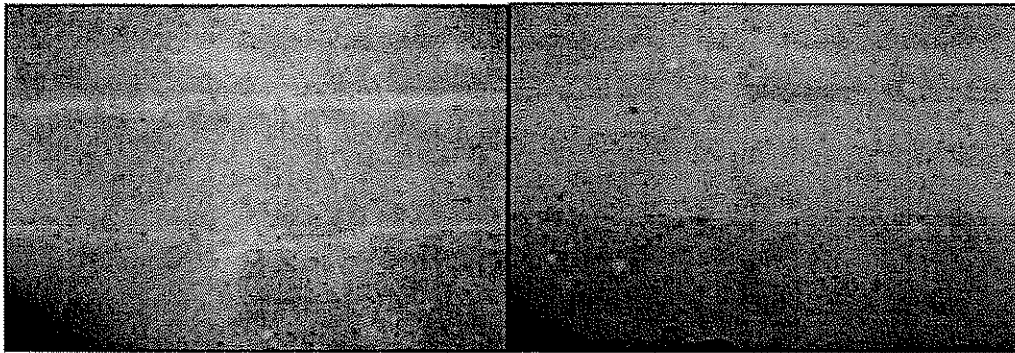
77 Cycles

100 Cycles

Figure 4.5: Progression of Deterioration for Specimen Ponded with Magnesium Chloride

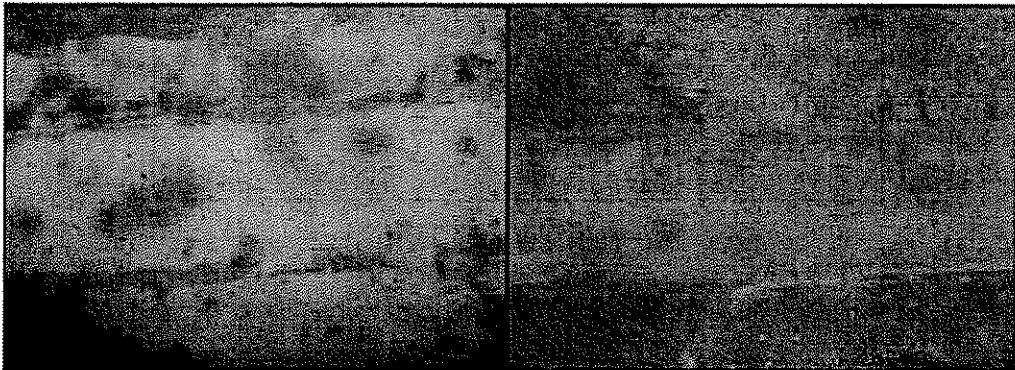


Initial Condition



20 Cycles

50 Cycles



77 Cycles

100 Cycles

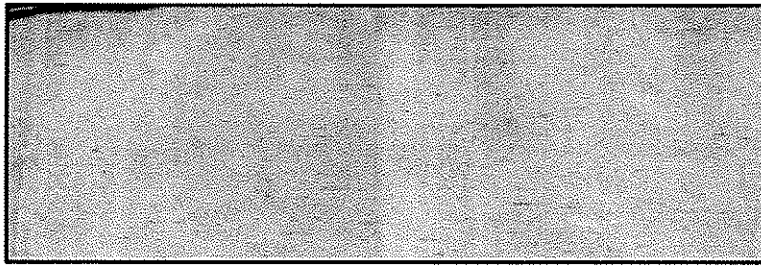
Figure 4.6: Progression of Deterioration for Specimen Ponded with Potassium Acetate

that the scaling would have been more severe if evaporation did not occur. At 100 cycles, the degree of scaling was considered to be "slight" with more flakes breaking away from the top concrete layer which resulted in a final average scale rating of 1 between the two specimens. Figure 4.7 illustrates the progression of deterioration for specimens ponded with distilled water.

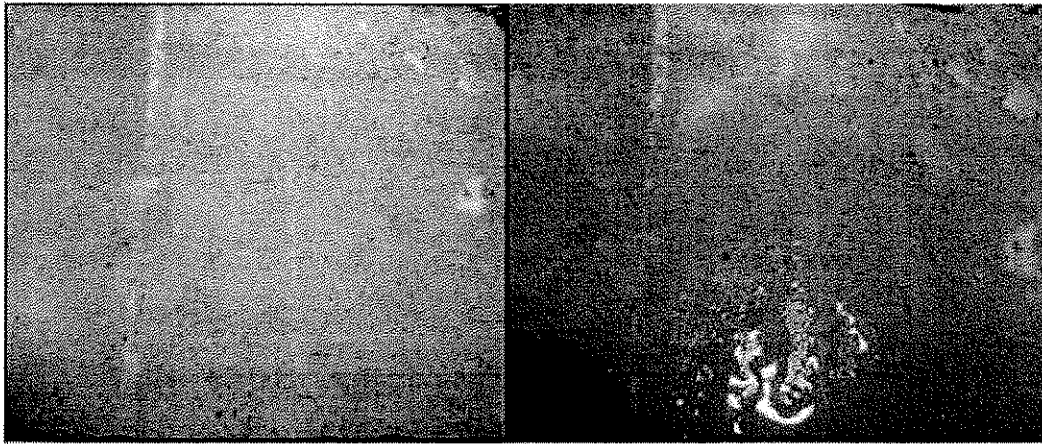
Mass of Scaled-off Particles

The cumulative mass of scaled-off particles after a specific number of freeze-thaw cycles was calculated and is plotted in Figure 4.8. After 77 cycles, the mass of scaled-off particles from the specimens ponded with sodium chloride exceeded 1 kg/m^2 , indicating that concrete no longer has adequate scaling resistance [52]. This corresponds to the visual scaling rating for the specimen described in the previous section.

The cumulative mass of scaled-off particles for the specimens ponded in calcium chloride, magnesium chloride, and potassium acetate after 100 cycles were 0.182 kg/m^2 , 0.216 kg/m^2 , and 0.164 kg/m^2 respectively. This also agrees with the visual rating in the previous section, where all the specimens received a scale rating of 0.5. From the plot, it is obvious that the resulting mass of scaled particles for the water specimens after 100 cycles is less than that of the other specimens even though, the final visual scale rating for the specimens is higher. This is because the scaling in the water specimens did not occur until approximately 84 cycles. At 100 cycles, the amount of scaled particles collected in the filter was at least four times the mass of particles collected for the specimens ponded in deicing chemicals. However, the scaling of the specimens ponded in deicing chemical was more consistent throughout the duration of freeze-thaw cycles, with small amounts of scaled particles collected each time the filtering process was carried out.

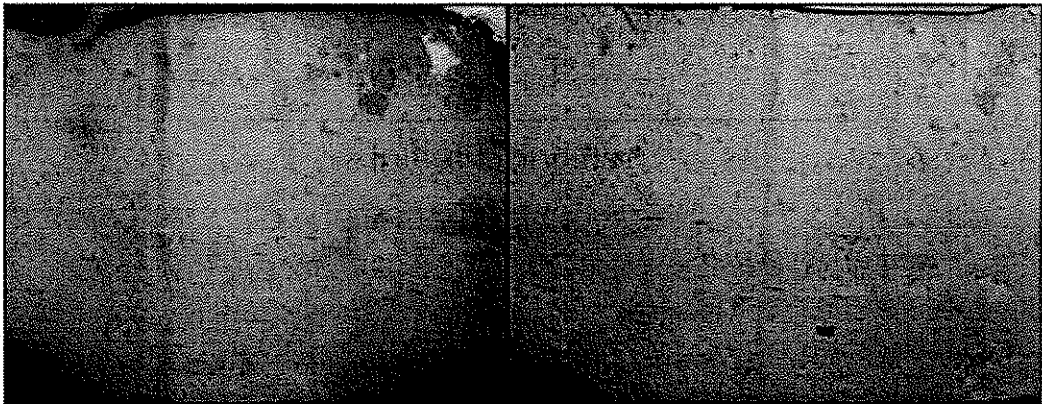


Initial Condition



20 Cycles

50 Cycles



77 Cycles

100 Cycles

Figure 4.7: Progression of Deterioration for Specimen ponded with Distilled Water

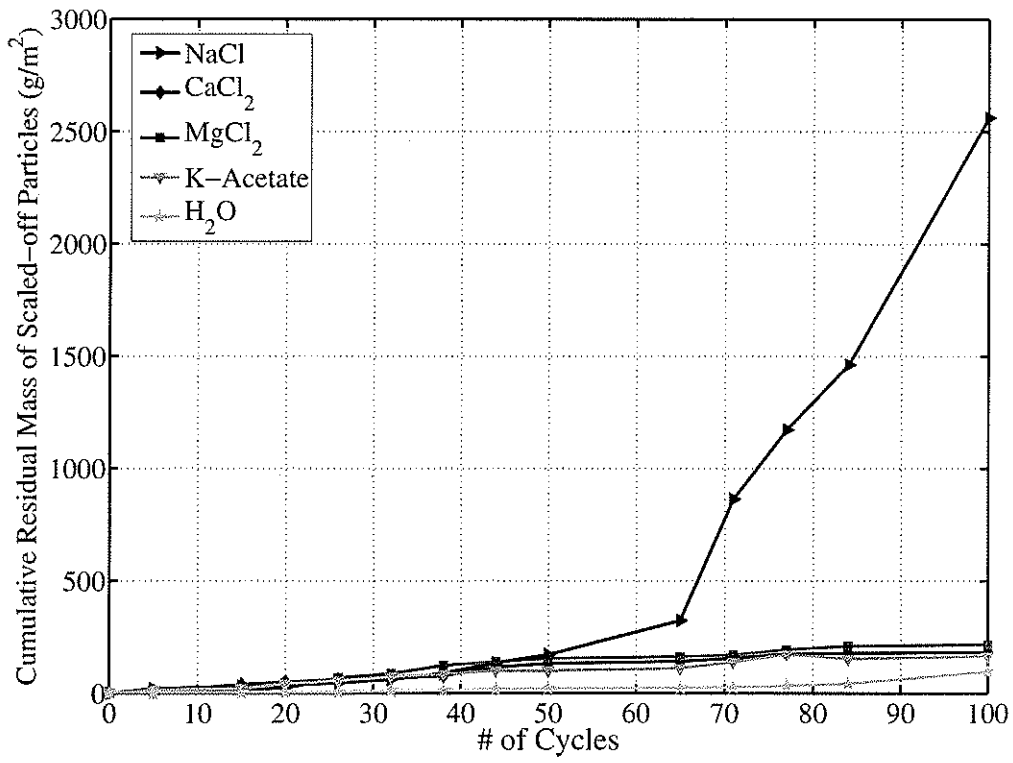


Figure 4.8: Cumulative Residual Mass of Scaled-off Particles

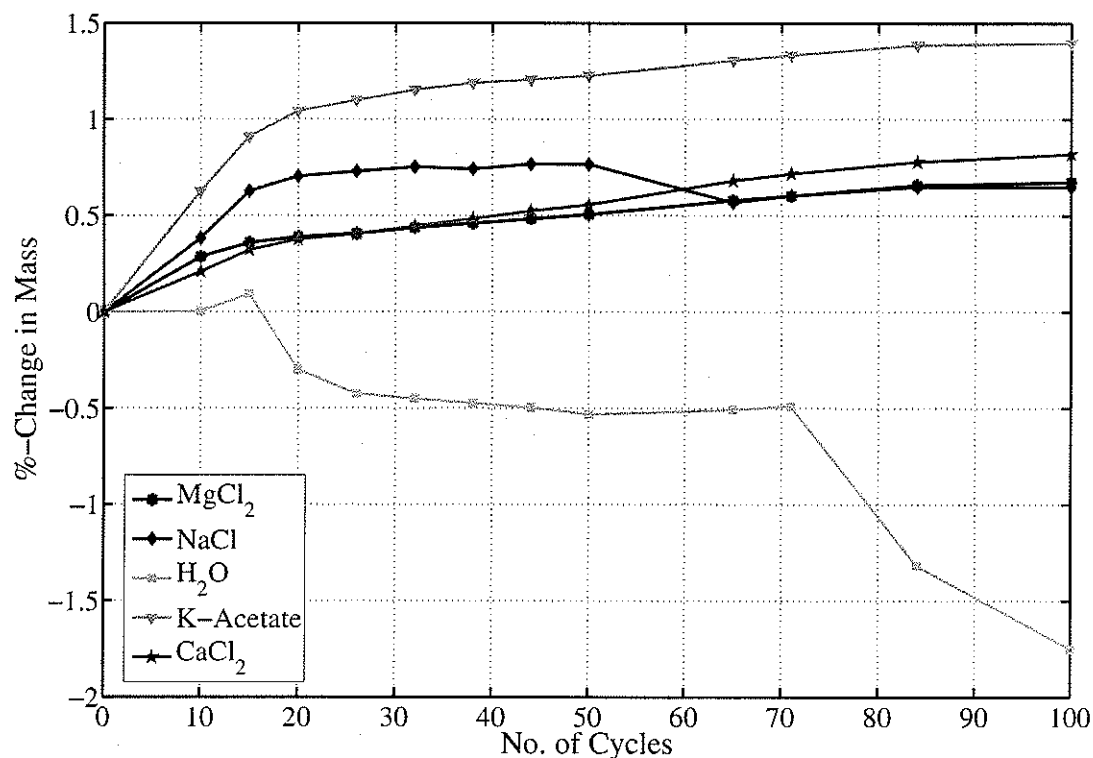


Figure 4.9: Mass-Change of Samples under Freeze-Thaw Cycles

4.3 Mass Change

Figure 4.9 presents the percent-change in mass throughout 100 cycles. The change in mass was calculated by dividing the change in weight after a specific number of cycles by the average saturated weight for the initial cycle. The initial saturated surface-dry weight was calculated using a representative cylinder for each deicing chemical. The initial weight of this cylinder was measured after the surface of the cylinder was wiped dry after 1 cycle. The difference between this weight and the the representative sample's initial dry weight was calculated and added to each cylinder in the deicing solution. As illustrated in the graph, all specimens experienced an initial weight gain during the initial cycles. However,

the damage and disintegration of the specimens in distilled water was evident after 20 cycles as the specimens were losing rather than gaining weight. The decrease in weight was most likely caused by the loss of aggregate and cement particles which accumulated in the bottom of the container. A visual inspection of the distilled water samples revealed that the outer surface was severely scaled along the length, and pieces of the top and bottom section of the cylinder had broken off. Based on previous research [37], [38], [54], [55], [56], this may be due to the lack of air entrainment in the concrete mix used, thus allowing the development of dilative pressures in the pore cavities when the growth of the ice crystal is larger than the capillary pore, and leads to eventual failure of the paste. The severity of scaling in the cylinders as opposed to the prism specimens was likely due to the saturated conditions of the cylinders.

The specimens immersed in the deicing solution did not experience any weight loss over the entire cycling period. This corresponds with results reported by other investigators [50], [68]. The rate of weight gain, however, decreased as the number of cycles increased. The greatest weight gain occurred in the specimens submerged in potassium acetate. The samples experienced a total weight gain of 1.4% at the end of 100 cycles. The percent-change in mass for specimens immersed in calcium and magnesium chloride were very similar to each other throughout the entire cycling period. In some cases, the plots even overlapped. The calcium chloride specimens experienced a 0.8% gain in mass, and the magnesium chloride specimens experienced a 0.7% gain in mass. Specimens submerged in sodium chloride exhibited a steady increase in weight until 50 cycles, and then a loss in weight until 65 cycles where a gain in weight occurred once more, but at a much slower rate than previous. According to Neville [50], if a previously unsaturated specimen is submerged in a solution, the increase in weight is caused by the absorption of the solution in which the specimen is immersed in. This was most likely the cause of weight gain for all of the deicer specimens in the initial 20 to 40 cycles. The increase in mass for the magnesium chloride specimens may also be due to the formation of brucite [64]. After this point, the slope of the percent-change in mass curve decreases for all deicer specimens, suggesting that saturation had occurred. Further weight

gain according to Neville [50], may be caused by the formation of crystals in voids previously occupied by solution. If the formation of crystals causes expansion and opens cracks, ingress of the solution or further crystals deposited in newly created spaces will lead to an increase in weight.

In the case of the sodium chloride solution, it was observed at 65 cycles that the amount of solution evaporated into the chamber air or absorbed by the cylinders was to such an extent that the cylinders were no longer fully submerged in deicing solution. This may explain the decrease in weight from 50-65 cycles. Another contribution to the decreased weight may be due to the scaling of the sodium chloride samples. It was observed that there was a significant quantity of cement particles in the bottom of the container at the end of the cycling period. After 65 cycles, the level of deicing solution was raised so that the specimens were once again fully submerged. This most likely explains why there was once again an increase in weight with corresponding cycles. An increase in weight in the sodium chloride specimens after 65 cycles may also be due to the deposition of salt crystals on the surface of the sodium chloride specimens and in the voids. This could have offset the weight loss previously incurred by the specimen. The sodium chloride specimens experienced an overall weight gain of 0.65% at the end of 100 cycles.

The percent-change in mass for the specimens continually immersed in deicing solution in the absence of freeze-thaw cycles is illustrated in Figure 4.10. Similar to the freeze-thaw samples, the continuous immersion specimens did not experience any weight-loss throughout the entire immersion period. All of the samples experienced a large weight-gain within the first two months of immersion before exhibiting a reduction in the rate of weight gain. Similar to the freeze-thaw samples, the potassium acetate specimens experienced the greatest weight gain. At the end of 6 months of continuous immersion, the K-Acetate samples experienced a total weight gain of 2.5%. In comparison, the total weight gain was 2.2% for the $CaCl_2$ samples, 1.8% for the $MgCl_2$ specimens, and 1.7% for the NaCl samples.

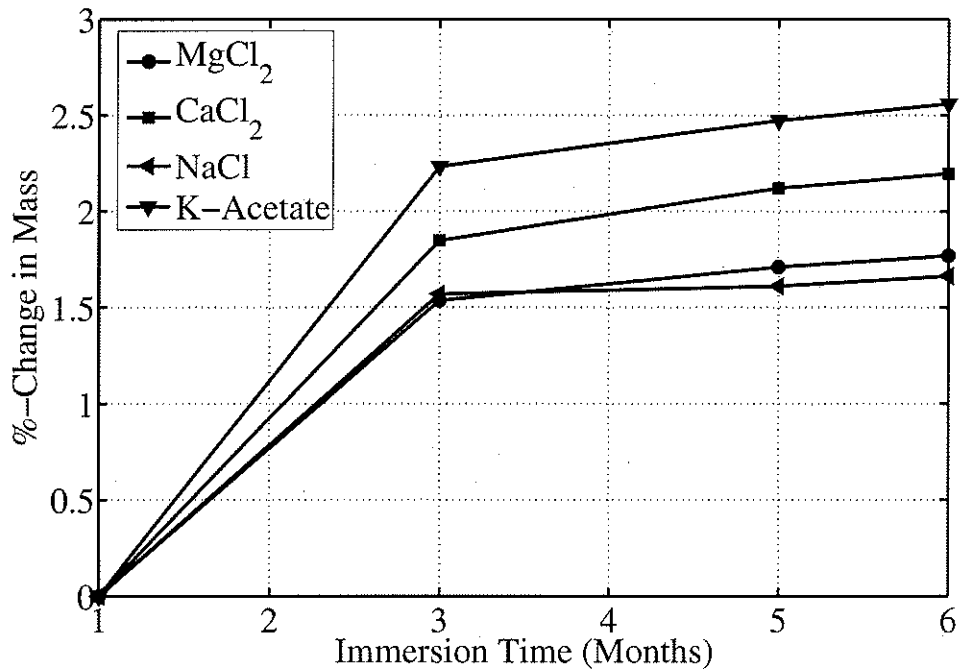


Figure 4.10: Mass-Change of Samples vs Immersion Time

A comparison of the mass-change in the continuous-immersion specimens to the freeze-thaw specimens, show that in general, the continuous-immersion specimens exhibited a larger weight gain than the samples subjected to freeze-thaw cycles. At the end of 6 months, the total gain in weight for the potassium acetate-immersed samples not subjected to freeze-thaw cycles was 1.8 times greater than the samples subjected to freeze-thaw deterioration. Similarly, the weight gain in the calcium and magnesium chloride samples without freeze-thaw cycles was 2.7 and 2.6 times greater than the freeze-thaw specimens in their respective deicing solutions. The weight gain in the NaCl specimens without F-T deterioration was 2.6 times greater than the samples subjected to F-T cycles. The results indicate that the deterioration caused by freeze-thaw cycles offset some of the weight gain caused by the absorption of the deicing chemicals. The results also may indicate the greater formation of brucite in the magnesium chloride samples not subjected to freeze-thaw cycles.

Chapter 5

Analysis of Strength Deterioration

5.1 Overview

This chapter describes the observations and results of the tension, compression and flexural strength tests carried out at the end of 100 cycles. The results of the test to determine the static modulus of elasticity is also presented. The results of the tensile and compressive strength tests are presented in terms of the percentage-change in strength from the control samples, as well as the magnitude of change relative to the deicing chemicals used. The results of the compression test are also compared to samples stored in deicing solutions in the absence of freeze-thaw cycles. An ANOVA analysis confirming the statistical significance of the test results is also presented. Analysis of the flexural strength test results for the beams is discussed in terms of load-deflection behavior, ultimate strength, and cracking load. Finally, the results of the Free Chlorides Test carried out by National Testing Laboratories are presented.

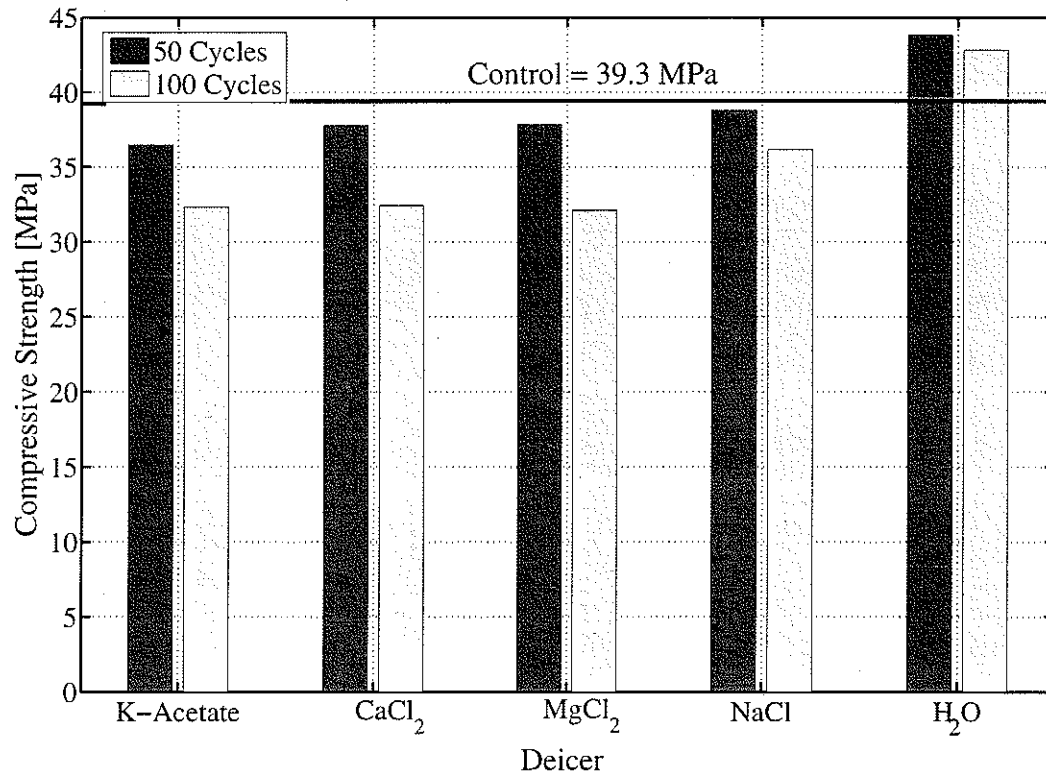


Figure 5.1: Mean Compressive Strength of Samples after Freeze-Thaw Cycling

5.2 Compressive Strength Tests

The compressive strength of the concrete samples after 50 and 100 cycles are illustrated in Figure 5.1. The specimens immersed in deicing solutions and distilled water were compared to the compressive strength of control samples exposed only to laboratory air. After 50 cycles, the specimens immersed in water showed an increase in strength in the order of 11% when compared to the control specimens. The increase in strength was attributed to the changes in the concrete microstructure as a result of continuous cement hydration during the freeze-thaw cycles. The continuous submergence of the samples in the distilled water created a more stable C-S-H structure as a result of the continued reaction between

Table 5.1: Concrete Compressive Strength Loss with Respect to Control Samples

Deicing Chemicals	Percent Change in Strength	
	50 Cycles	100 Cycles
K-Acetate	-7.13	-17.66
$CaCl_2$	-3.74	-17.41
$MgCl_2$	-3.67	-18.25
NaCl	-1.22	-7.88
H_2O	11.61	6.95

un-hydrated cement and the distilled water. After 100 cycles, the specimens showed a 7% increase in strength. The 4% decrease in strength from 50 cycles to 100 cycles was attributed to the severe scaling damage incurred by the water immersed specimens during this period. The decrease in mass, and the corresponding reduction in surface area offset the increased strength caused by continuous cement hydration.

Concrete samples immersed in all deicing solutions exhibited a decrease in compressive strength, when compared to the control samples. The strength loss after 50 freeze-thaw cycles from highest to lowest, was K-Acetate, $CaCl_2$, $MgCl_2$, and NaCl. The evidence of strength loss even after 50 cycles indicates that the deterioration was severe enough to offset the continuing hydration of the samples. After 100 cycles, the strength loss from highest to lowest was $MgCl_2$, K-Acetate, $CaCl_2$, and NaCl. The delayed deterioration in the calcium and magnesium chloride may have been partly attributed to the presence of corrosion inhibitors in the deicing solution. Table 5.1 summarizes the percent-loss in strength of the specimens submerged in deicing solution in comparison to the control specimens.

The percentage change in strength of the samples within a deicer group was also examined. Table 5.2 summarizes the percent-loss in strength between specimens from 50 to 100 cycles. The results show that the magnesium chloride samples experienced the greatest decrease in strength from 50 to 100 cycles equal to 15.14%. This was followed by the calcium chloride, potassium acetate, sodium chloride, and distilled water-immersed specimens. A comparison

Table 5.2: Change in Mean Concrete Compressive Strength

Deicing Chemical	Compressive Strength [MPa]		Strength Decrease [%]
	50 Cycles	100 Cycles	
K-Acetate	36.47	32.33	-11.34
$CaCl_2$	37.8	32.43	-14.73
$MgCl_2$	37.83	32.1	-15.14
NaCl	38.79	36.18	-6.74
H_2O	43.83	42.00	-4.18

of the percent-loss in strength from 50 to 100 cycles with the strength loss during the initial 50 cycles reveals that in general, the samples exhibited a greater decrease in strength in the latter freeze-thaw cycles. This infers that the rate of deterioration proceeded more rapidly once damage began. It therefore can be assumed that prolonged use of any of the deicing chemicals, especially $MgCl_2$, may lead to very rapid loss in concrete strength.

A comparison of the compression test results to the results of the scaling test indicated that the change in strength did not necessarily follow the trend in scaling damage. After 50 cycles, the specimens immersed in sodium chloride had the least amount of strength loss, but showed the most surface deterioration in the scaling tests. A visual rating of the cylinders at 100 cycles indicated that the sodium chloride specimens also underwent the most severe scaling damage when compared with samples immersed in the other deicing chemicals. After the completion of the freeze-thaw cycles, the sodium chloride-immersed specimens were considered to have "slight to moderate scaling", whereas the calcium chloride and magnesium chloride specimens exhibited "very slight scaling". The potassium acetate-immersed specimens experienced minimal scaling but not to the same degree as the calcium and magnesium chloride-immersed samples. This infers that the significant bulk of strength loss is due to the chemical mechanisms of deterioration rather than the reduction in cross-sectional area caused by surface scaling.

Compressive strength tests on concrete samples exposed only to deicing chemicals were also

Table 5.3: Continuously Immersed Samples Compared to Control Samples

Deicing Chemical	Mean Compressive Strength [MPa]	Change in Strength [%]
K-Acetate	30.16	-23.2
$CaCl_2$	31.9	-18.8
$MgCl_2$	27.4	-30.3
NaCl	41	+4.32
Control	39.3	

carried out to determine whether the effect of freeze-thaw cycles aggravated the mechanical deterioration of the test samples. Figure 5.2 illustrates the results of the compression tests of samples continually immersed in deicing chemicals for a period of 6 months. The results of the continuous immersion samples show a similar trend to the strength loss of the freeze-thaw specimens after 100 cycles. The strength loss from highest to lowest was $MgCl_2$, K-Acetate, $CaCl_2$, and NaCl. A comparison of the $MgCl_2$ samples to the control specimens revealed a 31% loss in compressive strength. In comparison, the K-Acetate samples exhibited a 23% decrease in strength, and the $CaCl_2$ specimens exhibited an 18% decrease in strength. The NaCl specimens experienced a 4% increase in strength. The increase in strength in the NaCl samples is attributed to the changes in concrete microstructure due to continuing hydration of the samples. Table 5.3 summarizes the percent-loss in strength of the the specimens submerged in deicing solution in comparison to the control specimens.

A comparison of the compression test results of the continuously immersed samples to the freeze-thaw samples revealed that the strength deterioration in the sodium chloride samples appeared to be aggravated by the presence of freeze-thaw cycles. As shown in Table 5.4, the mean compressive strength of sodium chloride samples not subjected to freeze-thaw cycles was 13% higher than the NaCl samples subjected to freeze-thaw cycles. It is believed that the continued submergence of the samples in the NaCl solution resulted in changes in the concrete microstructure through the deposition of hydration products in the pore structure.

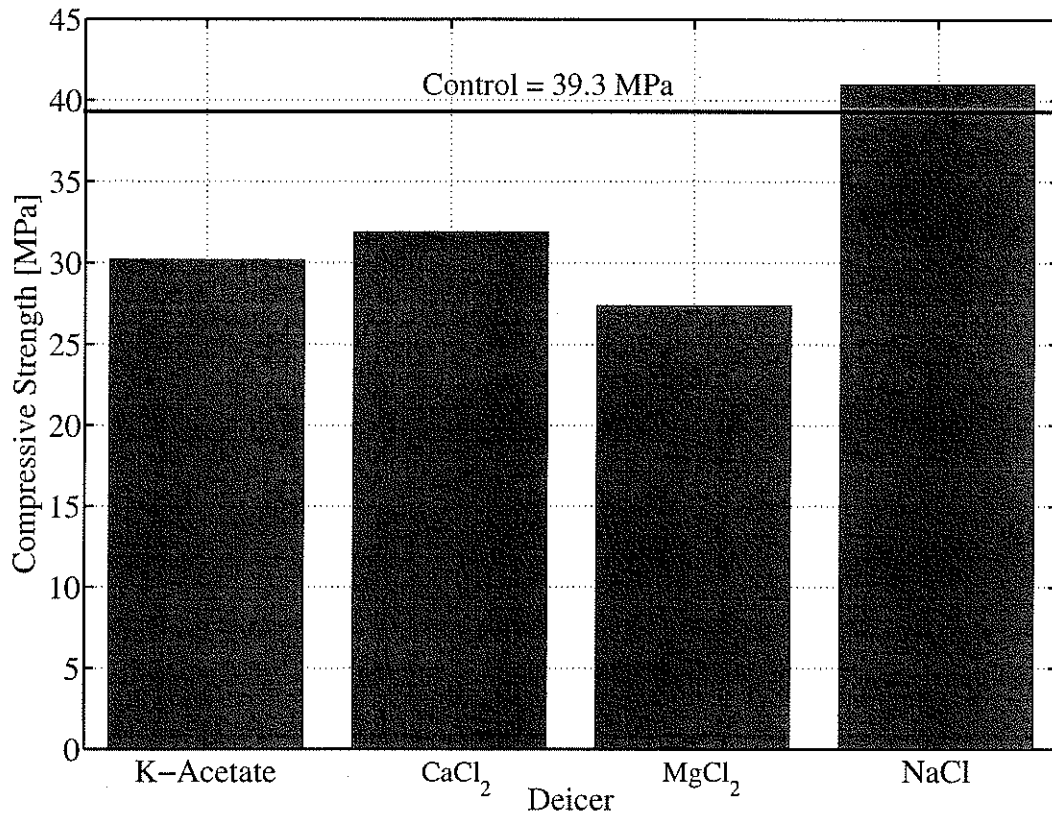


Figure 5.2: Mean Compressive Strength after 6 Months of Continuous Immersion

Table 5.4: Continuously Immersed Samples Compared to Freeze-Thaw Samples

Deicing Chemical	Change in Strength [%]
K-Acetate	-6.71
$CaCl_2$	-1.63
$MgCl_2$	-14.64
NaCl	13.32

In the case of the F-T samples, it is hypothesized that the submergence of the samples in the NaCl solution may have created damaging internal pressures caused by crystallization of the salts and increased water flow through the concrete as a result of the lower freezing point. These damaging mechanisms are believed to have offset the increased strength caused by the continued cement hydration. This damage manifested in the form of scaling, though not to the degree of severity as in the prism samples. In contrast, a comparison of the K-Acetate and $CaCl_2$ samples not subjected to freeze-thaw cycles to the samples that underwent the environmental weathering process revealed very little changes in the value of the mean compressive strength. The changes are attributed to natural sampling error as the range in the values of compressive strength were the same for both the F-T and continuous immersion samples. The mean compressive strength of the magnesium chloride samples not exposed to freeze-thaw cycles was 14.6% lower than the samples exposed to freeze-thaw cycles. It is hypothesized that the continuous immersion of the samples allowed for the formation of more advanced stages of brucite within the concrete microstructure, as evidenced by the increased weight gain of the sample. Growth of brucite crystals may induce expansive pressures leading to de-bonding of the aggregate between the paste-aggregate interface [13], [14], [64].

5.3 Tensile Strength Tests

The tensile strength of the concrete samples after 50 and 100 cycles is illustrated in Figure 5.3. As in the compression test, the specimens immersed in deicing solutions and distilled water were compared to the tensile strength of control samples exposed only to laboratory air. After 50 cycles, the tensile strength of all the specimens immersed in both distilled water and deicing chemicals exhibited a higher tensile strength than the specimens exposed only to laboratory air. The strength gain of specimens from lowest to highest was K-Acetate, $MgCl_2$, $CaCl_2$, H_2O , and NaCl. The increase in strength was attributed to the continuous hydration of the cement paste. The effect of hydration was most significant in the water and sodium chloride-immersed specimens which showed an increase in strength of 10.8% and 11.7%, respectively. After 100 cycles, the tensile strength of the deicer-immersed specimens decreased when compared to the control specimens. The water-immersed samples showed a continuous increase in strength throughout the entire cycling period. The strength loss from the highest to the lowest was $MgCl_2$, $CaCl_2$, K-Acetate, and NaCl. Table 5.5 summarizes the percent-change in strength of the specimens submerged in deicing solution in comparison to the control specimens.

It is evident that the tensile strength decreased significantly upon the onset of deterioration. It appears that the potassium acetate specimens deteriorated more rapidly, as the samples showed an earlier reduction in strength. However, the reduction in strength in the calcium and magnesium chloride specimens proved to be more severe with further freeze-thaw cycles. At 100 cycles, the magnesium chloride specimens experienced a 26% reduction in strength, which was 1.5 times greater than the strength loss incurred by the calcium chloride-immersed samples, 2.8 times greater than the strength loss incurred by the potassium acetate samples, and 11 times greater than the loss incurred by the sodium chloride samples. The calcium chloride-immersed samples performed slightly better, with a 16% reduction in strength. The rapid loss of strength upon the onset of deterioration demonstrates the significant mechanical

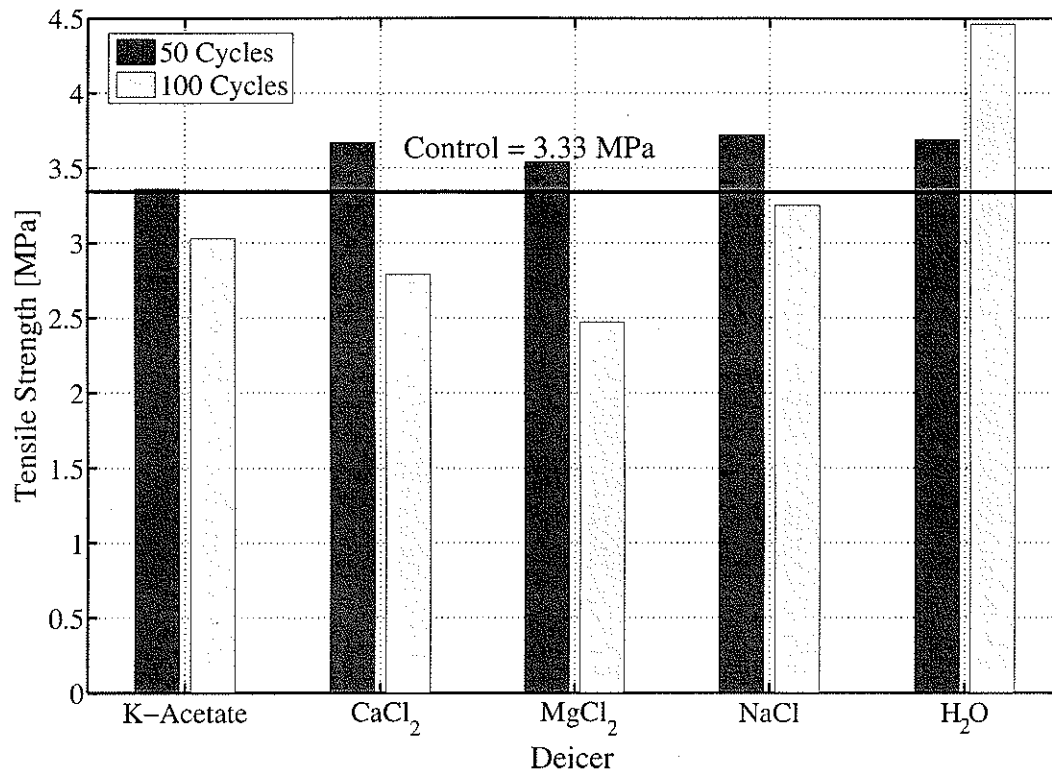


Figure 5.3: Tensile Strength of Samples after Freeze-Thaw Cycling

Table 5.5: Concrete Tensile Strength Loss With Respect to Control Samples

Deicing Chemicals	Percent Change in Strength	
	50 Cycles	100 Cycles
K-Acetate	+0.9	-9.07
$CaCl_2$	+10.2	-16.25
$MgCl_2$	+6.3	-25.8
H_2O	+10.8	+33.96
NaCl	+11.7	-2.26

Table 5.6: Change in Mean Concrete Tensile Strength

Deicing Chemical	Tensile Strength [MPa]		Strength Decrease [%]
	50 Cycles	100 Cycles	
K-Acetate	3.36	3.03	-9.92
$CaCl_2$	3.67	2.79	-24.08
$MgCl_2$	3.54	2.47	-30.22
NaCl	3.72	3.25	-12.6
H_2O	3.69	4.46	20.91

weakening of concrete when exposed to magnesium and calcium chloride samples. Table 5.6 summarizes the percent-loss between specimens from 50 to 100 cycles.

A comparison of the tensile strength of the specimens continuously immersed in deicing solution and specimens exposed to freeze-thaw cycles was not carried out. It was believed that the comparison would produce similar results to those for the compression test.

5.4 Statistical Analysis

5.4.1 Analysis of Variance

A statistical analysis was carried out to verify that the difference in the mean tensile and compressive strength values between the deicing chemicals were statistically significant. The statistical test used in the analysis was an Analysis of Variance Test. An Analysis of Variance test is a statistical hypothesis testing procedure that analyzes the differences between the means of two or more groups by analyzing the ratio of variances between groups and within the group [16]. The assumptions of an ANOVA test are that the dependent variable is drawn from a population of values that is normally distributed, and that the samples have been randomly assigned to a test group [16]. Because the distribution of individual strengths of comparable concrete specimens has been shown to be normal [53], and because the concrete specimens were randomly assigned to a deicing solution, the ANOVA analysis is determined to be valid.

Two null hypotheses were tested in the ANOVA analysis. The first null hypothesis was designed to determine whether the submergence of concrete samples in deicing solution had an effect on the mean compressive strength of concrete. The null hypothesis for both the tension and compression test specimens was given as follows:

$$H_0 = \mu_{CO} = \mu_{DW} = \mu_{NaCl} = \mu_{CaCl_2} = \mu_{MgCl_2} = \mu_{K-Acetate} \quad (5.1)$$

where μ_{CO} , μ_{DW} , μ_{NaCl} , μ_{CaCl_2} , μ_{MgCl_2} , and $\mu_{K-Acetate}$ are the mean values of compressive strength for the control specimens, distilled water, sodium chloride, calcium chloride, magnesium chloride, and potassium acetate, respectively. The second null hypothesis was designed to verify that the samples in deicing solution suffered damage between 50 and 100 cycles. The null hypothesis for both the tension and compression test specimens was given

as follows:

$$H_0 = \mu_{50} = \mu_{100} \quad (5.2)$$

A true null hypothesis inferred that all observations were taken from a normal distribution with mean μ , and variance σ^2 , and changing the level of the factors would have no effect on the mean response [16]. The alternative hypothesis was that the mean is not the same for all groups and the dependent variable is significantly affected by the independent variable. In order to determine whether the null hypothesis was true, variability between groups was compared to the variability within groups. If there was no significant difference between the means, it was expected that there would be little variability between groups, and the ratio of the variabilities would be close to 1.00. However, if there were significant differences between the means, then the variability would not be attributed to sampling error and the ratio was expected to be quite large [16],[8].

In order to determine the variances within and between the groups, the sum of squares within groups, between groups and the total sum of squares were calculated. The formulas are given as follows:

$$SSW = \sum^k \sum^{N_G} (X - \bar{X}_G)^2 \quad (5.3)$$

$$SSB = \sum^k N_G (\bar{X}_G - \bar{X}_T)^2 \quad (5.4)$$

where SSW refers to the sum of the squares of the deviation between an individual strength value to the mean value within a group, SSB refers to the sum of the mean deviation between each group from the total mean of all the groups, X = the individual value of strength for a sample, \bar{X}_G = the mean value of strength for a group, \bar{X}_T = the total mean of all the groups, N_G = the number of the group, and k = the number of groups.

The total sum of squares was calculated as:

$$SST = \sum^k \sum^{N_G} (X - \bar{X}_T)^2 \quad (5.5)$$

which is the sum of squares within each group plus the sum of squares between groups.

Next, the degree of freedoms within groups, degree of freedom between groups, and the total degree of freedom was calculated. The degree of freedom refers to the difference between the number of observations or groups in a study and values that limit the observations freedom to vary[16]. The equations are given as follows:

$$df_{SST} = N_T - 1 \quad (5.6)$$

$$df_{SSB} = k - 1 \quad (5.7)$$

$$df_{SSW} = df_{SST} - df_{SSB} \quad (5.8)$$

where N_T = number of observations, and k = number of groups.

The mean squares was calculated as the ratio of the sum of the squares divided by the appropriate degrees of freedom [8]. The equations are given as follows:

$$MSW = \frac{SSW}{df_{SSW}} \quad (5.9)$$

$$MSB = \frac{SSB}{df_{SSB}} \quad (5.10)$$

where MSW and MSB are the variance estimates within groups and between groups, respectively [8].

Finally, the F-statistic was calculated as:

$$F = \frac{MSB}{MSW} \quad (5.11)$$

Since equations 5.9 and 5.10 are an unbiased estimate of the population variance for a group, it followed that if the null hypothesis was true, the variance estimates would measure the same variance, and the F-statistic would be close to 1.00 [8]. If the population means differ, the between-groups variance was substantial, and the F-statistic would correspondingly become inflated. Thus, the null hypothesis was rejected when the value of the F-statistic is large. The critical F-value used to decide whether to accept or reject the null hypothesis was based on a probability value of 0.05, which is a generally accepted level of committing a Type I error [45]. A Type I error is committed if the null hypothesis is rejected when it is in fact true [8]. A p-value of 0.05 indicates that there is less 5 chances out of 100 of committing a Type I error.

5.4.2 Compressive Strength Analysis Using ANOVA

Table 5.7 summarizes the results of the ANOVA test after 50 cycles. As illustrated in the table, H_0 was rejected for even a low level of significance, meaning that there is a significant difference in compressive strength due to exposure to deicing chemicals and distilled water relative to the control samples. The test was repeated for the same null hypothesis, but excluding the control samples. In this case, H_0 was also rejected for even a low level of significance, indicating a significant change in compressive strength of samples submerged in deicing chemicals relative to samples submerged in distilled water. As explained in the previous section, the change in strength was due to the continued hydration of the cement

Table 5.7: Analysis of Variance for Compressive Strength at 50 Cycles

50-cycles		
Parameter	F-Statistic	P-value
All samples	11.97	0.000006911
Excluding Control Samples	13.25	0.000019703
Excluding Water Samples	2.23	0.1022

Table 5.8: Analysis of Variance for Compressive Strength at 100 Cycles

100-cycles		
Parameter	F-Statistic	P-value
All samples	18.83	0.00000134
Excluding Water Samples	8.76	0.0007

paste. The test of hypothesis was repeated a third time excluding water-immersed specimens to determine if the mean strength of the deicer-immersed specimens was significantly different from the mean strength of the control samples. In this case, the null hypothesis was accepted meaning that there was no significant change in compressive strength of the deicers relative to the control samples.

The ANOVA test was performed once more after 100 cycles. The results are summarized in Table 5.8. Similar to the results at 50 cycles, H_0 was again rejected for even a low level of significance. The test was again repeated, excluding the distilled water samples in order to determine if there was a significant change in strength as a result of the deicing chemicals. In contrast to the results at 50 cycles, H_0 was rejected indicating that one or more of the deicing solutions caused a significant change in the mean compressive strength of the samples.

The ANOVA test was performed a third time to determine whether the samples submerged in deicing chemicals suffered further damage between 50 and 100 cycles. The null hypothesis was $H_0: \mu_{50} = \mu_{100}$, where the μ_{50} and μ_{100} refers to the compressive strength of all samples at

Table 5.9: Analysis of Variance for Effect of Number of Freeze-Thaw Cycles

100-cycles		
Parameter	F-Statistic	P-value
All Samples	18.7	0.00000137

50 cycles and 100 cycles respectively. Table 5.9 summarizes the results of the analysis. The small p-value of 0.00000137 indicates that the probability of the samples being drawn from the same population with a normal distribution is 1.3 in 1,000,000. Thus, the test strongly supports the alternate hypothesis, and it is believed that there is a statistically significant difference between the means of one or more values of compressive strength.

5.4.3 Tukey's HSD Procedure for Compressive Strength

Because the ANOVA test does not indicate *which* differences between the means are significant a multiple comparisons test was carried out after the ANOVA test to determine the pattern of significance among the means [16],[8]. The procedure chosen for the analysis was Tukey's Honestly Significant Difference (HSD) Test because it has been shown to be neither too conservative in controlling the Type I error, nor too liberal so that the probability of controlling the Type I error is beyond acceptable limits [16]. Tukey's HSD Procedure was carried out at 50 and 100 cycles to determine which pairs of means were significantly different, and verify the results described in the ANOVA test above. Tukey's test was carried for all of the significant ANOVA tests when the null hypothesis was rejected. Each group mean was compared to every other group mean and the value of the difference between the means was compared to Tukey's HSD value [16]. The analysis was carried out in MATLAB, using a significance at the 0.05 level. The results were displayed on a graph with the group mean represented by a symbol and an interval around the symbol. The means were considered to be significantly different if their intervals were disjointed, and not significantly different, if

the intervals overlapped.

A comparison of the mean groups of deicing chemicals and control samples with the distilled water samples that was carried out at 50 and 100 cycles indicates that the mean values are statistically different from the distilled water samples. Figure 5.4 and Figure 5.5 illustrates the results of this comparison at 50 and 100 cycles, respectively. At 50 cycles, the mean values of the deicing solution and control specimens were significantly different from the distilled water specimen. At 100 cycles, the mean strength of the control specimen was no longer significantly different from the mean strength of the distilled water specimens. This reflects the decrease in compressive strength as a result of the severe scaling incurred by the water-immersed samples between 50 and 100 cycles.

A comparison of the compressive strength of the deicing chemicals with the compressive strength values of the control samples after 50 cycles does not indicate a statistical difference between the strength of the samples. After 100 cycles, however, the reduction in strength for the $CaCl_2$, K-Acetate, and $MgCl_2$ - immersed specimens were considered to be statistically significant from mean value of strength of the control specimens. The reduction in strength within the sodium chloride group, however was not considered statistically significant with respect to the control sample.

A comparison of the mean values of each deicing chemical at 50 cycles to the mean strength values at 100 cycles was also carried out. The results indicate that the sodium chloride and potassium acetate samples did not suffer further damage from 50 to 100 cycles, as the decrease in strength was not considered statistically significant at the 0.05 level. Figure 5.6 illustrates the results of the multiple comparisons test for the samples at the 0.05 level. In contrast, the decrease in strength for the calcium and magnesium chloride specimens were considered statistically significant and the results in Figure 5.6 indicate that the samples suffered further damage from 50 to 100 cycles.

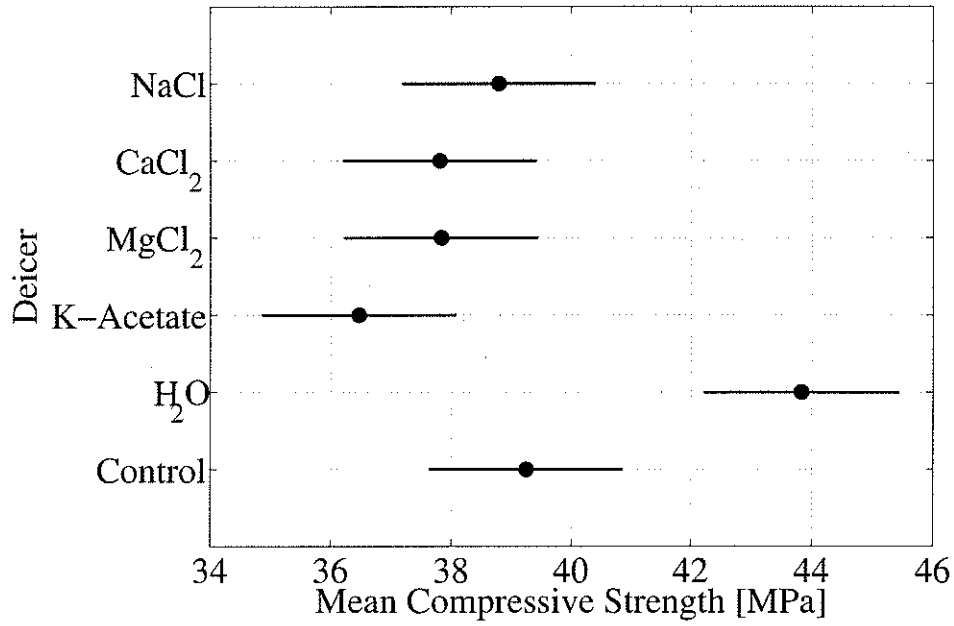


Figure 5.4: Comparison of Means After 50 Cycles

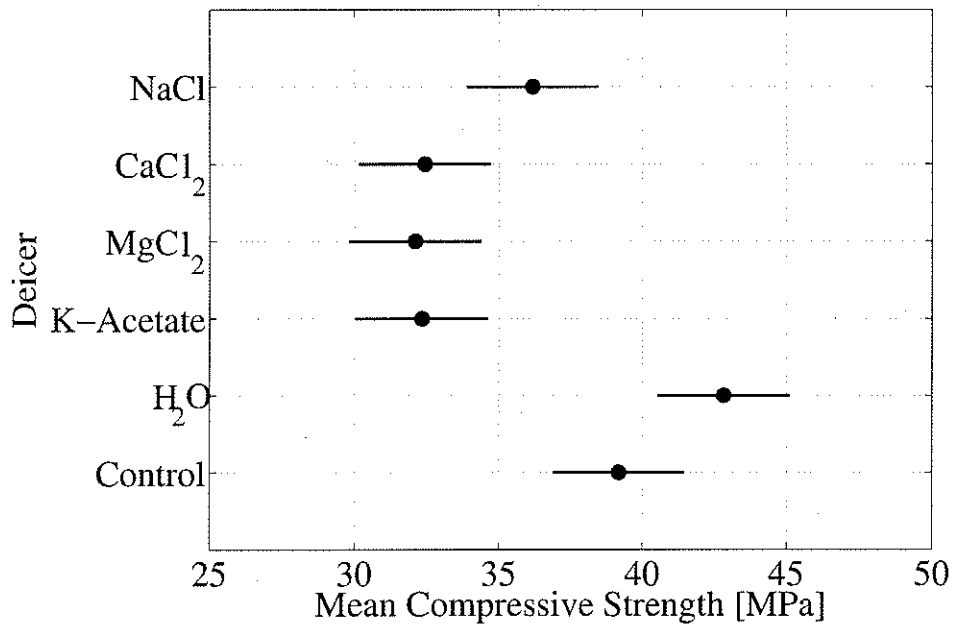


Figure 5.5: Comparison of Means After 100 Cycles

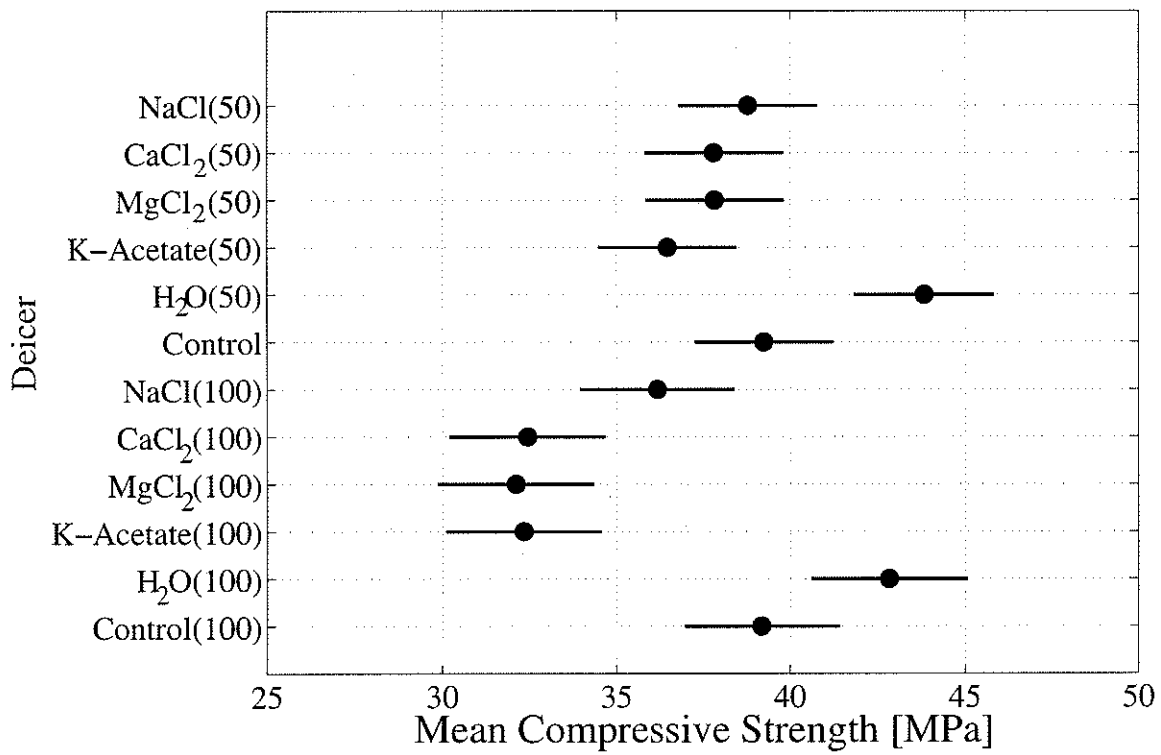


Figure 5.6: Comparison of Means Between 50 and 100 Cycles

Table 5.10: Analysis of Variance for Tensile Strength at 50 Cycles

50-cycles		
Parameter	F-Statistic	P-value
All samples	1.11	0.406

5.4.4 Tensile Strength Analysis Using ANOVA

A statistical analysis of the results of the tensile strength test was also carried out at 50 and 100 cycles to verify that the differences in the mean values between groups of deicing chemicals were statistically significant and that the specimens suffered damage with increased freeze-thaw cycling. Table 5.10 summarizes the results of the ANOVA test after 50 cycles. As illustrated in the table, H_0 was accepted at the 0.05 level, indicating that the difference in mean tensile strength between each group is not statistically significant.

The ANOVA test was performed once more at 100 cycles. The results are summarized in Table 5.11. In contrast to the results at 50 cycles, H_0 was rejected, indicating that there was a significant difference in the mean value of strength between one or more groups. The test was repeated, excluding the control specimens to determine whether there was a significant difference between the deicer immersed specimens and the distilled water specimens. Again, the significance was attributed to the changes in the microstructure of concrete due to continued hydration. The null hypothesis was once again rejected for even a low level of significance. The test was repeated a third time excluding the distilled water immersed specimens. The null hypothesis was rejected again, indicating significant differences between the deicer immersed specimens and the control specimens.

The test was performed again to determine if the samples suffered damage between 50 and 100 cycles. The results indicate that there is a significant difference between the means of one or more values of compressive strength. Table 5.12 summarizes the results of the analysis.

Table 5.11: Analysis of Variance for Tensile Strength at 100 Cycles

100-cycles		
Parameter	F-Statistic	P-value
All samples	30.46	0.00000217
Excluding Control Samples	40.62	0.00000374
Excluding Water Samples	10.09	0.0015

Table 5.12: The Effect of Number of Freeze-Thaw Cycles on Tensile Strength

100-cycles		
Parameter	F-Statistic	P-value
All Samples	12.07	.000000286

5.4.5 Tukey's HSD Procedure for Tensile Strength

Similar to the compression test analysis, Tukey's HSD procedure was used to determine the significance between two pairs of means. A comparison of the mean groups of deicing chemicals was not carried out at 50 cycles, because the ANOVA test showed that the change in mean values of each group of deicers was not significant with respect to one another. A comparison of the groups of means at 100 cycles, however, showed that the all of the mean groups were significantly different from the distilled water samples. The difference was attributed to the continued hydration of the water-immersed samples which led to an increase in tensile strength. The results are illustrated in Figure 5.7. From the figure, it is also evident that only the $MgCl_2$ samples were significantly different from the control samples after 100 cycles.

A comparison of the groups of means for 50 cycles and 100 cycles was also carried out to determine if the specimens suffered damage with further freeze-thaw cycles. The results for the sodium chloride specimens indicate that decrease in mean tensile strength was not considered statistically significant between 50 and 100 cycles. Figure 5.8 illustrates the results of the multiple comparisons test for all of the specimens. The results for the calcium

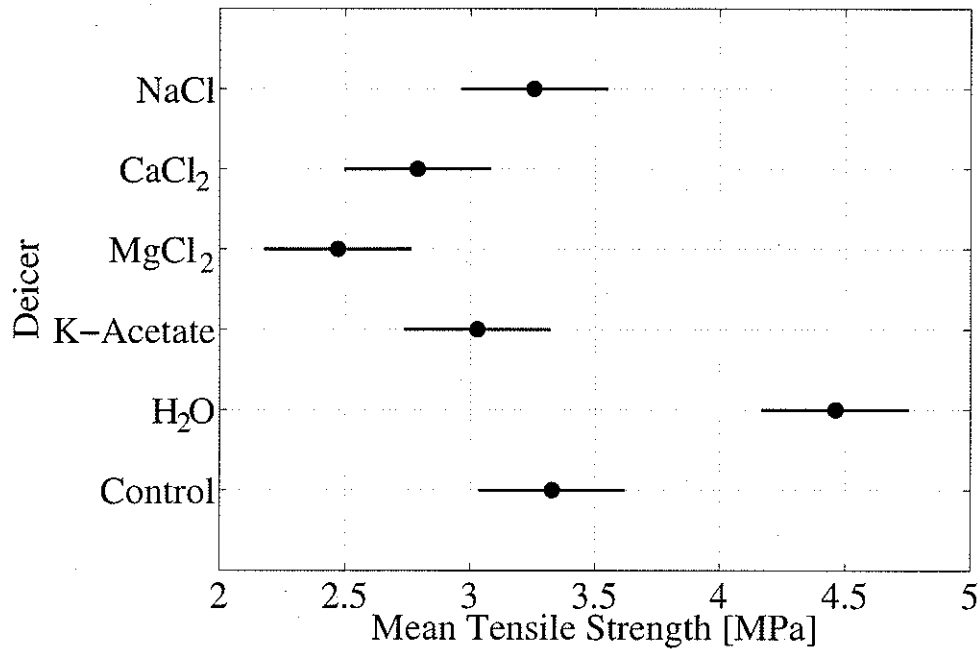


Figure 5.7: Comparison of Means After 100 Cycles

and magnesium chloride specimens show that the mean tensile strength was considered statistically significant meaning the specimens suffered further damage from 50 to 100 cycles. The results for the potassium acetate specimens show that the decrease in strength was not considered statistically significant between 50 and 100 cycles.

The results of the ANOVA analysis demonstrate that the reductions in tensile and compressive strength described in the previous section are significant and cannot be attributed to random sampling error. The analysis reinforces the severity of deterioration caused by the deicers.

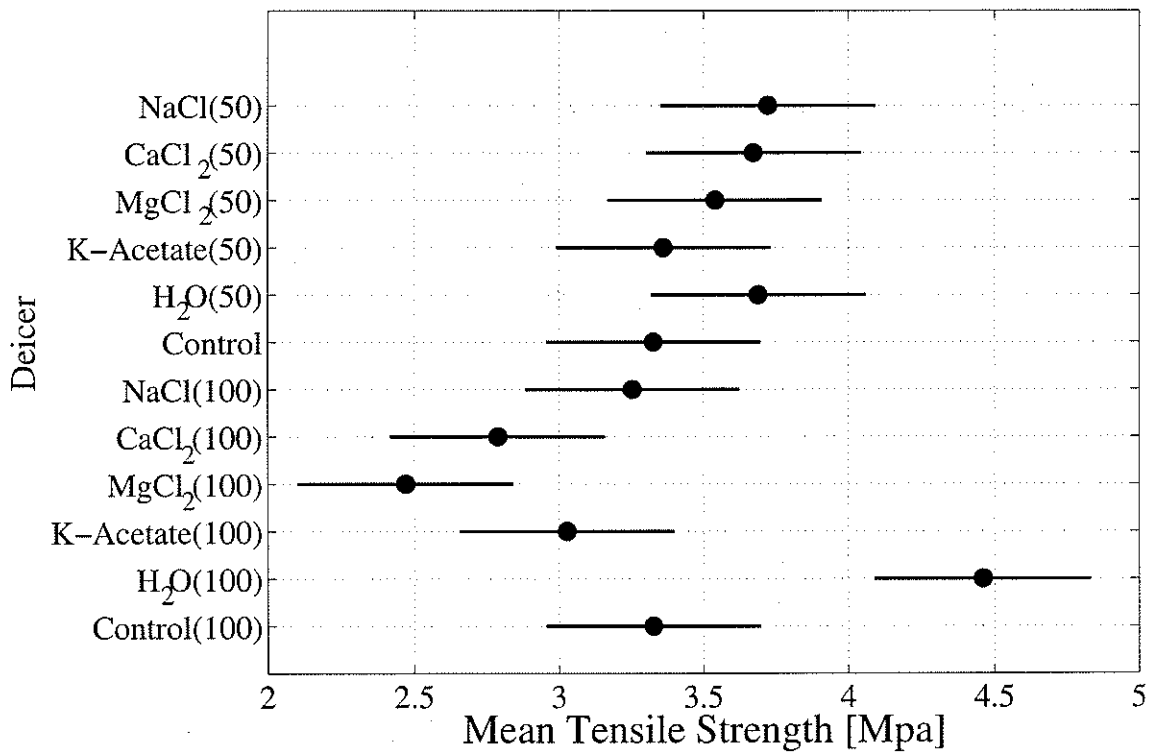


Figure 5.8: Comparison of Groups Between 50 and 100 Cycles

5.5 Flexural Strength Tests

Prior to the start of the test, visual examinations of the specimens were carried out. The calcium chloride samples exhibited “very severe” scaling, whereas the sodium chloride specimens exhibited “slight” scaling. The magnesium chloride, potassium acetate, and distilled water specimens exhibited no scaling at the end of cycling period. Figures 5.9 to 5.14 illustrate the initial condition of the sodium chloride, calcium chloride, magnesium chloride, potassium acetate, distilled water and control specimens, respectively.

5.5.1 Load Deflection Behavior

The load-deflection curves were plotted for all beam specimens. As mentioned in the previous chapter, the deflections of all beams were measured using LVDTs located at the mid-span of each beam. Figure 5.15 illustrates the load-deflection behavior of the control sample. Only one load-deflection curve is illustrated, as the LVDT on the second control specimen did not display a proper reading. The control specimen initially exhibited a linear load-deflection curve with virtually no deflection occurring in the beam until the onset of cracking in the tension zone. The control specimen cracked at 10.5kN at a deflection of 0.3mm. After the initiation of cracking, the load-deflection curve remained linear, but at a reduced slope than observed previously. At 35kN, the progressive cracking resulted in a further reduction in slope and the behavior became increasingly non-linear as prominent flexural cracks began to form. At 44kN, a large shear crack formed from near the support towards the mid-span of the beam, and was accompanied by a load drop on the load-deflection curve. The loading increased after 44kN, reflecting the redistribution of load to the un-cracked portions of the beam. At 64kN, yielding of the reinforcing steel began. Failure occurred at 78kN at a deflection of 16mm. The failure was caused by the crushing of concrete in the compression zone.



Figure 5.9: Condition of Sodium Chloride Specimen Prior to Flexure Test

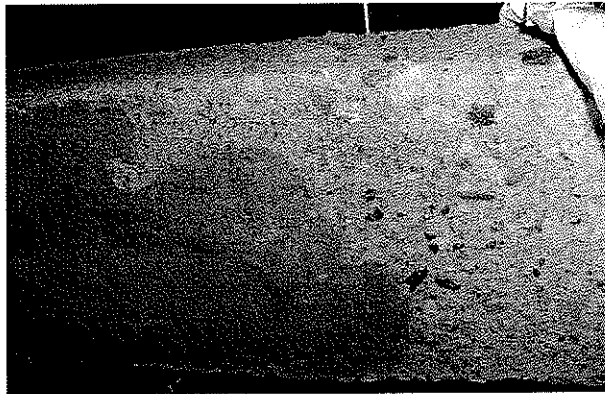


Figure 5.10: Condition of Calcium Chloride Specimen Prior to Flexure Test

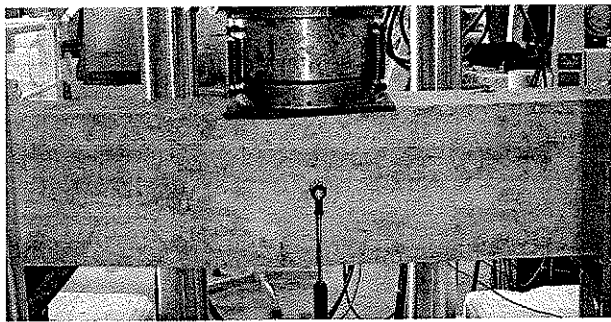


Figure 5.11: Condition of Magnesium Chloride Specimen Prior to Flexure Test

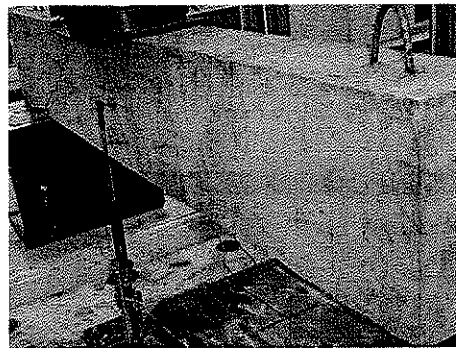


Figure 5.12: Condition of Potassium Acetate Specimen Prior to Flexure Test

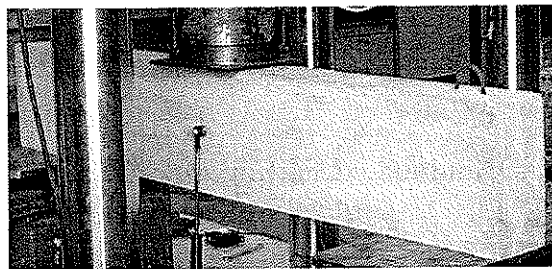


Figure 5.13: Condition of Distilled Water Specimen Prior to Flexure Test

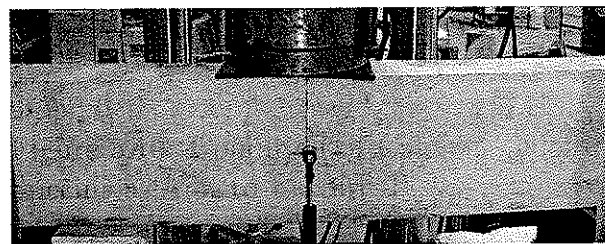


Figure 5.14: Condition of Control Specimen Prior to Flexure Test

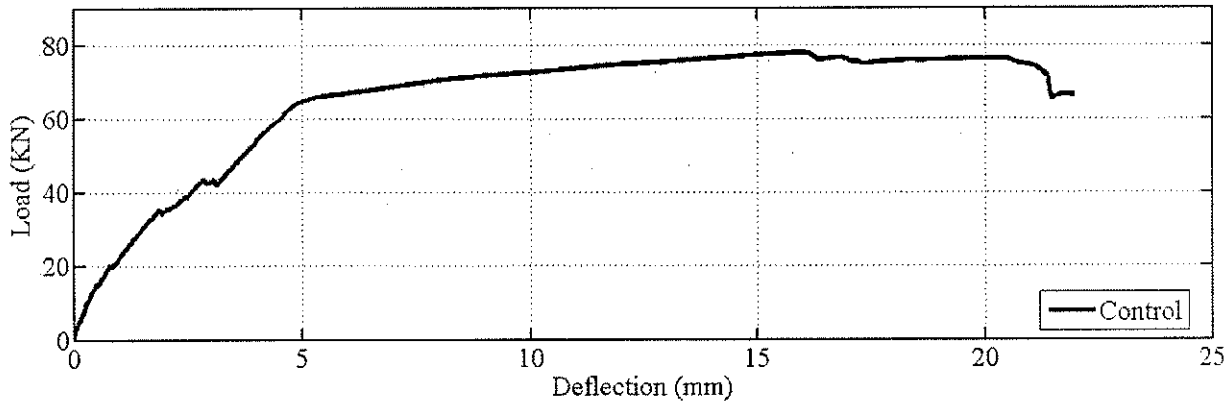


Figure 5.15: Load Deflection Behavior of Control Specimen

The load-deflection behavior of the concrete beams subjected to deicing chemicals and freeze-thaw cycles is illustrated in Figures 5.16 to 5.20, for NaCl, $CaCl_2$, $MgCl_2$, K-Acetate, and distilled water specimens, respectively. The sodium chloride specimens initially exhibited a linear load-deflection behavior until the onset of cracking in the tension zone. Specimen #1 cracked at 14kN at a deflection of 0.5mm, and Specimen #2 cracked at 12kN at a deflection of 0.56mm. After the initial cracking, the load-deflection curve for both specimens remained linear, but with a reduced slope until approximately 50kN. At this point, there was a slight dip in the load-deflection curve for both specimens indicating that further significant cracking occurred. It was observed at this point that a large shear crack formed from the support towards the mid-span of the beam. The load increased after 50kN, reflecting the redistribution of load to the un-cracked portions of the beam. Yielding of both samples began at approximately 64kN. Failure in Specimen #1 and Specimen #2 occurred at 77kN, and 78kN respectively at a deflection of 16.8mm. The failure was precipitated by crushing of the concrete in the compression zone.

The calcium chloride specimens exhibited a similar load-deflection relationship as the sodium chloride specimens. Both Specimen #1 and Specimen #2 exhibited a linear load-deflection relationship until the onset cracking. Specimen #1 cracked at 5kN at a deflection of

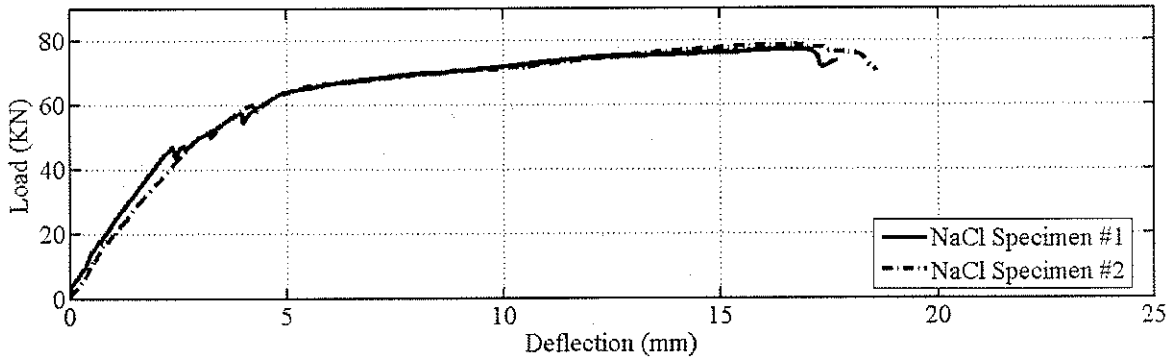


Figure 5.16: Load Deflection Behavior of Sodium Chloride Specimens

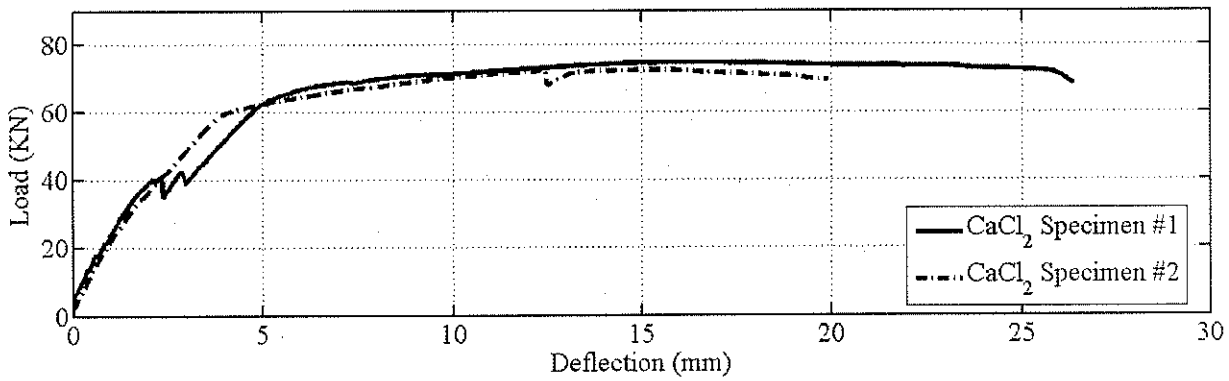


Figure 5.17: Load Deflection Behavior of Calcium Chloride Specimens

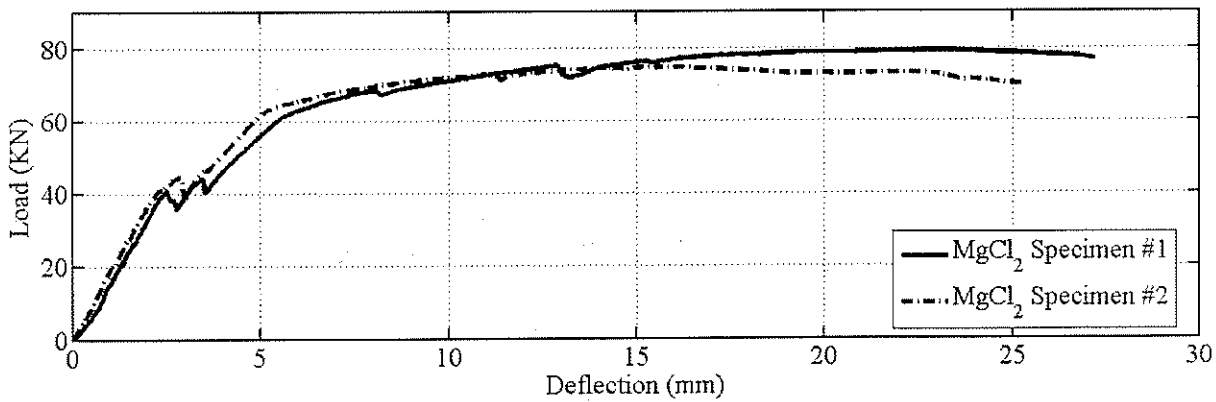


Figure 5.18: Load Deflection Behavior of Magnesium Chloride Specimens

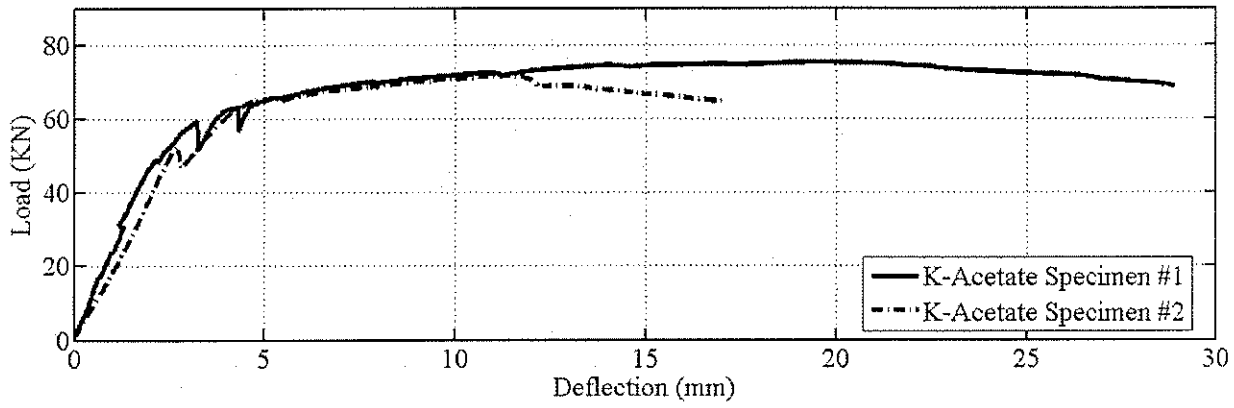


Figure 5.19: Load Deflection Behavior of Potassium Acetate Specimens

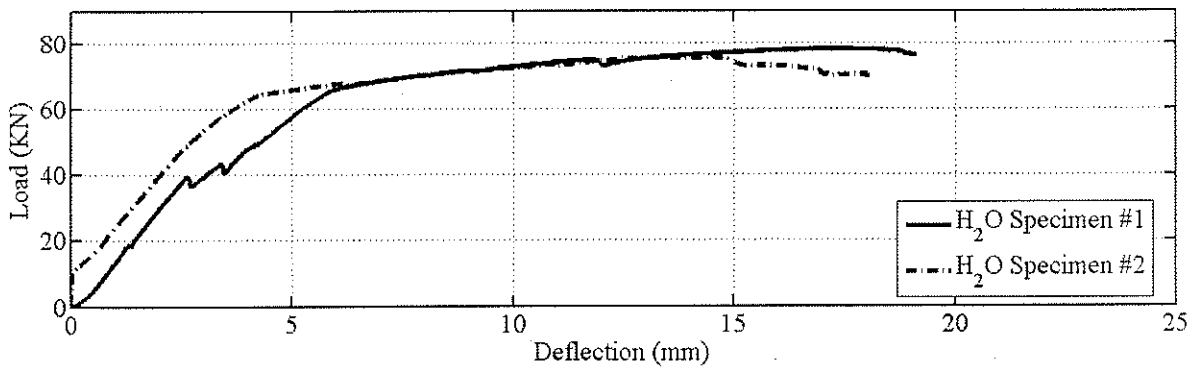


Figure 5.20: Load Deflection Behavior of Distilled Water Specimens

0.0067mm, and Specimen #2 cracked at 1.9kN at a deflection of 0.005mm. The lower cracking load for Specimen #1 and Specimen #2 may be attributed to the severe scaling in the beam as a result of the freeze-thaw and deicing chemical deterioration. After the initial crack, the slope of the load-deflection curve for both specimens was once again linear, but with a reduced slope. Further loading resulted in increasingly non-linear behavior caused by the progressive formation of cracks. Discontinuities in the curve reflected the redistribution of the load to un-cracked portions of the beam. Failure in Specimen #2 occurred at 72kN at a deflection of 12mm. Failure in Specimen #1 occurred at 74kN at a deflection of 16mm. Similar to the sodium chloride specimens, failure occurred by crushing of the concrete in the compression zone.

The magnesium chloride specimens exhibited an approximately linear load-deflection relationship until the onset of cracking in the tension zone. Specimen #1 cracked at 15kN at a deflection of 1mm and Specimen #2 cracked at 11kN at a deflection of 0.63mm. The slope of the load-deflection curve was linear for both specimens with a reduction in slope which reflected the initiation of cracking. Further loading resulted in increasingly non-linear behavior caused by the development of significant flexure and shear cracks. Yielding of the tension steel in both samples began at approximately 64kN. Further load caused the flexural cracks to migrate higher into the compression zone. At 72kN, horizontal cracks were observed in Specimen #1 at the level of the reinforcing steel, indicating that the reinforcing steel de-bonded from the concrete. Failure occurred at 74kN in Specimen #2 at a deflection of 18mm. Failure occurred in Specimen #1 at 79kN at a deflection of 23mm. The failure mode for both beams was concrete crushing.

Similar to the other test results, the potassium acetate specimens initially exhibited a linear load-deflection curve until initial cracking in the tension zone. Specimen #1 cracked at 10.3kN at a deflection of 0.4mm and Specimen #2 cracked at 7.1kN at a deflection of 0.37mm. After the initiation of cracking, the load-deflection curve remained linear, with a somewhat reduced slope. Yielding of the reinforcing steel in Specimen #2 occurred at

approximately 65kN. Failure in Specimen #1 occurred at 75kN at a deflection of 20mm. Failure in Specimen #2 occurred at 71kN at a deflection of 11mm. The failure in both beams was precipitated by crushing of concrete in the compression zone.

Cracking of the distilled water specimens occurred at 8.5kN at a deflection of 0.74mm Specimen #1. After the initiation of cracking, the slope of the load-deflection curve was reduced. At 65kN, yielding of the reinforcing steel occurred in both beams. Failure occurred at 78kN in Specimen #1 at a deflection of 19mm. The failure was precipitated by the crushing of concrete in the compression zone.

5.5.2 Cracking Load

The formation of cracks occur in concrete when the tensile stress in the beam exceeds the concrete tensile strength. Because cracking results in a reduction in the slope of the load-deflection curve, the magnitude of the cracking load is taken as the value at which the slope of the load-deflection plot deviates from its original straight line behavior. Table 5.13 summarizes the cracking load for all specimens and the percentage-change in cracking load with respect to the control sample. The results of the flexural strength test indicate that the $CaCl_2$ experienced a reduction in cracking load with respect to the control sample. The cracking load for Specimen #1 and Specimen #2 was 51% to 82% lower then the control samples. This was 2 times lower then the cracking load of the $MgCl_2$ specimens, 1.4 times lower then the K-Acetate specimens, and 2.5 times lower then the NaCl specimens. The low cracking load in the calcium chloride specimens is partly attributed to the severe scaling incurred by the specimens as the more severely scaled specimen had a lower cracking load.

The distilled water and potassium acetate samples both experienced increases and decreases in cracking load with respect to the control samples. The cracking load of the distilled water samples was approximately equal to or 20% less then the cracking load of the control

Table 5.13: Cracking Load

Deicing Chemicals	Cracking Load [kN]		%Change with respect to Control Samples	
	Sample #1	Sample #2	Sample #1	Sample #2
K-Acetate	7.1	17.1	-32.6	62.4
$CaCl_2$	1.9	5.1	-82.4	-52.0
$MgCl_2$	10.7	15.0	1.2	42.8
NaCl	12.4	14.3	17.3	35.7
H_2O	8.5	10.1	-18.9	-4.3
Control	10.5			

sample. Similarly, the potassium acetate samples showed a large range in cracking load from a 1.5 times reduction in cracking load to 1.7 times increase in cracking load. The reduction in cracking load for the distilled water specimens may be attributed to the freeze-thaw deterioration of the test samples. The ice crystals formed during freezing may have resulted in the development of hydraulic or osmotic pressures caused by the movement of water towards the freezing sites. However, the deterioration is limited due to the continuing hydration of the samples, which may have decreased the overall deterioration. The results obtained in the potassium acetate specimens suggest that the magnitude of cracking was sensitive to the formation of reaction products within the concrete microstructure.

The cracking load of both the $MgCl_2$ and NaCl samples were higher than the cracking load of the control samples. The cracking load of the $MgCl_2$ was approximately equal to or 1.4 times greater than the control sample. The cracking load of the NaCl samples was over 1.1 to 1.4 times greater than the control specimens. The higher cracking load in the $MgCl_2$ may have been caused by the formation of reaction products within the concrete microstructure. The higher cracking load in the NaCl specimens may be attributed to progressive densification of concrete structure as the sodium chloride penetrated the beam samples during the freeze-thaw deterioration and continued hydration of the samples cycling period.

Table 5.14: The Effect of Deicing Chemical Exposure on Ultimate Load

Deicer	Ultimate Load [kN]	% Change in Load
NaCl	77.1-78.9	-1.0 to 1.6
$MgCl_2$	79.1-74.7	-4.1 to 2.3
$CaCl_2$	74.1-72.3	-5.0 to -7.1
K-Acetate	71.4-75.3	-2.6 to -8.3
H_2O	78.1-75.4	-3.2 to 1.1
Control	77.3-77.9	

5.5.3 Ultimate Load

Table 5.14 summarizes the ultimate load and percent change in load compared to the control samples for all of the beam specimens. The ultimate strength was governed by the yielding of the reinforcing bar and subsequent crushing of concrete in the compression zone. An examination of the load-deflection curves in the previous section shows that with the exception of the severely scaled calcium chloride sample, all of the specimens began to yield at approximately 64kN. The severely scaled $CaCl_2$ specimen, however, began yielding at 60kN. This suggests that the reduced strength of the cement paste as a result of chloride ingress may have caused wider cracks in the concrete leading to earlier yielding of the bars. An examination of the cracks in the tension zone reveals that all of the beam specimens have approximately a similar cracking pattern. Figure 5.21, and Figure 5.22 illustrates the cracking pattern at failure for the control specimens. Figures 5.23 to 5.32 illustrate the cracks at failure for samples subjected to deicing chemicals.

5.6 Modulus of Elasticity

The static modulus test was carried out to measure the changes in the instantaneous elastic deformation of concrete when subjected to different deicing chemicals. The modulus of

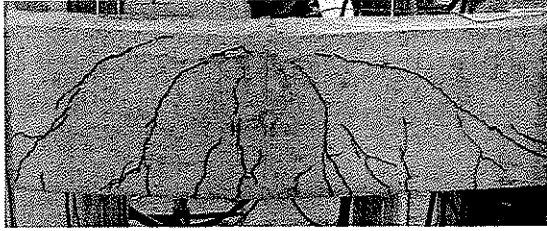


Figure 5.21: Crack Pattern of Control Specimen #1



Figure 5.22: Crack Pattern of Control Specimen #2

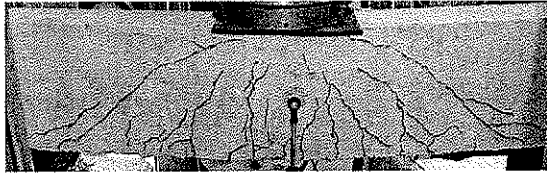


Figure 5.23: Crack Pattern of Sodium Chloride Specimen #1

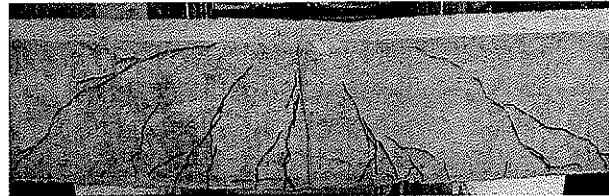


Figure 5.24: Crack Pattern of Sodium Chloride Specimen #2

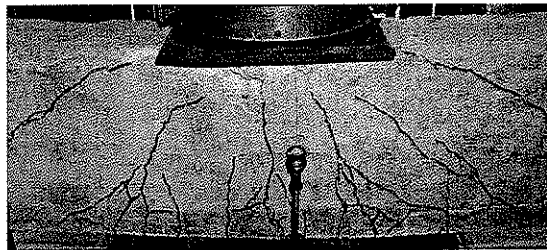


Figure 5.25: Crack Pattern of $MgCl_2$ Specimen #1

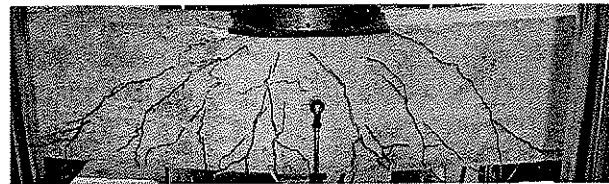


Figure 5.26: Crack Pattern of $MgCl_2$ Specimen #2

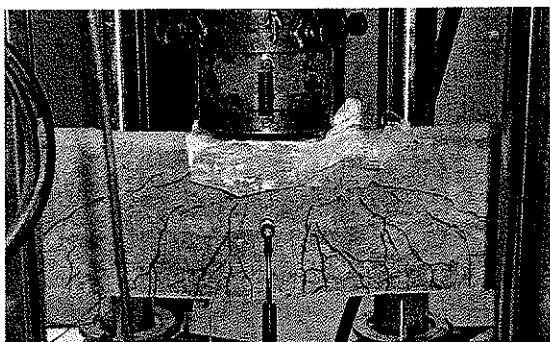


Figure 5.27: Crack Pattern of $CaCl_2$ Specimen #1

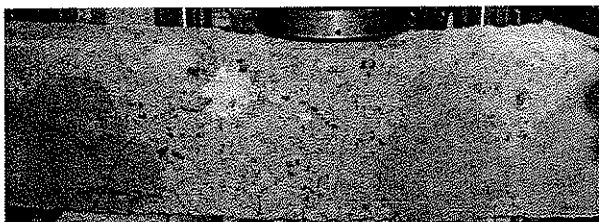


Figure 5.28: Crack Pattern of $CaCl_2$ Specimen #2

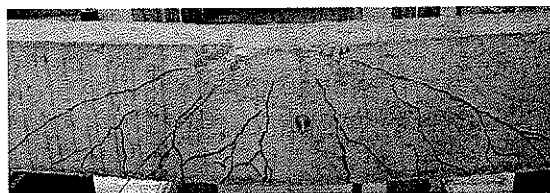


Figure 5.29: Crack Pattern of K-Acetate Specimen #1

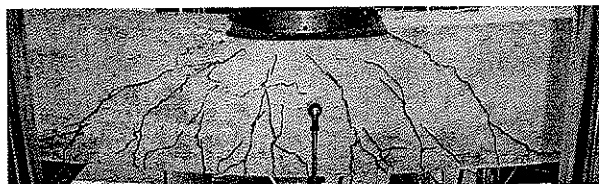


Figure 5.30: Crack Pattern of K-Acetate Specimen #2

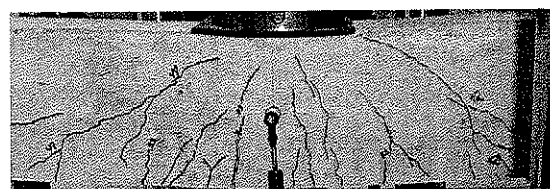


Figure 5.31: Crack Pattern of Distilled Water Specimen #1

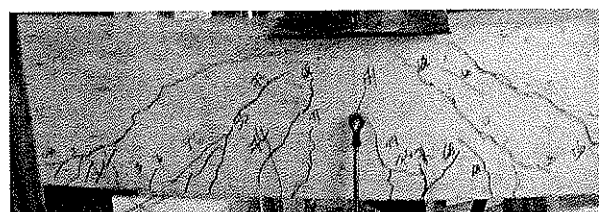


Figure 5.32: Crack Pattern of Distilled Water Specimen #2

Table 5.15: The Effect of Deicing Chemicals on the Static Modulus of Elasticity

Deicing Chemical	Modulus of Elasticity [MPa]	
	50 Cycles	100 Cycles
K-Acetate	24960	20508
$CaCl_2$	14997*	22488
$MgCl_2$	22521	19985
NaCl	23466	32977*
H_2O	21976	36852*
Control	18866	

*Values Appear Erroneous

elasticity values at 50 and 100 cycles were determined using longitudinal strains recorded during the static modulus test. As mentioned in the previous chapter, the strain profiles were measured using a 2-inch strain gage placed at center of each cylinder. A total of 5 cylinders were tested for the static modulus values (one cylinder per deicer group). The stress for each load point was calculated as the load divided by the cross-sectional area of the test sample. The modulus of elasticity was taken as the slope of the chord drawn between two specified points on the stress-strain curve. The equation is given as follows:

$$E = \frac{(S_1 - S_2)}{(\epsilon_2 - 0.000050)} \quad (5.12)$$

where E = the chord modulus of elasticity, S_2 = the stress corresponding to 40% of the ultimate load, (MPa), S_1 = the stress corresponding to a longitudinal strain of 0.5×10^{-4} , (MPa), and ϵ_2 = the longitudinal strain produced by stress S_2 [7]. Figure 5.33 and Figure 5.34 illustrate the stress-strain curves of the test samples at 50 cycles and 100 cycles, respectively. Table 5.15 summarizes the results of the static modulus of elasticity tests at 50 and 100 cycles.

The static modulus values of the specimens immersed in deicing solutions and distilled water were compared to the static modulus value of the control sample exposed only to laboratory

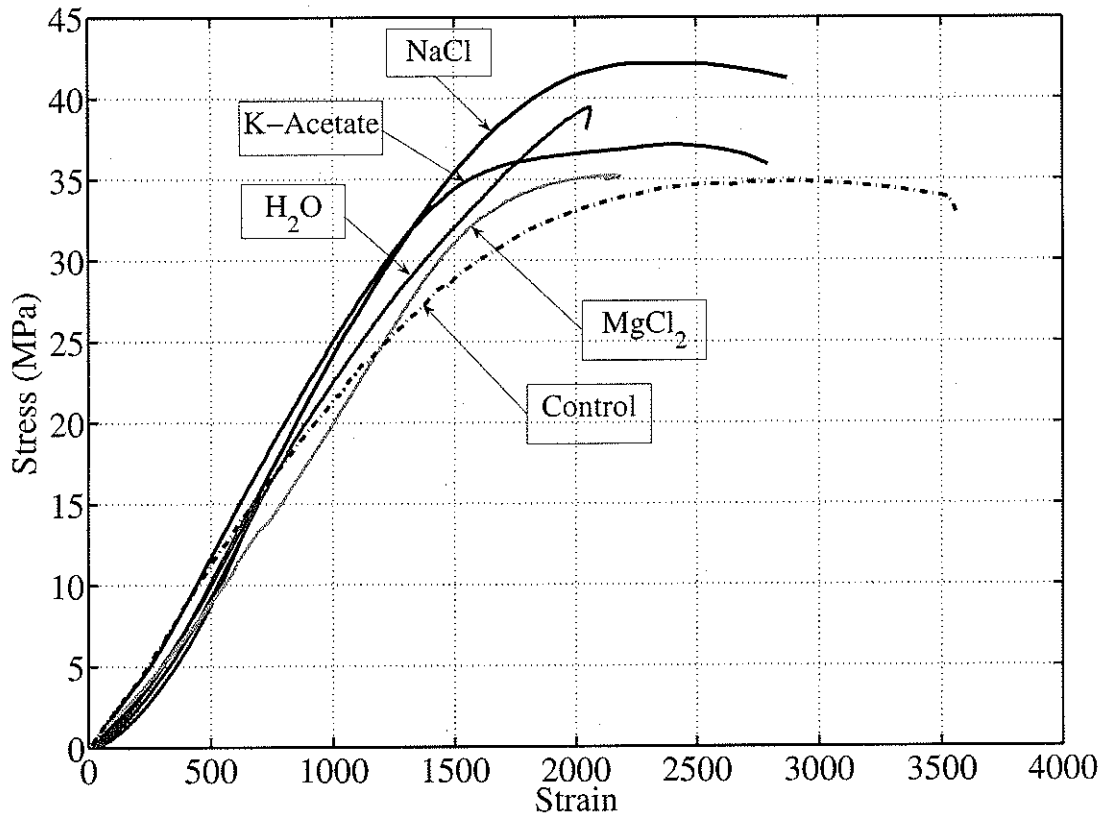


Figure 5.33: Stress-Strain Behavior of Test Samples at 50 Cycles

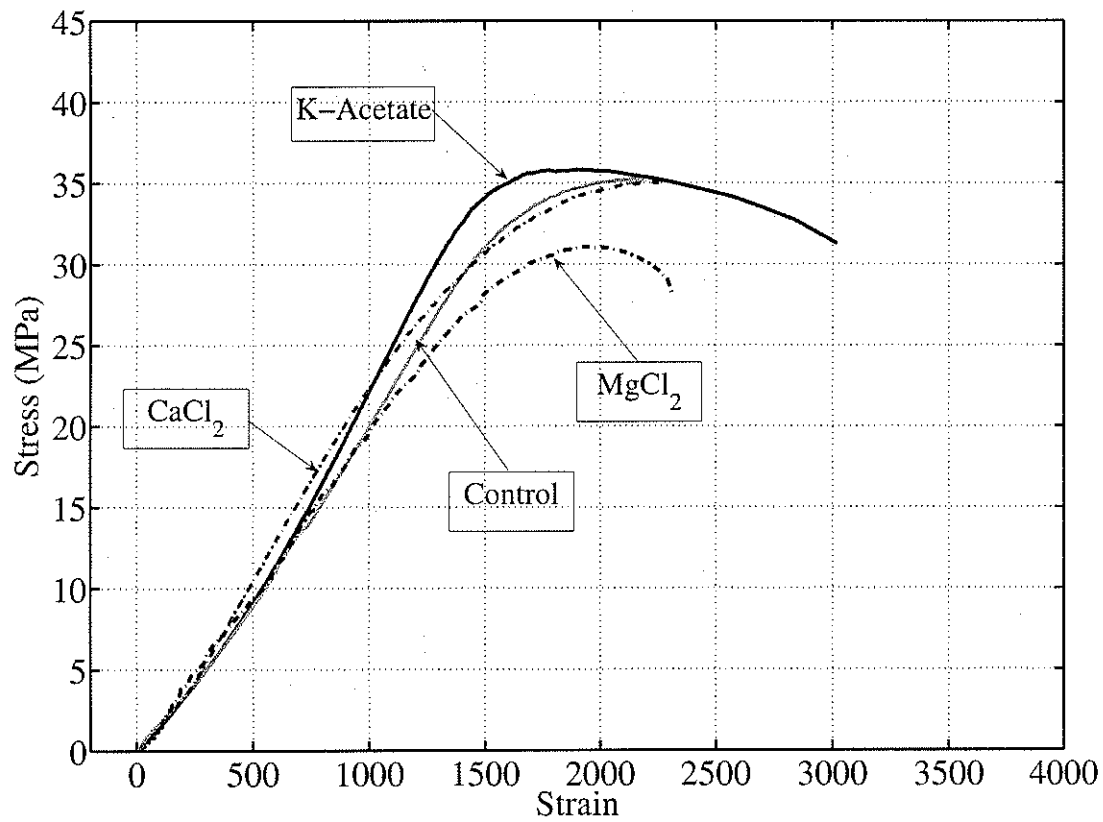


Figure 5.34: Stress-Strain Behavior of Test Samples at 100 Cycles

Table 5.16: Change in Chord Modulus of Elasticity Values Compared to Control Samples

Deicing Chemical	%Change in Chord Modulus	
	50 Cycles	100 Cycles
K-Acetate	+31	+9
$CaCl_2$	-21*	+19
$MgCl_2$	+19	+6
NaCl	+24	+75*
H_2O	+16	+95*

*Values Appear Erroneous

air. After 50 cycles, the static modulus of all samples increased. After 100 cycles, the calcium chloride-immersed specimen exhibited a 19% increase in the chord modulus value in comparison to the control specimen. The increase in chord modulus value is attributed the variations of the test samples due to the non-homogeneity of the concrete specimens. The increases and decreases in static modulus values are attributed to the presence or absence of coarse aggregates at the location of the concrete strain measurement. The strain gauge readings also appear to be extremely sensitive to the placement of the gauge on the test samples and the placement procedure. The presence of aggregates and the thickness of the adhesive layer between the strain gage and the concrete surface appear to significantly affect the strain readings measured by the gauge. To obtain the correct value of modulus of elasticity, the cylinder has to be loaded concentrically. In some cases, this may not have been carried out with due diligence and hence some results cannot be used for analysis. In general, however, it appears that the static modulus value was not affected by the deicing chemicals or freeze-thaw cycling. The change of the static modulus values at 50 and 100 cycles are summarized in Table 5.16.

Because of the high variability given by the results of the static modulus test, the apparent modulus of elasticity was calculated using the beam specimen data obtained during the flexural strength tests. The apparent modulus was calculated as the slope of the linear portion of the load-deflection curve for all beam samples. In addition, the moment-curvature

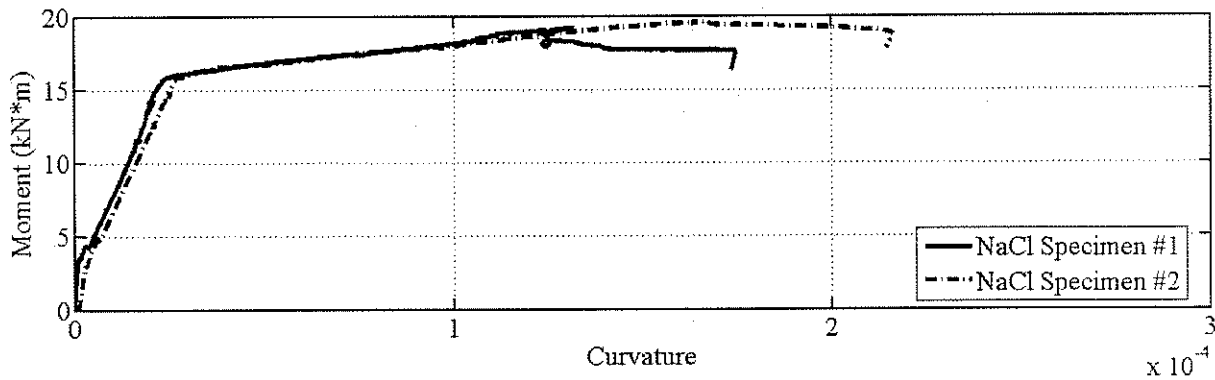


Figure 5.35: Moment-Curvature Relationship for Sodium Chloride Specimens

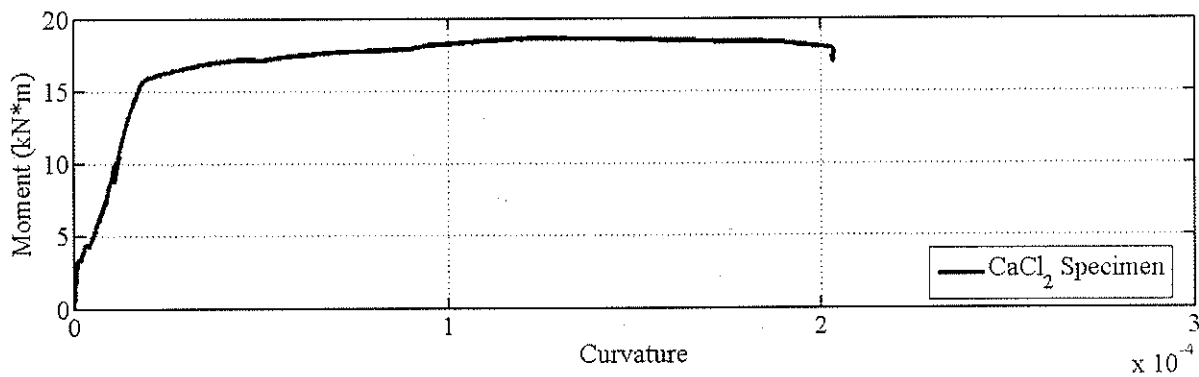


Figure 5.36: Moment-Curvature Relationship for Calcium Chloride Specimens

relationship for all of the beam samples were plotted, and the stiffness was calculated as the slope of the linear portion of the moment-curvature diagrams. The trend in stiffness was compared to the trend observed in the apparent modulus. Figures 5.35 to 5.38, illustrates the moment-curvature diagrams for NaCl, $CaCl_2$, $MgCl_2$, and control samples, respectively. The moment-curvature relationships for the distilled water and potassium acetate samples are not plotted, as the pi gages did not display proper readings. The apparent modulus of elasticity values are summarized in Table 5.17.

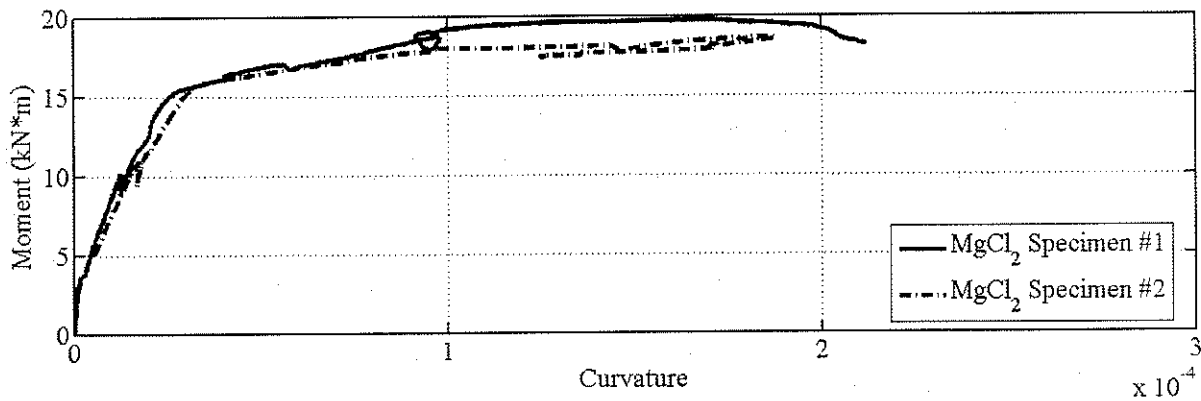


Figure 5.37: Moment-Curvature Relationship for Magnesium Chloride Specimens

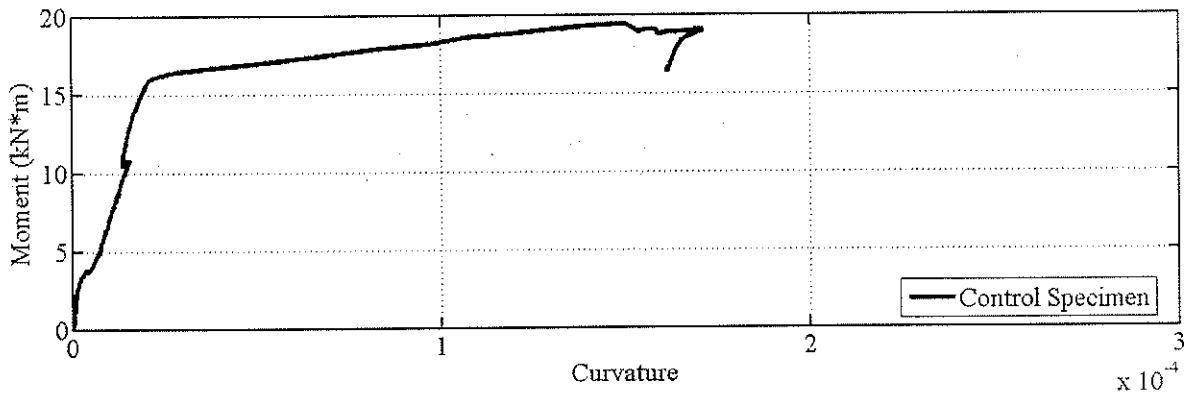


Figure 5.38: Moment-Curvature Relationship for Control Specimens

Table 5.17: Apparent Modulus of Elasticity

Deicing Chemicals	Apparent Modulus of Elasticity		% -Change with respect to Control Samples	
	Sample #1	Sample #2	Sample #1	Sample #2
K-Acetate	21.4	19.9	+38.9	+29.2
$CaCl_2$	17.8	14.1	+15.5	-8.6
$MgCl_2$	17.6	17.9	+14.3	+16.3
NaCl	18.4	16.1	+19.5	+4.5
H_2O	15	16	-2.6	+4.9
Control	15.4			

The results indicate that the slope of the moment-curvature diagrams for all of the beam specimens do not appear to deviate significantly from the control sample. The values of the apparent modulus indicate that only the severely scaled calcium chloride specimen exhibited a decrease in the modulus of elasticity with respect to the control specimens. The apparent modulus values for the other beam specimens, however, were approximately equal to or greater than the apparent modulus value of the control specimen. The results indicate that modulus of elasticity values were not severely affected by the deicing solution or freeze-thaw cycles.

5.7 Water Soluble Chlorides Test

The results of the water soluble chlorides test are illustrated in Figure 5.39. One sample was taken for each deicing chemical at the depths tested. The results show that in general, the chloride concentrations for all specimens decreased with sample depth. The magnitude of chloride concentration at a given depth, however, was influenced by the type of deicer. The calcium chloride samples had the greatest concentration of free chlorides near the surface layer when compared to the $MgCl_2$ and NaCl specimens. At the surface, the chloride concentration in the $CaCl_2$ was 1.3%, which was over 1.4 times greater than the chloride concentration in the $MgCl_2$ samples and 1.5 times greater than the chloride concentration of the NaCl sample at this depth. Below the surface layer, however, the chloride content in the $CaCl_2$ dropped considerably with depth. At 12mm-23mm, the concentration of chlorides was 0.29%, which was 77% lower than the chloride concentration at the surface layer. At 40mm-48mm, which was the maximum sampling depth of the $CaCl_2$ specimen, the chloride concentration decreased to 0.07%. In contrast, the NaCl samples had a much lower concentration of chlorides at the surface than the $CaCl_2$ specimens, but exhibited a more gradual decrease of water soluble chlorides with sampling depth. The NaCl samples had Cl concentration of 0.88% in the surface layer, and decreased by 34% to a chloride concentra-

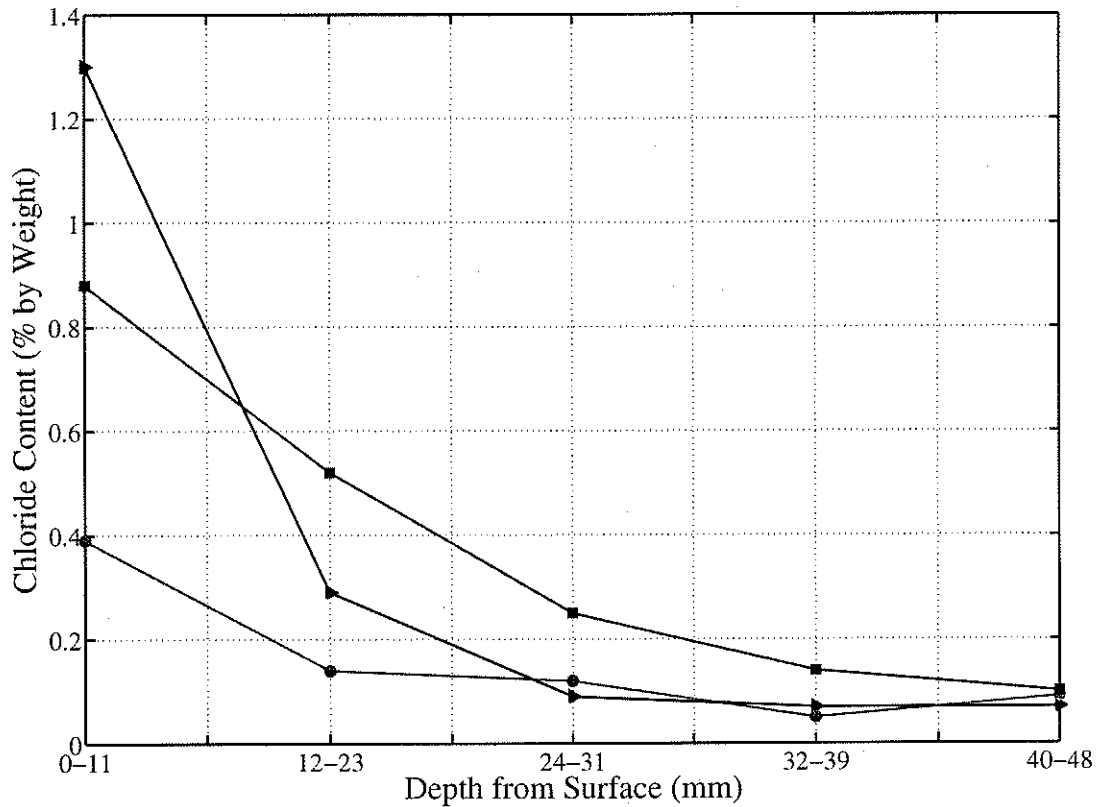


Figure 5.39: % Concentration of Water Soluble Chlorides with Depth

tion of 0.52% in the second layer. At the maximum sampling depth, the Cl concentration was 0.1%, which was 30% higher than the Cl concentration of the $CaCl_2$ specimen at this depth and 10% higher than the Cl concentration of the $MgCl_2$ specimen. The chloride ion data for the magnesium chloride samples indicates that at the surface layer, the $MgCl_2$ samples had a chloride concentration of 0.39%. At 10-20mm below the surface, the chloride concentration decreased to 0.14%. At 21mm-35mm, the Cl concentration decreased by 14% to 0.12%. The Cl concentration further decreased to 0.05% at a sampling depth of 36mm-44mm. The Cl concentration increased slightly at a sampling depth of 45mm-54mm to a final Cl concentration of 0.09%.

The results suggest that there is a considerably greater amount of chlorides in the free form in the calcium chloride deicing solution that have not bound with the hydration products of cement than in the sodium or magnesium chloride specimens. However, the results of the test did not indicate significant penetration of ions into the interior of the concrete. At the maximum sampling depth 40mm-48mm, the concentration of Cl ions in all of the specimens was approximately the same (ranging from 0.07% to 0.1%) despite the higher Cl ion concentration at the surface layer of the $CaCl_2$ specimens. The reduced quantity of the free chlorides in the interior of the concrete was most likely caused by the presence of the organic corrosion inhibitor in the deicing solution, which acts to protect the reinforcing steel by reducing the permeability of the concrete, and thereby limiting the access of oxygen, moisture, and chlorides to the level of reinforcement [47].

An examination of the chloride data for the $MgCl_2$ samples suggest further penetration of the chloride ions in comparison to the calcium chloride specimens, and less penetration of the chloride ions in comparison to the NaCl specimens. The reduced penetration of the Cl ions may have been attributed to the reduced permeability of the concrete material caused by the presence of the corrosion inhibitor in the deicing solution. The extent of the reduced ingress of the Cl ions, however, was not as effective as the suppression of chloride transport in the calcium chloride sample.

The chloride data indicates that the Cl ions in the NaCl samples penetrated deeper than those in the $CaCl_2$ and $MgCl_2$ solution, despite the higher concentration of free chloride ions at the surface of $CaCl_2$ sample. The severe scaling of the sample indicate that the freeze-thaw cycles generated internal pressures within the sample, causing internal micro-cracking, and thus increasing the permeability of the paste. The results suggests that the damage due to water soluble chlorides in the NaCl deicing chemical may be more severe than the damage caused by the chlorides in the $CaCl_2$ and $MgCl_2$ deicing chemicals. A faster rate of penetration may allow for rapid accumulation of chloride ions within the concrete over long-term applications. However, the larger quantity of free chlorides formed in the $CaCl_2$

solution suggests that in the absence of a corrosion inhibitor, the severity of damage caused by free chlorides could potentially be greater. The flexural test samples have shown that the permeability and concrete resistance is severely compromised upon the onset of scaling as shown by the severe deterioration incurred by the calcium chloride beam samples.

Chapter 6

Summary, Conclusions, and Recommendations

6.1 Summary

Many studies have demonstrated that deicing chemicals often exacerbate concrete damage originating from freeze thaw cycles. In North America, chloride-induced deterioration has been of major concern for many years. Furthermore, there has been an increasing demand for alternate deicers as traditional deicing chemicals have been associated with environmental and corrosion damage. The new deicers include calcium chloride, magnesium chloride, and potassium acetate. The deleterious effects caused by these deicing chemicals have not been fully documented.

This study is concerned with a comparative evaluation of several deicing chemicals currently used or considered for use by the industry in the presence of freeze-thaw cycles. The performance of the deicing chemicals is evaluated on the basis of changes in mechanical properties, and extent of concrete deterioration. In order to carry out the objectives of this investigation,

118 concrete cylinders, 10 concrete prisms, and 12 reinforced concrete beams were fabricated in order to determine the changes in scaling resistance, and physical and mechanical properties of the concrete elements. The samples were placed in an environmental chamber and subjected to freeze-thaw cycles ranging from $-25^{\circ}\text{C} \pm 3^{\circ}\text{C}$ to $23^{\circ}\text{C} \pm 2^{\circ}\text{C}$ over a period of 6 months. Concrete deterioration during the freeze-thaw cycles was evaluated on the basis of mass loss or gain and degree of scaling. The changes in the mechanical properties of concrete were determined in terms of loss of tensile, compressive and flexural strength, and changes in the static modulus of elasticity. The results of the compression test were also compared to samples stored in deicing solutions in the absence of freeze-thaw cycles. Finally a Water Soluble Chlorides Test was carried out by the National Testing Laboratories to evaluate the penetration of corrosion-inducing chlorides with depth. Table 6.1 summarizes the findings of the study. The deicing chemicals are rated based on their performance on the variables indicated. A deicing chemical was rated "severe" for a variable if the samples showed the greatest loss in strength or concrete damage when compared to the performance of the other deicers. A mild rating was given, if the deicer did not significantly affect the strength or deterioration of the concrete samples. Ratings of "moderate" and "significant" were given when a deicing chemical appeared to affect the strength and deterioration of the concrete samples, but did not represent the most severe case.

The results indicate that, in general, the magnesium chloride solutions produced the greatest severity of strength deterioration. The potassium acetate samples exhibited an earlier strength reduction; however, the severity of degradation was approximately equivalent or surpassed by the calcium and magnesium chloride solutions with progressive cycles. The delayed deterioration may have been partly attributed to the presence of corrosion inhibitors in the CaCl_2 and MgCl_2 solutions, which may have acted to reduce the permeability of the concrete samples. The lower cracking load in the flexural strength tests for the CaCl_2 indicates, however, that the onset of scaling may increase the severity of damage in the calcium chloride specimens. Finally, the NaCl samples experienced only a slight reduction

Table 6.1: Effect of Deicing Chemicals on the Strength and Deterioration of Concrete

Variable	Sodium Chloride	Calcium Chloride	Magnesium Chloride	Potassium Acetate	Distilled Water
Scaling	Severe	Mild	Mild	None	Moderate
Compressive Strength	Mild	Moderate	Severe	Significant	None
Tensile Strength	Mild	Significant	Severe	Moderate	None
Static Modulus of Elasticity	None	None	None	None	None
Cracking Load	None	Severe	None	Mild	Moderate
Ultimate Load	None	Moderate	None	None	None
Penetration of Water Soluble Chlorides	Significant	Moderate	Mild	N/A	N/A

in overall strength, but displayed significant surficial deterioration and chloride penetration. The decreased strength is attributed to the expansive internal pressures caused by the combination of the freeze-thaw cycles and the salt solution, as well as the reduction in surface area caused by scaling as a result of these damage mechanisms. This can substantially be reduced if air-entrained concrete is used. The deterioration of strength of the concrete samples was believed to be caused by the generation of pressures and reduction of inter-particle bonds between the paste and the aggregate. This experimental investigation supports the conclusions that follow.

6.2 Conclusions

6.2.1 Scaling

- The sodium chloride solution produced the most severe scaling deterioration of the 4 deicing chemicals considered in the current investigation. The scaling tests carried out on the prism specimens indicated that at 100 cycles, the sodium chloride samples exhibited a much greater degree of scaling than the other test samples with an average scale rating of 3.5, indicating moderate to severe scaling. All of the other specimens accumulated a maximum scale rating of 0.5 at the end of 100 cycles, indicating the occurrence of extremely minimal scaling. An examination of the cumulative mass of scaled-off particles taken at regular intervals throughout the cycling period reveals that the mass of scaled particles for the sodium chloride samples was over 12 times greater than for the other specimens. The severe scaling is believed to have manifested as a result of the damaging internal pressures which may form through the growth of crystals in the concrete pore structure.
- The potassium acetate specimens showed the least amount of scaling with virtually no scaling at the end of 100 cycles. Furthermore, none of the cylinders and beam specimens showed any scaling throughout the cycling period. The results agree with the investigation carried out by Wang et. al [68] which also indicated a lack of scaling in the samples subjected to potassium acetate. The results suggest that the potassium acetate deicer does not aggravate the deleterious physical damaging mechanisms caused by freeze-thaw cycles.
- The degree of scaling is sensitive to the non-homogeneity of the concrete samples. A comparison of the prism samples within the sodium chloride group revealed a difference in the severity of scaling between the two test samples. One of the test specimens exhibited extremely severe scaling with a layer of coarse aggregate exposed over the

entire surface. The other test sample experienced only "slight to moderate scaling", with coarse aggregate visible only in scattered areas. The scaling test demonstrates how the test sample and laboratory conditions impacts the results. The disparity of results is attributed to the surface preparation of the samples. Thus, concrete finishing needs to be carried out with greater care. It is hypothesized that second test specimen would have experienced a similar severity of scaling with continued cycles, as the scaling progressed in a similar manner, but at a slower rate. Also, despite very minimal scaling of the $CaCl_2$ samples during the freeze-thaw cycles, the beam specimens displayed "extremely severe scaling" at the end of 100 cycles. The results indicate that severity of scaling increases very rapidly upon the onset of deterioration.

- The saturation conditions of concrete is critical for freeze-thaw deterioration in water. The prism specimens exhibited extremely minimal scaling until approximately 85 cycles, at which point an increased volume of scaled particles were observed on the surface. In contrast to the prism samples, the distilled water-immersed specimens experienced severe scaling during the freeze-thaw cycles, and began scaling shortly after 20 cycles. The disparity of the results between the prism samples and the cylinders is attributed to the degree of saturation of the test samples. The cylinders were considered to be in a "saturated" condition, thus allowing the development of osmotic and hydraulic pressures within the concrete microstructure. The internal pressures generated disruptive stresses leading to eventual scaling. The saturated condition was not present in the prism samples, thus decreasing the severity of scaling.

6.2.2 Mass Change

- A measurement of mass change of the cylinders showed that in general, the specimens immersed in deicing solution experienced a net gain in mass throughout the freeze-thaw cycles. The initial gain in mass was attributed to the absorption of the deicing solution. Further gain in mass was associated with the precipitation of salt crystals in

the voids, and formation of new reaction products between the deicing chemicals and concrete materials.

- The samples submerged in potassium acetate showed the highest absorption when compared to the specimens submerged in NaCl , CaCl_2 , and MgCl_2 solutions.
- The distilled water-immersed samples experienced a loss of mass at the end of 100 cycles. The mass loss in the distilled water-immersed samples was attributed to the severe scaling incurred by the specimens as a result of freeze-thaw damage. It is hypothesized that the the formation of ice crystals during freezing caused the development of dilative pressures in the pore cavities, which lead to eventual paste failure.
- A comparison of the mass change of specimens submerged in deicing chemicals in the absence of freeze-thaw cycles revealed a larger total weight gain at the end of 6 months. The results suggest that the deterioration caused by freeze-thaw cycles offset the total weight gain caused by the absorption of the deicing chemicals.

6.2.3 Compressive Strength

- The reduction of compressive strength in the samples immersed in calcium chloride, magnesium chloride and potassium acetate indicates that there is chemical reaction that occurs between the deicing chemicals and cement paste. In contrast, the sodium chloride-immersed samples did not show a significant reduction in strength, indicating that deterioration is more likely caused by physical mechanisms. This is in agreement with the results obtained by other researchers. A comparison of the strength of NaCl samples not subjected to freeze-thaw cycles to the samples that underwent environmental weathering showed a 13% increase in compressive strength. This further confirms that the damaging effects of sodium chloride on concrete are significantly influenced by freeze-thaw cycles. It is believed that the accumulation of freeze-thaw cycles created damaging internal pressures through the crystallization of salts and the movement of

fluid through the pore structure. The damage manifested in the form of scaling. In the absence of the freeze-thaw cycles, the NaCl samples underwent changes in the concrete microstructure through the deposition of hydration products in the pores, which lead to an increase in compressive strength.

- The calcium chloride, magnesium chloride, and potassium acetate samples all exhibited similar losses in strength when compared to the control samples. However, of the 4 deicing chemicals considered in the investigation, the magnesium chloride specimens exhibited the greatest loss in strength when the specimens were compared to the control samples. After 100 cycles, the specimens exhibited an 18.3% decrease in strength when compared to the control samples. An ANOVA test conducted on the experimental results showed that the changes in mean values of strength between the samples immersed in deicing solution and the control sample were statistically significant and not attributed to sampling error. The decrease in strength in the magnesium chloride-immersed samples is believed to be caused by the formation of reaction products between the magnesium chloride and the cement paste. Previous research has demonstrated that these products include brucite, and magnesium silicate hydrate. It is believed that the $MgCl_2$ reacted with calcium-silicate hydrate to form non-cohesive magnesium-silicate hydrate. The replacement of C-S-H with M-S-H reduces concrete strength because its reduced binding capacity destroys the inter-particle bonds between the cement paste and aggregate, thus weakening the cement paste.
- The strength reduction observed in the $CaCl_2$ -immersed specimens is also attributed to the formation of reaction products between the calcium chloride solution and the concrete. The growth of newly precipitated salts such as calcium oxychloride has been demonstrated in previous research to produce expansive pressures similar to hydraulic stresses generated during freeze-thaw deterioration [15]. These stresses may induce fractures at the interface between the aggregate and cement paste, thus decreasing the strength of the concrete.

- The comparable loss of strength in the potassium acetate-immersed specimens to the calcium and magnesium chloride-immersed samples indicates that there is a deleterious reaction that occurs between the potassium acetate deicer and cement paste. The specimens immersed in potassium acetate exhibited only a slightly lower reduction in compressive strength than the $MgCl_2$ samples. At 100 cycles, the potassium acetate-immersed samples exhibited a 17.6% decrease in strength when compared to the control group. An ANOVA analysis confirmed that the result was statistically significant. The specific mechanisms of deterioration are unknown at this time.
- The loss of strength as a result of calcium chloride, magnesium chloride and potassium acetate solutions is not aggravated by the presence of freeze-thaw cycles. A comparison of the compressive strength of the $CaCl_2$ -immersed samples in the absence of freeze-thaw cycles to the $CaCl_2$ -immersed samples that underwent environmental weathering reveals very little changes in the value of the mean compressive strength. The changes are attributed to natural sampling error as the range in values of strength were the same for both the F-T and continuous immersion samples. A comparison of the compressive strength of the K-Acetate samples in the absence of freeze-thaw cycles to the K-Acetate samples subjected to cycling revealed similar results. A comparison of the compressive strength of the $MgCl_2$ samples in the absence of freeze-thaw cycles to the samples subjected to freeze-thaw cycles shows a 14.6% reduction in mean compressive strength. An examination of the mass change of the samples shows that the weight gain of the specimens without freeze-thaw cycles was 2.6 times greater than the samples subjected to freeze-thaw cycles. The gain in weight is attributed in part to the formation of brucite and it is hypothesized that the continuous immersion of the samples allowed for the formation of more advanced stages of brucite within the concrete microstructure. Growth of brucite crystals in advanced stages of formation may induce expansive pressures leading to de-bonding of the aggregate between the paste-aggregate.

- The rate of deterioration in the calcium and magnesium chloride samples increased with progressive cycles. The potassium acetate samples initially experienced greater reduction in strength during the initial 50 cycles with almost two times greater strength reduction. However, from 50 to 100 cycles, the K-Acetate samples experienced an 11% reduction in strength whereas the calcium and magnesium chloride samples exhibited a 15% reduction in compressive strength. The delayed deterioration of the calcium and magnesium chloride specimens may be attributed to the presence of the corrosion inhibitor. It is suspected that the reduced permeability of the concrete as a result of the corrosion inhibitor increased the time required for the chemicals to penetrate and react with the concrete.
- The specimens immersed in distilled water experienced continuing hydration throughout the freeze-thaw cycles. At 100 cycles, the distilled water-immersed samples experienced a 7% decrease in strength. A portion of the increased strength caused by the continuing hydration was offset by the severe scaling incurred by the samples, and the resulting reduction in cross-sectional area.

6.2.4 Tensile Strength

- Of the 4 deicing chemicals considered in this investigation, the magnesium chloride specimens exhibited the greatest loss in tensile strength when compared to the control sample. At 100 cycles, the magnesium chloride specimens experienced a 26% reduction in strength, which was 1.5 times greater than the strength loss incurred by the calcium chloride-immersed samples and 2.8 times greater than the strength loss incurred by the potassium acetate samples. The reduced tensile strength of the magnesium chloride samples is again attributed to the replacement of C-S-H with M-S-H, which would lead to weakening of the cement paste.
- The potassium acetate-immersed specimens lost strength earlier than the calcium and

magnesium chloride-immersed samples. At 50 cycles, the potassium acetate samples exhibited 0.9% increase in tensile strength compared to the 6% and 10% increase incurred by the calcium and magnesium chloride specimens respectively. Between 50-100 cycles, however, the strength of the potassium acetate-immersed samples decreased by 10%, whereas the strength of the calcium and magnesium chloride-immersed specimens decreased by 25% and 30% respectively. The delay in concrete damage may be attributed to the time required to activate the deterioration mechanism and/or the presence of the corrosion inhibitor. Regardless, the results indicate that once concrete damage begins, the loss of strength occurs very rapidly with progressive cycles.

- The sodium chloride specimens did not experience a significant decrease in tensile strength at 100 cycles. The ANOVA test demonstrated that the decrease in strength was not considered statistically significant. The changes in concrete microstructure as a result of continuous hydration off-set the slight decreases in strength as a result of crystal precipitation and concrete scaling. The results support the conclusion that NaCl deterioration is primarily a physical mechanism.

6.2.5 Flexural Strength

- The flexural strength test results showed that the beam specimens sprayed with $CaCl_2$ exhibited the lowest cracking load of the samples tested. The magnitude of cracking load for the $MgCl_2$ and K-Acetate samples were over 3 and 1.4 times greater than the $CaCl_2$ specimens respectively. The cracking load of the NaCl specimens was over 2.5 times the cracking load of the $CaCl_2$ samples. The low cracking load in the calcium chloride specimens is partly attributed to the severe scaling incurred by the specimens as the more severely scaled specimen had a lower cracking load. The scaling diminished the concrete cover, and allowed greater ingress of deicing chemicals to the interior of the concrete. The precipitation of new reaction products such as calcium oxychloride may have produced harmful hydraulic pressures, inducing fracture between the

aggregate-paste interface and leading to micro-crack development and propagation at this interface.

- The cracking load of the NaCl specimens was 1.1 times higher than the control samples. The higher cracking load in the NaCl specimens may be attributed to progressive densification of concrete structure as the sodium chloride penetrated the beam samples during the freeze-thaw deterioration and continued hydration of the samples cycling period. Based on previous investigations, it is hypothesized that the intrusion of sodium chloride introduced the formation of reaction products that acted to partially block the coarser pores and convert them into finer pores. The reduction in coarser pores acts to increase the tensile and compressive strength of the cement matrix, which results in a higher cracking load.
- The cracking load for the $MgCl_2$ samples was equal to or 1.5 times greater than the cracking load of the control samples. The absence of a reduced cracking load suggests that the conditions of the test did not result in the formation of magnesium-silicate-hydrate, which would cause weakening of the paste, and a lower cracking load. The spraying of the beams may have created a saturated condition near the surface of the specimen. The diffusion of chloride ions towards the interior may have resulted in the formation of reaction products in the layers close to the beam surface. The resulting “protective shell” may have prevented further ingress of the magnesium chloride solution, and a higher cracking load may have resulted from changes in microstructure due to continuing hydration. It is believed, however, based on the tension and compression test results, that the precipitating front would have disappeared upon further saturation of the beam due to the chemical reactions between the magnesium chloride and the cement paste and the precipitation of new mineral phases in the cracks and voids.
- The cracking load of the distilled water samples was approximately equal to or 20% less than the cracking load of the control sample. The reduction in cracking load for the distilled water specimens may be attributed to the freeze-thaw deterioration of the test

samples. The ice crystals formed during freezing may have resulted in the development of hydraulic or osmotic pressures caused by the movement of water towards the freezing sites. The development of these pressures may induce micro-cracking leading to the reduction in tensile strength and resulting cracking load. Previous research has also indicated that mechanical processes such as freeze-thaw deterioration may result in an increased number of coarser pore volumes [49]. Again, this would lead to a reduction in cracking load. However, the degree of reduction is quite small, suggesting that if micro-cracking took place, it was not severe. Based on the tensile and compressive strength tests in the previous section, it is hypothesized that the continuing hydration of the samples may have decreased the overall deterioration.

- The results for the potassium acetate specimens indicate both a slight increase and decrease in cracking load. Based on the tensile and compressive strength tests, there appears to be a chemical reaction that occurs between the deicing chemical and concrete. The nature of the chemical reaction or the mechanism of deterioration cannot be explained at this time without further research.
- The dominant failure mode of all beam specimens was governed by yielding of the reinforcing bars and concrete crushing. No significant changes in the ultimate load were observed regardless of the deicing chemical used, however, the severely scaled calcium chloride specimen yielded at a slightly lower load. It is believed that the reduced strength of the cement paste as a result of chloride ingress may have caused the bars to yield earlier.

6.2.6 Static Modulus of Elasticity

- The static modulus of elasticity did not appear to be influenced by the deicing chemicals or freeze-thaw cycles. However, it was found that the concrete composition, test procedure, and placement of the strain gage had a significant effect on the modulus

values. Thus, it was difficult to draw conclusions due to the variability of the results and the small sample size. Apparent modulus values and the beam stiffness given by the moment-curvature relationships for the beam specimens also indicate that the modulus of elasticity was not severely affected by the deicing chemicals or freeze-thaw cycles.

6.2.7 Water Soluble Chlorides Test

- The samples subjected to the calcium chloride solutions developed the greatest amount of corrosion-forming water soluble chlorides at the surface layer. A comparison of the concentration of water soluble chlorides in the samples revealed that the chloride concentration in the $CaCl_2$ was over 3 times the concentration in the $MgCl_2$ samples and 1.5 times greater than the chloride concentration of the NaCl sample at this depth.
- The chloride data for the $CaCl_2$ samples show, however, that the chloride ions did not significantly penetrate the interior of the concrete. At depths below the surface layer, the chloride data indicates that the Cl ions in the NaCl samples penetrated deeper than those in the $CaCl_2$ solution. The reduced quantity of the free chlorides in the interior of the $CaCl_2$ samples is attributed to the presence of the organic corrosion inhibitor in the deicing solution, which reduced the permeability of the concrete, thereby limiting the chloride ingress.
- The chloride data for the $MgCl_2$ specimens show further penetration of the chloride ions in comparison to the calcium chloride specimens, and less penetration of the chloride in comparison to the NaCl specimens. A lower Cl ion ingress is attributed to the presence of the corrosion inhibitor in the deicing solution. It is hypothesized however, that the formation of early stages of brucite near the surface as the Cl ions migrated towards the concrete interior inhibited further ingress of both the Cl ions and the corrosion inhibitor towards the concrete interior.

- The chloride data for the NaCl samples show further penetration of the Cl ions within the sample in comparison to the calcium and magnesium chloride specimens. This indicates that prolonged use of the sodium chloride deicer may result in a higher potential for corrosion.
- The results suggest that the damage due to the NaCl deicing chemical may be more severe than the $CaCl_2$ and $MgCl_2$ deicing chemicals. However, a larger quantity of free chlorides formed in the $CaCl_2$ solution suggest that in absence of a corrosion inhibitor, the severity of damage by the water soluble chlorides may be potentially greater. The onset of scaling severely reduces the permeability as shown by the flexure test samples, and would allow the penetration of the free chlorides towards the interior, inducing a greater possibility for corrosion.

To summarize the findings of this study, the specimens subjected to magnesium chloride solutions exhibited severe strength deterioration. The loss of strength, however, was followed closely by the calcium chloride-immersed samples. The specimens subjected to potassium acetate solutions also exhibited significant losses in strength though not to the same degree of severity as the magnesium chloride specimens. The sodium chloride solutions produced severe scaling in the presence of freeze-thaw cycles, however, the surface deterioration does not significantly impact the mechanical properties of concrete. The scaling damage does, however, allow for greater ingress of deicing chemicals into the concrete interior. This is emphasized by the severe penetration of the chloride ions with depth for the sodium chloride specimens, and the lower cracking loads exhibited by the severely scaled calcium chloride beam specimens. Despite previous research to the contrary [68], the potassium acetate solutions do not appear chemically innocuous as significant reductions in tensile and compressive strength comparable to the calcium and magnesium chloride specimens were observed. The results of this study have many important implications in the effort to obtain a greater understanding of the impact that alternative deicing chemicals may have on the long-term durability of concrete materials. The results of this investigation suggest that the proposed

deicing chemicals react with concrete through various deterioration mechanisms to reduce the strength and durability of concrete structures. This research will provide transportation industries with greater knowledge to better select effective yet benign deicing chemicals. As a result, the long-term durability and life of transportation infrastructure and assets will be maintained.

6.3 Recommendations for Future Research

- The results of this investigation indicated evidence of chemical interactions between potassium acetate and concrete materials due to the significant reduction in tensile and compressive strength caused by the deicing chemicals. Further experimental investigations are warranted to determine the nature of the reaction and the reaction products formed.
- The influence of different concrete mixtures on the performance of the calcium chloride, magnesium chloride and potassium acetate needs to be studied in a systematic way. Variables need to include the effect of air entrainment, water-cement ratio, and type and size of aggregates. In addition, the effect of these deicers on aged core samples should be investigated.

Bibliography

- [1] ACI Committee 201, *Guide to Durable Concrete- ACI 201.2R-01*. American Concrete Institute, Farmington Hills, Michigan, USA, October, 2001, 41 pp.
- [2] American Society of Testing Materials. Standard Test Method for Scaling Resistance of Concrete Surfaces Exposed to Deicing Chemicals. ASTM 672/C-98, American Society of Testing and Materials, 1994, Philadelphia, PA
- [3] American Society of Testing Materials. Standard Specification for Moist Cabinets, Moist Rooms, and Water Storage Tanks Used in the Testing of Hydraulic Cement Concretes. ASTM C511, American Society of Testing and Materials, 1994, Philadelphia, PA
- [4] American Society of Testing Materials. Standard Practise for Capping Cylindrical Concrete Specimens. ASTM C617, American Society of Testing and Materials, 1994, Philadelphia, PA
- [5] American Society of Testing Materials. Standard Test Method for Compressive Strength of Cylindrical Concrete Specimens. ASTM C39/C, American Society of Testing and Materials, 1994, Philadelphia, PA
- [6] American Society of Testing Materials. Standard Test Method for Splitting Tensile Strength of Cylindrical Concrete Specimens. ASTM C496/C, American Society of Testing and Materials, 1994, Philadelphia, PA
- [7] American Society of Testing Materials. Standard Test Method for Static Modulus of

Elasticity and Poisson's Ratio of Concrete in Compression. ASTM C496/C, American Society of Testing and Materials, 1994, Philadelphia, PA

- [8] Bartz, A.E. Basic Statistical Concepts, Fourth Edition, Prentice Hall, Upper Saddle River, New Jersey, 1988, 456 pp
- [9] Beltaos, S. "Climatic change and River Ice Breakup." *Canadian Journal of Civil Engineering* v 30 n 1, February 2003, p 145-155
- [10] Brown, F.P., Cady, P.D. "Deicer Scaling Mechanisms in Concrete". *Durability of Concrete, ACI Special Publication SP 47-7* American Concrete Institute, Detroit, MI 1975, p 101-119
- [11] Canadian Center for Climate Modeling and Analysis (2003)
<http://www.cccma.bc.ec.gc.ca/models/models.shtml>
- [12] Chatterji, S. "Mechanism of the $CaCl_2$ on Portland Cement Concrete". *Cement and Concrete Research*, v 8, 1978, p 461-468
- [13] Cody, R.D, Spry, P.G. *The Role of Magnesium in Concrete Deterioration*. Final Report HR-355, Iowa Department of Transportation, 1994, 171 pp.
- [14] Cody, R.D., Cody, A.M., Spry, P.G., Gan, G. "Concrete Deterioration by Deicing Salts: An Experimental Study". *Semisequicentennial Transportation Conference Proceedings* May 1996, Department of Geological and Atmospheric Sciences, Iowa State University, Ames, Iowa
- [15] Colleparidi, M., Coppola, L., Pistolesi, C. "Durability of Concrete Structures Exposed to $CaCl_2$ Based Deicing Salt". *Durability of Concrete*, ACI SP-145-5, p 107-120
- [16] Coolidge F.L. *Statistics: A Gentle Introduction*. Sage Publications, Inc, London, UK, 2006, 397 pp.
- [17] Dow Chemical Company, http://grounds-mag.com/mag/grounds_maintenance_deicersand_degrees.t

- [18] Filion, Y. "Implications for Canadian Water Resources and Hydropower production". *Canadian Water Resources Journal v 25 n 3*, 2000, p 255-269
- [19] Fischel, M. Evaluation of Selected Deicers Based on a Review of the Literature Colorado Department of Transportation Report No. CDOT-DTD-R-2001-15, 2001
- [20] Foy, C., Pigeon, P., Banthia, N. "Freeze-thaw Durability and Deicer Salt Scaling Resistance of a 0.25 Water-Cement Ratio Concrete". *Cement and Concrete Research v 18, n 4*, 1988, p 604-614
- [21] Ftikos, C., Parissakis, G. "The Combined Action of Mg^{2+} and Cl^{-} Ions in Cement Pastes". *Cement and Concrete Research v 15*, 1985, p 593-599
- [22] Ghafoori, G., Mathis, R.P. "Scaling Resistance of Concrete Paving Block Surfaces". *ACI Materials Journal v 94 n 1*, January- February 1997, p 32-38.
- [23] Hansen, W.C. "Crystal Growth as a Source of Expansion in Portland Cement Concrete". *American Society for Testing Materials, Proceedings, v 63*, 1963, p 932-945
- [24] Harnik, A.B., Meier, U., Rosli, A. "Combined Influence of Freezing and Deicing Salt on Concrete- Physical Aspects". *Durability of Building Materials and Components ASTM Special Technical STP-691 ASTM Special Technical STP- 691*, P.J. Sereda and G.G. Litvan, Eds. American Society for Testing and Materials, 1980, p 474-84.
- [25] Hartmann, D.L. *Global Physical Climatology*, First Edition, Academic Press, Inc., San Diego, California, USA, 1994, 411 pp.
- [26] Hassan, Y., Halim, A.O., Razaqpur, W., Bekheet, W., Farha, M.H. "Effects of Runway Deicers on Pavement Materials and Mixes: Comparison with Road Salt". *Journal of Transportation Engineering v 128 n 4*, July/August 2002, p 385-391
- [27] Heller, L., Ben-Yair, M. "Effect of Chloride Solutions on Portland Cement". *Journal of Applied Chemistry, v 16*, August 1966, p 223-226

- [28] Hengeveld, H. "Projections for Canada's Climate Future". *Climate Change Digest Special Edition*, Meteorological Service of Canada, Environment Canada, Minister of Public Works and Government Services, 2000, 32 pp.
- [29] Hershfield, D.M. "The Frequency of Freeze-Thaw Cycles". *Journal of Applied Meteorology v 13 n 3*, April 1974, p 348-354
- [30] Hope, B.B., Page, J.A., Poland, J.S. The Determination of the Chloride Content of Concrete. *Cement and Concrete Research v 15*, 1985, p 863-870
- [31] Kleinlogel, A. *Influences on Concrete*, Translation by Morgenroth, F.S., Frederick Ungar Publishing Co., New York, 1950
- [32] Kuenning, W.H. "Resistance of Portland Cement Mortar to Chemical Attack- A Progress Report". *Highway Research Record Number 113- Symposium on Effects of Aggressive Fluids on Concrete*, National Research Council, January, 1965, p 43-87
- [33] Intergovernmental Panel on Climate Change (IPCC) "Climate Change 2001: The Scientific basis." <http://www.grida.no/climate/ipcc.tar/>
- [34] Lee, H., Cody, R.D., Cody, A.M., Spry, P.G. "Effects of Various Deicing Chemicals on Pavement Concrete Deterioration". *Mid-Continent Transportation Conference Proceedings*, 1998, p. 71-75.
- [35] Lee, H., Cody, A.M., Cody, R.D., Spry, P.G. "PCC Pavement Deterioration and Expansive Mineral Growth". *Mid-Continent Transportation Conference Proceedings*, 1998, p. 71-75
- [36] Lindmark, S., "Mechanisms of Salt Frost Scaling Resistance of Portland Cement-bound Materials: Studies and Hypothesis", Ph.D Thesis (Report TVBN 1017), Lund Inst. Tech., Lund, Sweden, 1998

- [37] Litvan, G.G., "Phase Transitions of Adsorbates: IV, Mechanism of Frost Action in Hardened Cement Paste", *Journal of American Ceramic Society* v 55 n 1, January 1972, p 38-42
- [38] Litvan, G.G., "Frost Action in Cement Paste". *Material Construction, Materials Structures* v 6 n 34, July-August 1973, p 293-298
- [39] Litvan, G.G., "Frost Action in Cement in the Presence of Deicers", *Cement and Concrete Research* v 6, September, 1976, p 351-356
- [40] MacGregor, J.G., Bartlett, F.M., *Reinforced Concrete Mechanics and Design*, First Canadian Edition., Prentice Hall, Scarborough, ON, Canada, 2000, 1042 pp
- [41] Marchand, J., Pleau, R., Pigeon, M. "Precision Tests for Assessment of the Deicer Salt Scaling Resistance of Concrete". *Cement, Concrete, and Aggregates* v 18, n 2, December 1996, p 85-91
- [42] Marchand, J., Sellevold, E.J., Pigeon, M. "The Deicer Salt Scaling Deterioration of Concrete- An Overview." *Proceedings of the Third CANMET/ACI International Conference on Durability of Concrete Structures*, Nice, France, May 22-28, 1994, p 1-46
- [43] Marchand, J., Pleau, R., Gagne, R., "Deterioration of Concrete due to Freezing and Thawing" *Materials Science of Concrete IV* eds. J. Skalny and S. Mindess American Ceramic Society, Westerville, OH, 1995, p 283-354
- [44] McDonald, D.B., Perenchio, W.F. "Effects of Salt Type on Concrete Scaling". *Concrete International* v 19 n 7, July, 1997, p 23-26
- [45] Mendenhall, W. *Beginning Statistics A to Z*, Duxbury Press, Belmont, CA, USA, 1993, 219 pp.
- [46] Mills, B., Andrey, J. "Climate Change and Transportation: Potential Interactions and Impacts." *Potential Impacts of Climate Change on Transportation Workshop Proceed-*

ings, October, 2002, Bookings Institution, Washington D.C., United States Department of Transportation

- [47] Mindess, S., Young, J.F., Darwin, D. *Concrete, 2nd Edition*, Pearson Education, Upper Saddle River, NJ, USA, 2003, 644 pp
- [48] Minsk, L.D. *Snow and Ice Control Manual for Transportation Facilities*, McGraw-Hill, New York, NY, USA, 1998, 289 pp
- [49] Moukwa, M., Aitcin, P., Regourd, M. "Durability of Concrete Under Simulated Arctic Conditions." *Cement, Concrete, and Aggregates*, v 11 n 1, 1989, p 45-51
- [50] Neville, A.M. "Behavior of Concrete in Saturated and Weak Solutions of Magnesium Sulphate or Calcium Chloride". *Journal of Materials in Civil Engineering* v 4, n 4, 1969, p 781-816
- [51] Petersson, P., Lundgren, M. "Influence of the Minimum Temperature on the Scaling Resistance of Concrete". *Proceedings of the 1996 7th International Conference on Durability of Building Materials and Components*, 1996, p 523-531
- [52] Pigeon, M., Pleau, R. *Durability of Concrete in Cold Climates*. E & FN Spon, Boundry Row, London, UK, 1995, 244 pp
- [53] Popovics, S. *Strength and Related Properties of Concrete: A Quantitative Approach*. Jon Wiley & Sons Inc., USA, 1998, 535 pp
- [54] Powers, T.C. "Working Hypothesis for Further Studies of Frost Resistance of Concrete". *Journal of the American Concrete Institute* v 16 n 1, February 1945, p 245-272
- [55] Powers, T.C. "Mechanisms of Frost Action in Concrete". Maryland. University – Stanton Walker Lecture Series on Materials Sciences n 3, November 1965, 35 p
- [56] Powers, T.C. "Freezing Effects in Concrete". *American Society of Mechanical Engineers*, 1975, p 1-11

- [57] Harnik, A.B. and Rosli, A. "Improving the Durability of Concrete to Freezing and Deicing Salts". *Durability of Building Materials and Components ASTM Special Technical STP-691 ASTM Special Technical STP- 691*, P.J. Sereda and G.G. Litvan, Eds. American Society for Testing and Materials, 1980, p. 464-473.
- [58] Santagata, M.C., Collepari, M. "The Effect of CMA Deicers of Concrete Properties". *Cement and Concrete Research v 30 n 9*, September, 2000, p 1389-1394
- [59] Stark, D.A., "Effect of Length of Freezing Period on Durability of Concrete". PCA Research and Development Bulletin RD096T, Portland Cement Association, 1989, 9 pp.
- [60] Sellevold, E.J. "Frost/Salt Testing of Concrete: Effect of Test Parameters and Concrete Moisture History". *Nordic Concrete Research Report TVBM-3048* RILEM Committee TC-117 FDC meeting in Lund 1991. Lund Institute of Technology, Div. Of Building Materials, 1991, p 83-100
- [61] Snyder, M.J. "Protective Coatings to Prevent Deterioration of Concrete by Deicing Chemicals". *National Cooperative Highway Research Program Report 16, Highway Research Board of the Division of Engineering and Industrial Research*, National Academy of Sciences, National Research Council, 1965
- [62] Studer, W. "Internal Comparative Tests on Frost-Deicing Salt Resistance". *International Workshop on the Resistance of Concrete to Scaling due to Freezing in the Presence of Deicing Salts*, Centre de Recherche Interuniversitaire sur le Beton, Université de Sherbrooke- Université Laval, Quebec, August 1993, p 175-187
- [63] Suryavanshi A., Swamy, R.N. "Influence of Penetrating Chlorides on the Pore Structure of Structural Concrete". *Cement, Concrete, and Aggregates, v 20, n 1*, June 1998, p 169-179
- [64] Sutter, L.L. "Investigation of the Long Term Effects of Magnesium Chloride and Other Concentrated Salt Solutions on Pavement and Structural Portland Cement Concrete-

Interim Report". South Dakota Department of Transportation Office of Research, January, 2005

- [65] Valenza II, J.J., Scherer, G.W. "Mechanisms of Salt Scaling". *Materials and Structures* v 38 n 278, May, 2005, p 479-488
- [66] Vaysburd, A.M., Emmons, P.H. "Corrosion Inhibitors and Other Protective Systems in Concrete Repair: Concepts or Misconcepts". *Cement & Concrete Composites* v 26, 2004, p 255-263
- [67] Verbeck, G.J. and Klieger, P. "Studies of Salt Scaling of Concrete". *Bulletin No. 150, Highway (Transportation) Research Board*, 1957, p 1-13
- [68] Wang, K., Nelson, D.E., Nixon, W.A. "Damaging Effects of Deicing Chemicals on Concrete Materials." *Cement and Concrete Composites*, v 28, n 2, February, 2006, p 173-188